

LITHUANIAN UNIVERSITY OF HEALTH SCIENCES

Rugilė Dragūnaitė

**IDENTIFICATION OF
EPITRANSCRIPTOMIC m⁶A BIOMARKERS
IN GLIOMA THROUGH PROFILING OF
STEM CELLS AND TUMOR TISSUES**

Doctoral Dissertation
Natural Sciences,
Biology (N 010)

Kaunas, 2025

The dissertation has been prepared at the Laboratory of Molecular Neuro-oncology of the Neuroscience Institute of the Lithuanian University of Health Sciences during the period of 2020–2025.

Scientific Supervisor

Dr. Daina Skiriutė (Lithuanian University of Health Sciences, Natural Sciences, Biology – N 010).

Dissertation is defended at the Biology Research Council of the Lithuanian University of Health Sciences:

Chairperson

Prof. Dr. Jurgita Skiecevičienė (Lithuanian University of Health Sciences, Natural Sciences, Biology – N 010).

Members:

Dr. Rūta Steponaitienė (Lithuanian University of Health Sciences, Natural Sciences, Biology – N 010).

Prof. Dr. Elona Juozaitytė (Lithuanian University of Health Sciences, Medicine and Health Sciences, Medicine – M 001).

Dr. Giancarlo Russo (Vilnius University, Natural Sciences, Biochemistry – N 004).

Dr. Anna Olszewska (Gdansk University of Medicine (Poland), Natural Sciences, Biology – N 010).

Dissertation will be defended at the open session of the Biology Research Council of the Lithuanian University of Health Sciences on the 26th of August 2025 at 1 p.m. in the A-202 auditorium of “Santaka” Valley Centre for the Advanced Pharmaceutical and Health Technologies of the Lithuanian University of Health Sciences.

Address: Sukilėlių Ave. 13, LT-50162 Kaunas, Lithuania.

LIETUVOS SVEIKATOS MOKSLŲ UNIVERSITETAS

Rugilė Dragūnaitė

**NAUJŲ GLIOMOMS SPECIFINIŲ
m⁶A RNR ŽYMENŲ PAIEŠKA
GLIOMŲ KAMIENINĖSE LĄSTELĖSE
IR NAVIKUOSE**

Daktaro disertacija
Gamtos mokslai,
biologija (N 010)

Kaunas, 2025

Disertacija rengta 2020–2025 metais Lietuvos sveikatos mokslų universiteto, Neuromokslų instituto Molekulinės neuroonkologijos laboratorijoje.

Mokslinė vadovė

dr. Daina Skiriutė (Lietuvos sveikatos mokslų universitetas, gamtos mokslai, biologija – N 010).

Disertacija ginama Lietuvos sveikatos mokslų universiteto Biologijos mokslo krypties taryboje:

Pirmininkė:

prof. dr. Jurgita Skiecevičienė (Lietuvos sveikatos mokslų universitetas, gamtos mokslai, biologija – N 010).

Nariai:

dr. Rūta Steponaitienė (Lietuvos sveikatos mokslų universitetas, gamtos mokslai, biologija – N 010);

prof. dr. Elona Juozaitytė (Lietuvos sveikatos mokslų universitetas, medicinos ir sveikatos mokslai, medicina – M 001);

dr. Giancarlo Russo (Vilniaus universitetas, gamtos mokslai, biochemija – N 004);

dr. Anna Olszewska (Gdanskio medicinos universitetas (Lenkija), gamtos mokslai, biologija – N 010).

Disertacija bus ginama viešajame Biologijos mokslo krypties tarybos posėdyje 2025 m. rugpjūčio 26 d. 13 val. Lietuvos sveikatos mokslų universiteto Naujausių farmacijos ir sveikatos technologijų centro A-202 auditorijoje. Disertacijos gynimo vietos adresas: Sukilėlių pr. 13, LT-50162 Kaunas, Lietuva.

*I dedicate this thesis to my late father, Stasys Dragūnas.
Though you are no longer here, your spirit lives on
in every page of this thesis.
Not a day has passed that I do not think of you.*

CONTENTS

ABBREVIATIONS	10
INTRODUCTION	11
AIM AND OBJECTIVES.....	13
The uniqueness and significance of the investigation.....	13
Study outline	14
1. REVIEW OF THE LITERATURE	16
1.1. Malignant brain tumors	16
1.1.1. General overview	16
1.1.2. Glioblastoma	17
1.1.3. Glioblastoma molecular classification	19
1.1.4. Current stemness biomarkers of glioblastoma	20
1.1.5. Treatment resistance in glioblastoma.....	21
1.2. Epitranscriptomics	21
1.2.1. N6-methyladenosine (m ⁶ A) modification.....	22
1.2.2. m ⁶ A modification in cancer	23
1.2.3. m ⁶ A methylation topology	24
1.3. Experimental and computational approaches for identification of m ⁶ A	25
1.4. Stemness-related m ⁶ A candidate biomarkers in glioma tumors	26
1.4.1. mRNA <i>OS9</i>	26
1.4.2. mRNA <i>PAGRI</i>	27
1.4.3. mRNA <i>TOBI</i>	27
1.4.4. mRNA <i>PIK3R2</i>	28
1.4.5. mRNA <i>GP1BB</i>	28
1.4.6. mRNA <i>RETREG1</i>	29
1.4.7. mRNA <i>LUC7L3</i>	29
2. METHODS AND MATERIALS.....	31
2.1. Specimen collection and ethics	31
2.2. Covariate screening	31
2.3. Reagents, barcodes, reagent suppliers and catalogue numbers ...	32
2.4. Human cell lines	33
2.5. RNA extraction and polyA RNA enrichment	34
2.6. Enzyme-linked immunosorbent assay (ELISA).....	34
2.7. N6-methyladenine immunoprecipitation (MeRIP-seq) by next-generation sequencing	35
2.8. MeRIP-seq m ⁶ A peak calling	36
2.8.1. Differential gene expression and methylation of MeRIP-seq.....	36

2.9.	Direct RNA library preparation and MinION sequencing (dRNA-seq) by Oxford Nanopore Technologies (ONT).....	36
2.9.1.	dRNA-seq sequencing library preparation.....	36
2.9.2.	ONT MinION flow cell loading and sequencing.....	37
2.9.3.	Mapping of sequencing data.....	37
2.9.4.	Differential gene expression and methylation of dRNA-seq.....	37
2.10.	Quantitative RT-PCR.....	37
2.11.	Silhouette Plot.....	38
2.12.	m ⁶ A methylation and stemness score calculations.....	38
2.13.	Random forest algorithm (Alluvial plot).....	39
2.14.	Nomogram analysis.....	39
2.15.	Pathway enrichment analysis.....	39
2.16.	Statistical analysis.....	40
3.	RESULTS.....	41
3.1.	The composition of RNA profile from m ⁶ A epitranscriptome aligned MeRIP-seq in glioblastoma U87-MG and glioma stem cell NCH421k lines.....	41
3.2.	The composition of RNA profile from m ⁶ A epitranscriptome aligned dRNA-seq in glioma patient samples.....	44
3.3.	Protein-coding RNA m ⁶ A modification target selection via MeRIP-Seq and dRNA-seq data.....	46
3.3.1.	Target selection in mRNA in MeRIP-seq data.....	46
3.3.2.	Selection of m ⁶ A-modified mRNA targets in glioma patients dRNA-sequencing data.....	49
3.4.	Clustering of glioma patients based on m ⁶ A epitranscriptomic signatures.....	52
3.4.1.	Relationship between mRNA m ⁶ A methylation and patients' clinical data in combination of RRACH motifs.....	55
3.4.2.	AAACA 2129 <i>OS9</i> RRACH m ⁶ A modification is significantly associated with gliomas survival and Ki-67.....	61
3.4.3.	AGACA 1210 <i>PAGRI</i> RRACH m ⁶ A modification is significantly associated with gliomas survival and glioblastoma subtypes.....	63
3.4.4.	GGACA 2173 <i>OS9</i> RRACH is strongly associated with glioma patients clinicopathological characteristics.....	64
3.4.5.	Weak link between GGACT 2187 <i>TOBI</i> RRACH methylation and glioma patients' clinical characteristics.....	66
3.4.6.	Strong link between AAACC 3283 <i>PIK3R2</i> RRACH methylation and glioma patients'.....	68
3.4.7.	GAACC 3068 <i>GP1BB</i> RRACH methylation associated with and glioma patients' clinical outcome.....	69
3.4.8.	GGACA 3110 <i>RETREG1</i> RRACH is a very promising molecular marker for glioma prognostics.....	71
3.4.9.	Weak link of GGACT 3122 <i>LUC7L3</i> RRACH in glioma patients' clinical data.....	73

3.5. Unraveling stemness: a deep dive into glioma patients' stemness scores.....	74
3.6. Analysis of expression levels in target genes.....	81
3.6.1. Target gene expression relations to epitranscriptomic data.....	87
3.6.2. Individual target genes' expression relations to patients' clinical data in clusters.....	88
3.7. mRNA signaling pathways related to stemness in m ⁶ A methylation-based clusters.....	91
DISCUSSION.....	96
CONCLUSIONS.....	104
PRACTICAL RECOMMENDATIONS.....	105
SANTRAUKA.....	106
REFERENCES.....	121
LIST OF PUBLICATIONS.....	138
PHD CANDIDATE'S CONTRIBUTION.....	142
CURRICULUM VITAE.....	144
ACKNOWLEDGMENTS.....	146

ABBREVIATIONS

ATP	–	adenosine triphosphate
ATRX	–	alpha-thalassemia mental retardation X-linked
CD15	–	X hapten or Lewis X antigen
CD44	–	non-kinase transmembrane glycoprotein
CD90	–	membrane GPI-anchored protein
CD133	–	Prominin-1, a trans-membrane glycoprotein
CDKN2A	–	cyclin dependent kinase inhibitor 2A
CDS	–	protein coding region
CHI3L1	–	chitinase-3-like protein 1
CNS	–	central nervous system
DEG	–	differentially expressed genes
EGFR	–	epidermal growth factor receptor
FBS	–	fetal bovine serum
GAS1	–	growth arrest-specific protein 1
GB	–	glioblastoma
GLI2	–	GLI family zinc finger 2
GSC	–	glioma stem cells
GSEGO	–	gene set enrichment analysis
IDH	–	isocitrate dehydrogenase
JAG1	–	jagged canonical notch ligand 1
Ki-67	–	marker of proliferation Kiel 67
LFNG	–	fucose-specific beta-1,3-N-acetylglucosaminyltransferase
LGG	–	low grade glioma
LncRNA	–	long non-coding ribonucleic acid
m ⁶ A	–	N6-methyladenosin
MeRIP	–	methylated RNA immunoprecipitation
MGMT	–	O-6-methylguanine-DNA methyltransferase
NEFL	–	neurofilament light polypeptide
NF1	–	neurofibromin 1
NF-kB	–	nuclear factor kappa B subunit 1
NOTCH3	–	notch receptor 3
NSC	–	neural stem cells
ONT	–	Oxford Nanopore Technologies
OS	–	overall survival
PDGFRA	–	platelet derived growth factor receptor alpha
polyA RNA	–	polyA ribonucleic acid
PTEN	–	phosphatase and tensin homolog
S100A4	–	fibroblast-specific protein 1 (Fsp1) or metastasin 1
SLC12A5	–	solute carrier family 12 member 5
SOX2	–	SRY-Box transcription factor 2
SMO	–	smoothened, frizzled class receptor
TERT	–	telomerase reverse transcriptase
TMZ	–	temozolomide
TP53	–	tumor protein p53
WHO	–	World Health Organization

INTRODUCTION

Malignant brain tumors gliomas are the most prevalent type of central nervous system (CNS) tumors originating from glial cells [1]. Standard care and prognosis for gliomas vary drastically. Glioblastoma (GB) is the most common malignant brain tumor with a 5-year survival of 7.2%. The standard of glioblastomas treatment is surgical resection followed by radiotherapy, temozolomide chemotherapy, however, the heterogeneity, infiltrative nature and protection from the blood-brain barrier still remain a challenge for GB treatment strategies [1, 2]. Resistance to all available treatment therapies is encouraged by the strong DNA repair and self-renewing of glioma initiating cells [1].

There is growing evidence of tumor-initiating glioma stem cells (GSCs), which exhibit properties associated with GB resistance to therapy and tumor recurrence [3, 4]. Certain stem cells can be identified using cell surface markers such as *CD133*, *CD44* or *A2B5*, and studies are showing promising results in glioma patients [1, 3]. Therefore, it is crucial to target treatment-resistant stem cells and look for therapeutic targets against them.

The role of mRNA m⁶A modification in gliomas just begun to be appreciated. It is already demonstrated that m⁶A methylation is a reversible and dynamic modification [5–7] and critical for GB stem cell tumorigenesis and self-renewal [8]. In addition, it is already known that m⁶A-modified mRNAs engage in cellular processes such as cell differentiation, DNA damage response, cell growth or cellular stress response [8, 9]. Studies of m⁶A modifications in glioma stem cells conducted to date suggest that mRNA m⁶A modification may be a promising target for GSCs.

Advances in technology have laid the foundation for the field of epitranscriptomics to define the role of m⁶A mRNA modifications in cancer biology. Development of high-throughput sequencing MeRIP-seq [10] and Oxford Nanopore sequencing [11] provides new insight into mRNA m⁶A modification detection in gliomas with high accuracy. Current work including glioma stem cells, II and IV grade astrocytic glioma tumors as study material with purpose to define and analyze potential biomarkers for gliomagenesis. The screening of molecular markers enabled to select the most significant targets in glioma tumor tissues and specify a set of prognostically relevant genes for glioma tumor malignancies. Screening of specific stemness-related biomarkers enabled to define the most significant targets for glioma pathogenesis and selection of gene set of combined prognostically and diagnostically relevant data for glioma malignancies. Overall, our study demonstrated the

feasibility of sequencing in glioma tumor samples that uncovered brain cancer epitranscriptomes and transcriptomes at single-transcript resolution and revealed m⁶A alterations occurring in the mRNA of clinically relevant targets.

AIM AND OBJECTIVES

Aim:

To identify glioma-specific mRNA N6-methyladenosine (m⁶A) modifications in glioma stem cells and tumors for novel clinically relevant molecular markers in gliomas.

Objectives:

1. To determine the N6-methyladenosine (m⁶A) profile of mRNAs in glioma stem cells (NCH421k) compared to glioblastoma cells (U87-MG), and to identify candidate m⁶A-modified transcripts potentially associated with glioma stemness and progression.
2. To define a set of mRNAs with characteristic m⁶A epitranscriptomic modifications associated with glioma pathogenesis and patient prognosis.
3. To investigate glioma stem cells specific candidate m⁶A-modified transcripts in glioma tumors for evaluation with tumor pathology and patient clinical characteristics.

The uniqueness and significance of the investigation

Since research into post-transcriptional chemical modifications of RNA is fresh and innovative, a little more is already known about RNA modifications and their functional importance, although significant results are still lacking. Even with m⁶A, the most well-studied methylation mark mechanism by which it modulates mRNAs remains unclear. The focus on mRNA modifications is particularly intriguing because they serve as substrates for protein translation. m⁶A modifications change in certain malignancies can enhance the translation of a subset of mRNAs, many of which are oncogenes.

In glioblastoma (GB), an aggressive and treatment-resistant primary brain tumor, examining m⁶A changes in glioma stem cells (GSCs) and tumor tissues is a novel and significant path of research. This area of research is particularly placed at the crossroads of RNA biology, cancer stem cells, and neuro-oncology, providing both mechanistic insights and translational prospects. The reversibility and targetability of m⁶A modifications indicate their potential as novel therapeutic vulnerabilities in glioma. Therapeutic regulation of epitranscriptome modifications in glioma stem cells could help control their growth, renewal, and tumor development.

This study analyzed m⁶A-modified and stemness-related mRNA gene candidates in patients' glioma tumor tissues with different glioma grades for the first time. Also, this study provides insights into a set of selected mRNAs suitable for future investigations for the development of prognostic and diagnostic glioblastoma treatment methods targeting glioma stem cells. Furthermore, patients' m⁶A methylation data were deposited in the public repository GEO under the accession number GSE282642. For our information, it was the first methylation data placed into database.

The significance of this study goes beyond glioma biology. Studying m⁶A in glioma stem cells can shed light on how RNA modifications influence stem-like behavior in malignancies and potentially enlighten similar mechanisms in other cancers.

Study outline

This study is divided into two sections:

- A search of potential m⁶A modified mRNAs for glioma prognostic and diagnostic using glioma stem cells (NCH421k) and glioblastoma (U87-MG) cell lines after MeRIP-seq analysis.
- Validation of potential m⁶A modified mRNAs in glioma post-surgical tissue after direct RNA-seq analysis.

Simplified graphical design of the dissertation are represented in Fig. 1 below.

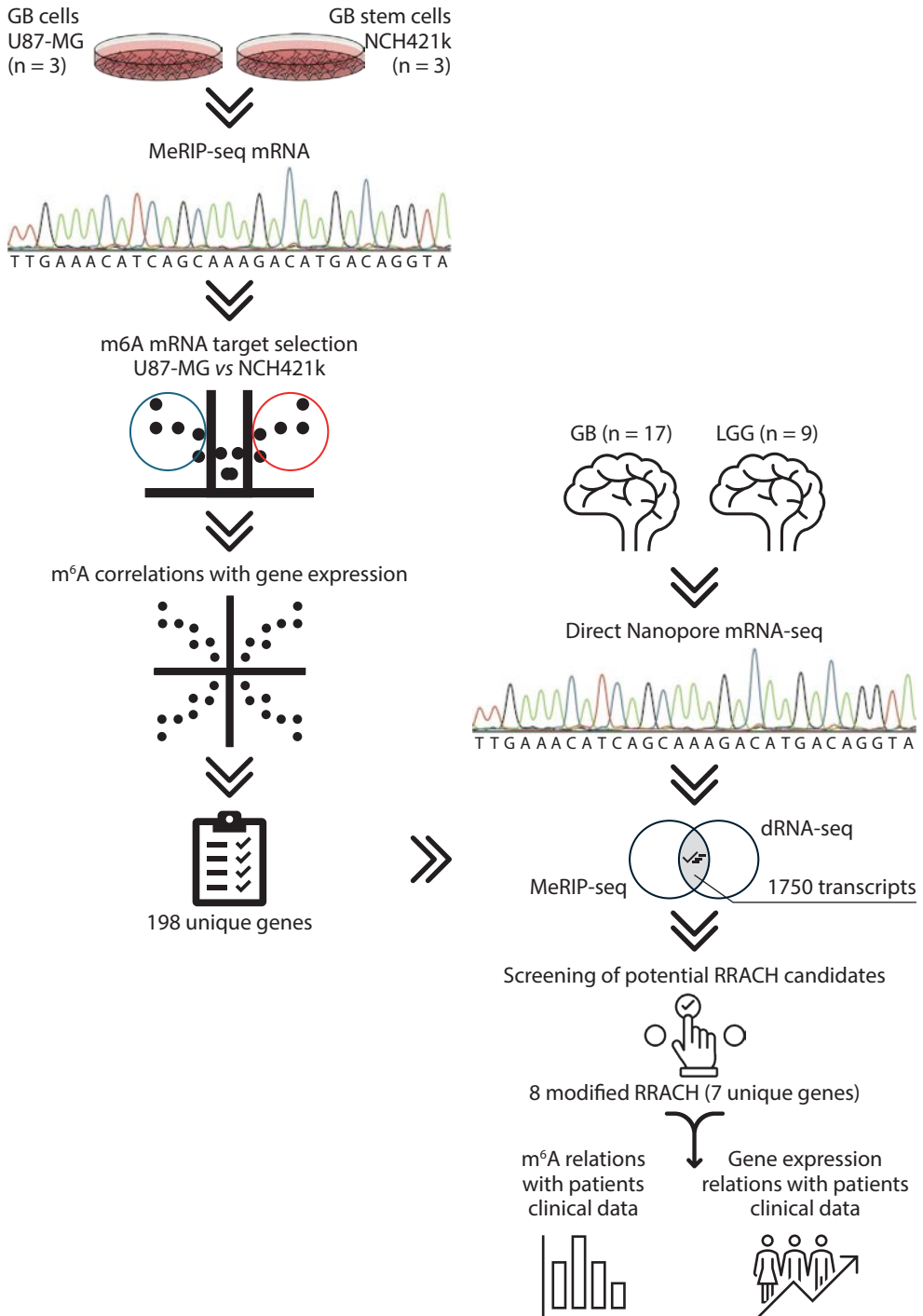


Fig. 1. Graphical design of the thesis

Illustrations provide a quick reference of the sample sets and main methods of the thesis.

1. REVIEW OF THE LITERATURE

1.1. Malignant brain tumors

1.1.1. General overview

Malignant brain tumors include glioblastoma (49%), other gliomas in parenchyma (30%), primary lymphoma (7%), and ependymomas (3%) and meningiomas (2%). Neurocognitive impairment (30–40%), localized neurologic impairments (10–40%), headache (50%), and seizures (20–50%) are all signs of malignant brain tumors [12]. Less than 5% of adults who develop a malignant brain tumor have a cancer predisposition syndrome [13, 14] or a family history of brain tumors. However, based on germline sequencing [15] and genome-wide complex trait analysis [16], heredity plays a larger role in the development of brain tumors.

The best technique for assessing brain malignancies is magnetic resonance imaging. Tumor biopsy is necessary for diagnosis, considering molecular and histological features. Treatment varies according to the type of tumor and frequently consists of radiation, chemotherapy, and surgery [12].

Countries and regions vary in the occurrence and mortality rates of brain tumors (Fig. 1.1.1.1). Europe, Australia, the United States, and Canada have the highest rates of the CNS brain tumors, while economically poor nations such as Africa and some parts of Asia face lower rates [17]. Of all incidences of primary malignant brain tumors 49% of brain tumors are glioblastomas [12].

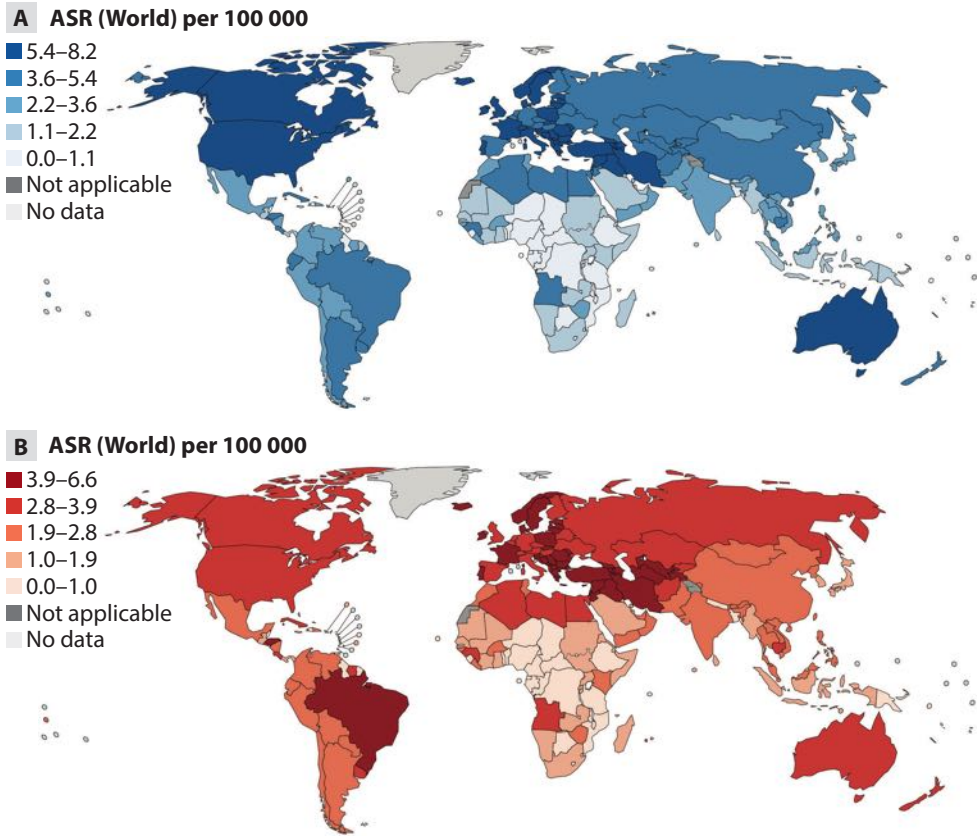


Fig. 1.1.1.1. *The epidemiology of the central nervous system brain tumors*

The figure represents standardized incidence by age (0–85), (A) disease related mortality (B) and rates in both men and women (per 100 000 individuals) across the world. Adapted from GLOBOCAN 2022.

1.1.2. Glioblastoma

Approximately 57% of all gliomas and 49% of all primary malignant central nervous system (CNS) tumors are glioblastoma (GB), the most frequent and aggressive malignant primary brain cancer in adults [18]. The tumors always grow resistant to treatment and recur despite surgical intervention and chemoradiotherapy, leading to mortality with a median survival of only 15 months [19]. GBs are grade IV diffuse gliomas, which are distinguished by their capacity for cancer cells to penetrate into surrounding brain tissue and the 5-year survival rate is about 5% [20–22]. According to National Cancer Institute of Lithuania, between 2020 and 2024, Lithuania’s glioblastoma death rates varied from 3 to 4.6 cases per 100 000 population. With a

population of approximately 2.8 million, this translates to an estimated 84 to 129 glioblastoma-related fatalities during this period.

Glial cells, which represent the connective tissue that envelops and shields neuronal cells in the brain and spinal cord, develop uncontrollably and eventually give rise to gliomas. Microglia, ependymal cells, oligodendrocytes, and astrocytes are examples of glial cells [23]. In 1863, Dr. Rudolf Virchow became the first to identify GB as a tumor originating from glial cells [24]. Previously believed to originate only from glial cells, new research indicates that high grade gliomas, such as GB, could originate from a variety of cell types with characteristics like neural stem cell-like [25].

Primary and secondary GBs are distinguished from one another. Primary GBs are tumors that form without a recognized precursor, while secondary GBs are tumors that have signs of developing from a lower-grade malignancy, either clinically, radiologically, or histopathologically [26, 27]. Primary and secondary GBs exhibit unique genetic modifications during their evolutionary history, despite their histological indistinguishability. This observation was initially published by H. Ohgaki and colleagues in 1996. The most common genetic changes observed in primary GB were overexpression of the epidermal growth factor receptor (*EGFR*) gene, mutations in the phosphatase and tensin homolog (*PTEN*) gene, or complete deletion of chromosome 10 [27]. While secondary GB was more likely to have genetic changes involving tumor protein 53 (*TP53*) and *IDH1* gene mutations [28].

GB is still an incurable disease, despite advances in our knowledge of its cellular and molecular features. Chemotherapy, radiation therapy, and surgical resection are some of the conventional techniques used in the management of GB. The entire tumor could not be eliminated during surgical resection due to the infiltrative tendency of GB to the surrounding normal tissues. Nonetheless, surgery is essential to minimize the size of the tumor, relieve symptoms before receiving radiation and chemotherapy, and make tumor tissue available for histologic and genetic tumor analysis. The intricacy of managing and treating glioblastoma is further complicated by its heterogeneous nature [29]. Almost all GB tumors recur despite developments in molecular characterization and the creation of individualized treatment plans [20] and treatment resistance makes recurrence a significant clinical problem.

There has been evidence that glioblastoma stem cells (GSCs), which are cancer cells that resemble stem-like cells characteristics, may play a role in tumor growth and recurrence [30]. GSCs exhibit resistance to chemotherapy and radiation, have greater capacities for self-renewal, and are slow-cycling tumor cells with an enhanced capacity to create tumors [31–33]. Some researchers questioned the existence of GSCs, claiming that the cells that were discovered might not be truly representative of the tumor material but

rather a population that was acquired through in vitro cultivation. While there are disagreements and discussions surrounding the GSC hypothesis about how difficult it is to find a dependable GSC marker and the best system to enrich and functionally isolate GSC, there is growing experimental and clinical evidence that GSCs exist and are significant in glioblastoma [34, 35]). Due to significant changes in genomic stability, GSCs have an increased stemness potential. Since GSCs are distributed throughout the brain's hemispheres, eliminating this cell type is difficult. GSC differentiation and dedifferentiation in glioblastoma are intimately associated with tumorigenic potential, and these processes may be impacted by epigenetic modifications [36].

1.1.3. Glioblastoma molecular classification

Tumor grading established by the World Health Organization (WHO) is used for diagnosis and to predict therapeutic outcome. More molecular traits were incorporated with immunohistochemistry data and histology in the 2021 WHO CNS tumor classification to determine tumor kinds and grading. Empirical evidence suggests that this enhances diagnosis precision, facilitates customized therapy, and eventually improves patient outcomes [37, 38].

The 2021 revision to the World Health Organization's categorization system for brain tumors has improved the standards for glioblastoma diagnosis, giving more weight to molecular characteristics than to conventional histological indicators [37]. According to this revised classification, glioblastomas are now classified as having one or more of the following characteristics: microvascular proliferation, necrosis, *TERT*-promoter mutation, *EGFR* gene amplification, or +7/ π 10 chromosome copy number changes. IDH-wildtype status, which indicates the absence of mutations in *IDH1* or *IDH2* genes, is no longer the only way to identify glioblastomas. This change is a reflection of a better knowledge of the molecular mechanisms behind the aggressive nature of glioblastoma [39, 40].

Based on variations in genomic expression profiles, GB was later divided into four subtypes after large-scale next-generation sequencing techniques were developed: proneural, neural, mesenchymal, and classical [41]. All four subgroups are supported by different percentages of individual cells inside each tumour; the most common subgroup is indicative of the total bulk tumor subtype and is determined by the genetic changes that are present. *EGFR* amplification, which is defined by chromosome 7 amplification combined with chromosome 10 loss, absence of *TP53* gene alterations, and cyclin-dependent kinase inhibitor 2A (*CDKN2A*) gene deletion, which impacts the RB pathway and its constituent parts was observed in 100% of the classical

subtype [41]. The Notch (*NOTCH3*, *JAG1*, *LFNG*) and Sonic hedgehog (*SMO*, *GAS1*, *GLI2*) components, as well as the neural stem cell marker nestin, which is encoded by the *NES* gene, are all strongly expressed in the classical subtype. When patients with the classical subtype are treated aggressively with chemotherapy and radiation, their mortality significantly improves. Tumors of the mesenchymal subtype had the highest frequency of mutations in the *NFI* (Neurofibromatosis type 1) tumour suppressor gene, markers such as MET receptor tyrosine kinase and Chitinase 3-like 1 (*CHI3L1*). Mesenchymal subtypes have high expression levels of genes involved in the nuclear factor kappa-light-chain-enhancer of activated B cells (*NF-kB*) pathway and the tumour necrosis superfamily pathway [41]. Despite having the best overall prognosis of all the subtypes, mesenchymal subtypes have a higher risk of invasion and react effectively to therapy [42]. The proneural subtype is characterized by two major genetic alterations: point mutations in the *IDH1* gene and platelet-derived growth factor receptor alpha (*PDGFRA*) [41] and lastly, expression of neural markers, such as neurofilament light peptide (*NEFL*) and Solute carrier family 12 members 5 (*SLC12A5*), are indicative of a neural subtype. Despite not exhibiting a discernible improvement in response to intensive therapies, patients with proneural subtype tumors may have higher survival rates [41, 43].

1.1.4. Current stemness biomarkers of glioblastoma

Biomarkers are endpoints that are objectively assessed as indicators or metrics of normal biological processes, pathogenic processes, or pharmacological reactions to a therapeutic intervention. They are essential to the practical development of medical diagnostics and treatments [44, 45].

Despite the lack of a single, universal marker for GSCs, several markers are currently in use and are frequently used to distinguish GSCs, including *SOX2*, *CD133*, *Nestin*, *OLIG2*, *NANOG*, *Musashi*, *CD44*, *c-Myc*, *Bmi1* and *Oct4* [46–49]. One important marker in GB is *Nestin*. Lower survival rates have been demonstrated to relate to increased levels of *Nestin* [50]. These proteins are crucial for cancer and stem cell activity, and they are expressed in GSCs. For example, *CD44* increases survival and differentiation [51], *CD133* promotes proliferation [52], and *SOX2/NANOG* self-renewal and stemness [53, 54]. Additional possible marker to identify GSCs include integrin *ITGA6*, *CD171* (*LICAM*), *CD90* (*THY1*), *CD15* (*FUT4*), ATP-binding cassette transporters, *CD44* and *ID1* together, and *S100A4* [55].

In conclusion, there is still opportunity for advancement in the treatment of glioblastoma despite numerous recent findings and current trials. The scientific community continues to face challenges in developing novel

therapeutic drugs due to the aggressive nature of this malignancy and the limitations of continually emerging approaches. However, the desire to improve patients' conditions and accomplish what presently appears unattainable motivates constant exploration for solutions.

1.1.5. Treatment resistance in glioblastoma

Treatment resistance is a problem in practically all cancers, but it is especially important in GB since it plays a part in the nearly 100% patient mortality rate. Finding the genetic mechanisms causing resistance has been the goal of research in the past years on patients who have received conventional therapy [56–59]. But there was not much data to support these mechanisms in GB. Only few genes are frequently identified to be specifically changed in glioblastoma. Studies have investigated more specialized and alternative treatment methods in an effort to address the insufficient effectiveness of conventional therapy, but with limited success [60–62].

Additionally, it has been demonstrated that some gene changes make cells more likely to undergo the cellular states associated with GBs [63]. Consequently, they might have an impact on cells' capacity to develop adaptive resistance. Additionally, there may be pathways that are critical and harmful when changed, which would stop cells with these mutations from surviving to the recurrent stage. Although some research [56, 59] have already identified specific genes that are more frequently altered in GB, they have not used comprehensive techniques to look into changes throughout cellular pathways. These investigations could reveal new therapeutic targets and provide insight into the mechanisms influencing GB cells' capacity to endure treatment.

1.2. Epitranscriptomics

Changes in gene expression in molecules are one of the main causes of tumor development. Numerous regulatory mechanisms actively modulate gene expression at the DNA, RNA, and protein levels without making any changes to the DNA sequence. Those processes include epigenetic, transcriptional, and epitranscriptomic layers. Epitranscriptomics is a relatively new, variable, and dynamic science of gene regulation, which refers to chemical modifications of RNA molecules without changing the nucleotide sequence [64].

1.2.1. N6-methyladenosine (m⁶A) modification

N6-methyladenosine (m⁶A) is an RNA modification found at the adenine base of all types of RNA molecules, including rRNA, tRNA, lncRNA, mRNA, miRNA, and other non-coding RNAs such as circular RNA (circRNA) [65]. This modification is the most common in eukaryotes, occurring in more than 25% of all transcripts [10, 66]. Recent studies have demonstrated the key role of m⁶A modification in various cellular processes, including differentiation [67], development [68] also plays an important role in regulating gene expression including mRNA stability [69], splicing [70], miRNA biogenesis [71] and etc. Dysregulation of m⁶A modification is associated with various diseases such as neurological disorders [72, 73], viral infections [74] and cancer [75, 76]. Therefore, it is crucial to understand the molecular mechanisms underlying m⁶A regulation and the possibility of targeting them for therapeutic purposes.

Many researchers focused on m⁶A modifiers known as “readers”, “writers” and “erasers” in glioma cancer. “Readers” are m⁶A-specific binding proteins include YTHDF1/2/3 and IGF2BP1 [77]. Studies have shown that those “readers” mRNA expression positively correlated with gliomas malignancy and increased in high grade gliomas [78, 79]. In addition, to stabilizing MYC and VEGFA transcripts in GSCs, YTHDF2 may identify highly methylated mRNAs, causes their degradation, and thereby reduce cell death and differentiation, which in turn promotes glioblastoma growth and dedifferentiation [80, 81]. “Writers” are methyltransferase-like 3 and 14 (METTL3 and METTL14) and their cofactors such as WTAP, RBM15/15B or KIAA1429 [82] while “erasers” include ALKBH5 and FTO genes [83–85] contribute to glioblastoma carcinogenesis, particularly GSCs [86]. In summary, glioblastoma formation and incidence are linked to changed m⁶A modifications, most likely through controlling stem cell self-renewal. It seems that m⁶A “readers” contribute to the progression of glioblastoma growth, while both m⁶A “writers” and “erasers” have an oncogenic effect. Nevertheless, contradictory findings suggest that m⁶A modifications contribute to the development of tumors, most likely by controlling different downstream genes [87].

According to Liu, 2014 [82], the m⁶A has been placed in the specific consensus motif RRACH (R = A or G; H = A, C, or U), which is sufficient to prevent methylation in the event of a mutation [88]. m⁶A modifications participate in many biological and pathological processes, therefore, after the distribution of m⁶A modifications in cells, various disorders occur. It has been observed that m⁶A regulates the balance between cellular differentiation and pluripotency during organismal development [89, 90] while modified m⁶A levels on specific gene transcripts are important for cancer. Reduced m⁶A

levels on *NANOG* or *FOXMI* mRNAs, stabilize the mRNA, which increase the number of cancer stem cells [89, 90]. Conversely, increased m⁶A level on oncogene c-myc mRNA improves transcript stability and translation, which in turn encourages self-renewal and proliferation [91, 92]. Regarding the biology, regulation, and function of m⁶A, there are still various controversies in the field. According to the traditional perspective, m⁶A is a dynamic and reversible modification that can undergo controlled methylation and demethylation during its lifecycle [68]. According to recent hypotheses, the primary function of m⁶A is to signal mRNA for degradation, and its modification is more static and influenced by genes, such as the length and location of exons and introns [93].

The primary points of conflict center on how, and when m⁶A levels and locations are controlled, as well as the primary consequences of m⁶A change on mRNA. Our understanding of m⁶A biology, regulation, and function will increase with the development of advanced m⁶A profiling methods, particularly those that can locate every m⁶A site in the molecules [94].

1.2.2. m⁶A modification in cancer

Changes of m⁶A methylation levels can impact numerous cellular functions, including those linked to the initiation and development of tumors, in keeping with its pivotal function in regulating the production of mRNA genes. Interestingly, both high and low levels of m⁶A have been linked to carcinogenesis and many malignancies show changes in m⁶A abundance. Rising pool of research in recent years has demonstrated m⁶A levels in both solid and liquid tumors [65].

It is important to highlight that, even for the same tumor type, different research has produced conflicting findings about the role of m⁶A methylation in tumor growth. For instance, high m⁶A levels are related with high tumor aggressiveness in leukemia [95, 96] while increased FTO expression in leukemia subtype leads to the lack of m⁶A levels which contributes with leukemogenesis [97]. In the *ANKLE1* gene's exon with a G to A mutation in colon-rectal cancer has been identified by a large-scale population analysis. YTHDC1 recognizes the methylated [A] allele, which inhibits cell proliferation by increasing the protein expression of the tumor suppressor *ANKLE1* [98]. Environmental variables influence m⁶A modification and aid in the development of cancer in addition to intracellular dysregulation of m⁶A machinery and mutations on m⁶A sites. According to recent research, exposure to cigarette smoke condensate in immortalized human pancreatic duct epithelial cells [99] and chemical carcinogens can significantly alter the abundance of m⁶A in epithelial cells [100, 101].

In 2017, Cui's team reported that glioblastoma was associated with m⁶A RNA methylation and m⁶A-related proteins [102]. Glioma stem cells, which are considered the initial cells of glioblastoma, have been studied which are responsible not only for the emergence of glioblastomas but also for resistance to treatment and tumor recurrence [103]. The first mechanistic study that connected glioblastoma oncogenesis and m⁶A modification was released, showing GSC lines' levels of m⁶A RNA methylation and it was demonstrated that these levels decreased with in vitro development [104]. Epigenetic changes are thought to be promising indicators for the diagnosis of GB. Some epigenetic conditions do explain GB development and can also be utilized to diagnose GB or predict the prognosis of GB patients [105, 106]. There is evidence that reduced m⁶A RNA methylation promotes the tumorigenesis of glioma stem cells [102]. Through immunological checkpoints (ICPs) and the GALECTIN signaling pathways, m⁶A modification promotes an immunosuppressive environment and helps GB cancer cells reach the stemness stage according to a single-cell sequencing [107]. We believe that the new knowledge of the functions of m⁶A modification in gliomas will help with the progress of precision GB treatment.

On top of that, the idea of using the m⁶A signature of specific transcripts as biomarkers for early cancer diagnosis and classification, outcome prediction and risk stratification is gaining interest.

1.2.3. m⁶A methylation topology

All forms of RNA contain m⁶A, though the amounts of each kind might vary. An analysis of the distribution of m⁶A across RNA species revealed that 94% of the relevant m⁶A peaks matched to the intragenic area [108]. However, only 1% to 2% of the peaks were mapped to non-coding RNA, which indicates that m⁶A is more prevalent in mRNA than in other RNAs.

Many years ago, the number of m⁶A per mRNA was estimated [109]. According to their estimation, human cells have one m⁶A for every nine hundred nucleotides. It corresponds to 3 m⁶A per mRNA, given that the average length of mRNA is approximately 3000 nucleotides. At least one m⁶A is present in human cells in between 4000 and 5000 transcripts transcribed by different genes [10, 66]. Therefore, transcripts encoded by 4000–5000 genes can have between 2 and 3 m⁶A deposited on them.

m⁶A site localization in mRNA is essential to understand its function. Two domains can be distinguished in mRNA. First one, untranslated regions, which have regulatory functions, might be in either 3' (3'UTR) or 5' (5'UTR). The second is the coding sequence that proteins are translated from. The location of m⁶A is crucial to its function since distinct parts of mRNA have

different roles [110]. m⁶A distribution across mRNA is not random. Approximately 80% of m⁶A are found in the regions next to stop codon in both CDS and 3'UTR, according to the metagene profile [10, 66, 111, 112].

As mentioned before, sequencing study of m⁶A sites has shown a motif RRACH that may dictate methylation, which is consistent with its specific distribution [66]. Nevertheless, motifs are not limited to regions where m⁶A is enriched, so it is also determined by other factors.

Recent advancements in m⁶A sequencing presented the possibility for large-scale research and allowed m⁶A mapping from low-input material [112]. Overall, there is no tissue specificity in the m⁶A profile. m⁶A is abundant at Transcription start site (TSS) and at the stop codon in all tissues [113].

1.3. Experimental and computational approaches for identification of m⁶A

Although RNA modifications have been discovered for a long time the field of these modifications is still poorly explored. Along with the emergence of Next Generation sequencing (NGS), increasingly m⁶A detection methods have been developed to understand the functions of m⁶A. Primary way to identify m⁶A modifications using the MeRIP-seq method based on m⁶A antibodies. Methylated adenosines are specifically bound by antibodies, which makes it possible to find the approximate location of m⁶A [10, 66].

A new, promising method for nanopore sequencing has recently been developed. The direct RNA-seq (dRNA-seq) approach developed by Oxford Nanopore Technologies (ONT) has recently allowed for the discovery of RNA modifications. ONT sequencing device records nucleotides allowing for the accurate identification of RNA modifications, including m⁶A in its native form. Together with an electric current, the RNA to be sequenced travels through the nanopore. At a level unique to each nucleotide, the current is disrupted as the nucleic acid passes through the nanopore. This makes it possible to identify uridine, adenosine, cytosine, or guanosine. Despite being a well-established technique that can record RNA modifications at a single nucleotide precision, dRNA-seq still needs to be improved in terms of accuracy and efficiency [114]. In order to map m⁶A from nanopore sequencing data, a bioinformatic technique has been developed by error calling is the basis of the algorithm. Adenosine is misidentified when m⁶A passes through a nanopore and the mismatch made it possible to estimate the m⁶A position with 87% accuracy [114].

1.4. Stemness-related m⁶A candidate biomarkers in glioma tumors

Understanding the basic principles of stem cell biology and their consequences in glioma cancer requires an understanding of target genes related to stemness [115]. Key details about the chromosomal locations, position in genome and other factors of candidate target genes are provided in Table 1.4.1. Target genes' epitranscriptome interactions with patients' clinical data and their potential as therapeutic targets analyzed by this focused investigation.

Table 1.4.1. Annotations and physical locations of 7 candidate genes.

Gene	Chromosome	Region	Strand	Annotation
<i>OS9</i>	12	3'_utr	-	<i>OS9</i> endoplasmic reticulum lectin
<i>PAGR1</i>	16	3'_utr	+	<i>PAXIP1</i> associated glutamate rich protein 1
<i>TOBI</i>	17	cds	-	Transducer of <i>ERBB2,1</i>
<i>PIK3R2</i>	18	3'_utr	+	Phosphoinositide-3-kinase regulatory subunit 2
<i>GP1BB</i>	22	3'_utr	+	Platelet glycoprotein Ib beta chain
<i>RETREG1</i>	5	3'_utr	-	Reticulophagy regulator 1
<i>LUC7L3</i>	17	3'_utr	+	<i>LUC7</i> like 3 pre-mRNA splicing factor

1.4.1. mRNA *OS9*

The effective ubiquitination of glycosylated substrates of endoplasmic reticulum-associated degradation (ERAD) depends on the *OS9*. Prior research has linked *OS9* to transcription factor turnover and ER-to-Golgi transit [116]. In human malignancies, genes involved in cellular growth control are often amplified and overexpressed. A hybrid-selection technique based on chromosome microdissection was used to identify the mRNA gene *OS9* inside the 12q13-15 region, which is commonly amplified in human cancers. Findings indicating the widespread expression of *OS9* in human tissues [117]. Typically, *OS9* is suggested as a lectin that was essential to the hypoxic stress response [118]. A protein that is highly expressed in osteosarcomas is encoded by this gene. By binding to the hypoxia-inducible factor 1 (HIF-1), a crucial regulator of angiogenesis and the hypoxic response, this protein encourages the breakdown of one of its subunits [116]. Although no comprehensive studies of the *OS9* mRNA gene have been performed in gliomas, overview shows that *OS9* mRNA could play as a key target for further study and clinical research since it is essential for maintaining cellular homeostasis, disease processes, and possible therapeutic uses.

1.4.2. mRNA *PAGRI*

The histone methyltransferase MLL2/MLL3 complex is linked to the *PAGRI* gene, *PAXIP1* associated glutamate rich protein 1, which may play a part in epigenetic transcriptional activation. It was suggested to be drawn by *PAXIP1* to DNA damage sites where, apart from the MLL2/MLL3 complex, the *PAGRI* is necessary for cell survival in response to DNA damage [119] may be significant for glioma cell survival, response to radiation therapy or treatment resistance mechanisms. In a Set1-like histone methyltransferase complex known as the PTIP complex, *PAGRI* gene was initially found to be linked to PTIP [120]. *PAGRI* gene landscape could be relevant to analyze molecular and genetic profile for diagnosis. Although there is currently little direct study on *PAGRI* in gliomas, its basic biological roles point to its relevance in the biology of gliomas. Its function in the development of gliomas and its potential as a therapeutic target require more investigation. The protein is a promising target for further glioma research because of its role in chromatin remodeling and DNA damage response.

1.4.3. mRNA *TOBI*

Transducer of *ERBB2*, 1 (or *TOBI*) suppresses tumors and has anti-proliferative qualities that may control cell division by lowering the activity of the AKT/mTOR signaling pathway [121, 122]. Studies have shown that decreased expression of *TOBI* promotes gastric cancer and related with tumor aggressiveness and poor patients' prognosis [123]. Recent research shows that malignant nature of gastric cancer cells is actively suppressed by the tumor-suppressive protein *TOBI* and inhibits the development and activation of certain immune cells. *TOBI* may increase the life span of patients with gastric cancer by promoting neutrophil anti-tumor polarization, inhibiting their apoptosis, and enhancing their receptivity to immunotherapy [124]. The morphogens including Wnt, BMP, EGF, and TGF β , function as genetic oscillators that coordinate patterning events in cancer stem cells [125]. It was discovered that the IDH-WT glioblastoma had *TOBI*, which is engaged in the EGFR and BMP signaling pathways. These results emphasize that neuro-transmission and the neuro-immune axis contribute to glioma plasticity [126]. Also, ERN1 protein kinase activity also primarily regulated the downregulation of *TOBI* gene expression. The changes in *TOBI* gene expression may also be involved in the inhibition of glioblastoma cell proliferation brought on by ERN1 knockdown [122]. Additionally, it was recently found that *TOBI* is an anti-proliferative protein that has been linked to the development and progression of cancer [127]. mRNA genes were positively associated with

immune response and the tumor microenvironment and low expression of *TOBI* associated with poor survival prognosis in LGG [128].

Through its participation in important signaling pathways and anti-proliferative activities, mRNA *TOBI* contributes significantly to the biology of gliomas. Although its fundamental molecular properties and certain functional elements have been established by current research, more study is required to completely comprehend its potential as a therapeutic target in the treatment of gliomas. The protein is an intriguing target for further study in glioma therapy because of its involvement in several cancer-related processes.

1.4.4. mRNA *PIK3R2*

Phosphoinositide-3-kinase regulatory subunit 2 (*PIK3R2*) is a widely distributed isoform that has received little attention up to this point, information from The Cancer Genome Atlas indicates that elevated expression of *PIK3R2* is also common in cancer. *PIK3R2* specifically expressed in the brain and testis of adults [129–131]. In mouse models, *PIK3R2* overexpression causes metastases, however preclinical *PIK3R2* elimination causes tumor regression and decreases invasion. This mRNA also considered as an oncogene, which suggests that increased *PIK3R2* expression induces tumor progression [132]. Tumor regression was also caused by *PIK3R2* reduction without additional PI3K pathway reactivation [133, 134]. As cancers reach more advanced stages, *PIK3R2* expression rises. Gene expression alterations should be considered when designing treatments because of the carcinogenic properties of overexpressed but not severely modified gene in cancer. The optimal treatment strategy for tumors with increased *PIK3R2* expression demands a clearer understanding of what makes *PIK3R2* a cancer driver and. It also supposed to considered in clinical management of cancer [132].

To summarize, the expression of the mRNA *PIK3R2* gene is highly expressed in many cancers and is associated with clinical prognosis and immune response of patients [135], which provides essential information in tumorigenesis.

1.4.5. mRNA *GP1BB*

Glycoprotein Ib beta chain *GP1BB* has not been consistently studied in cancer. However, there is evidence that *SEPT5-GP1BB* plays a significant role in cellular processes that may influence cancer progression [136]. Ineffective use of an imperfect polyA signal in the upstream *SEPT5* gene results in naturally occurring read-through transcription between the neighboring *SEPT5* and *GP1BB* genes on chromosome 22, where transcription

proceeds into the *GP1BB* gene [137–139]. Several read-through variations are produced via alternative splicing. It is improbable that the read-through transcripts will result in protein products because they are candidates for nonsense-mediated mRNA degradation [138]. According to Gene Expression Profiling Interactive Analysis (GEPIA), the expression of the *GP1BB* gene between GB and LGG is quite similar, but compared to healthy tissue, the expression of this gene is significantly reduced in both pathologies.

Although there is not much concrete proof connecting *GP1BB* to cancer, its involvement in platelets and thrombosis raises the possibility that it contributes significantly, yet indirectly, to the development of cancer. Its contributions to tumor biology and its potential as a therapeutic target or biomarker in cancer-associated thrombosis and metastasis require more investigation.

1.4.6. mRNA *RETREG1*

Generally considered as a tumor suppressor gene, reticulophagy regulator 1 (*RETREG1*) controls apoptosis and endoplasmic reticulum stress [140]. In some cancer types, tumor aggressiveness and a poor prognosis are associated with decreased *RETREG1* expression. *RETREG1* functions as a tumor suppressor, controlling the development and proliferation of cancer cells by modifying the endoplasmic reticulum turnover through selective autophagy [140, 141]. It was also reported that *RETREG1* has the potential to function as biomarker for pluripotent stem cells in mice and predicted to be used to identify stem cells [142]. Lack of or inability to function *RETREG1* had a role in the buildup of misfolded and aggregated proteins, which impairs proteostasis and, thus, reduces the survival of neurons [143–146]. In both in vitro and in vivo, *RETREG1* inhibits the growth of colorectal cancer [147]. Both oesophageal and colon tumors had advanced cancer stages linked to *RETREG1* expressions and mutations [148, 149]. The reticulophagy receptor *RETREG1* is the primary mediator of LOP-induced reticulophagy and cell death, indicating that ER-phagy receptors can trigger autophagic cell death [150]. Lastly, lysophagy – specific autophagy for damaged lysosomes – has been identified as a potential GB treatment target [151, 152].

1.4.7. mRNA *LUC7L3*

In A549 and HeLa cells, *LUC7L3* depletion dramatically reduced cell proliferation; this reduction was followed by an increase in apoptotic cell death. It was also demonstrated that this gene exhibits some functions associated with cell survival [153]. Additionally, *LUC7L3*, alternative splicing-associated protein considered as prognostic biomarker of hepatocellular

carcinoma (HCC). Patients with high mRNA expression had shorter survival time and higher risk of postoperative recurrence. It was proposed that the overexpression of *LUC7L3* mRNA may be intricately linked to the aggressive proliferation of HCC [154]. It was discovered that SRSF1 increases the translation of *LUC7L3*, hence positively regulating its protein levels. It is interesting to note that, like SRSF1 in protein translation, *LUC7L3* also controls the mRNA translation of genes linked to mitotic spindle assembly. Depletion of *LUC7L3* can cause genome instability [153, 155]. According to GEPIA database, better survival prognoses are found in gliomas that have significant lower *LUC7L3* gene expression.

LUC7L3 may have an indirect impact on the development of glioblastoma because of its function in RNA splicing and genomic stability. Many malignancies, including glioblastoma, exhibit dysregulation of RNA splicing, and proteins involved in splicing regulation, such as *LUC7L3*, may be involved in the biology of tumors. However, to prove a direct connection between *LUC7L3* and glioblastoma, more investigation would be required.

2. METHODS AND MATERIALS

2.1. Specimen collection and ethics

At the Department of Neurosurgery, Hospital of Lithuanian University of Health Sciences Kauno klinikos (Kaunas, Lithuania), tumor tissues from a total of 16 glioblastomas (GB) and 9 diffuse astrocytoma's (LGG) were collected between 2002 and 2020. Diagnosis of glioma was confirmed by pathologist on tumor tissues. The study was approved by the Kaunas Regional Biomedical Research Ethics Committee (P2-9/2003 and BE-2-3) and conducted in strict adherence to the declaration of Helsinki. All patients provided informed consent to participate in the research study prior to sample collection. Following surgical removal, tissue samples were snap frozen in liquid nitrogen ($-196\text{ }^{\circ}\text{C}$).

2.2. Covariate screening

Of all the considered covariates the screening criteria was met by age, sex, tumor location and size, Ki-67, MGMT, subtype and survival time (in days). These variables were included in the of all subsequent analyses. Details of glioma patients' clinical characteristics data outlined in the table below (Table 2.2.1).

Table 2.2.1. Glioma patients' clinical characteristics

		Glioblastoma (GB) (n = 17)	Low-grade glioma (LGG) (n = 9)
Age*, years	Median (range)	67 (50–85)	33 (24–71)
Sex	n (F, M)	17 (10, 7)	9 (6, 3)
Survival (in days)**	Median (range)	290 (32–2215)	3093 (1192–3829)
Location	n (temporal, frontal, parietal, occipital, fronto-temporal, cerebellum)	17 (9, 3, 2, 2, –, 1)	9 (2, 3, –, –, 2, 2)
Size, cm ³	Median (range)	50.43 (7.3–293.18)	116.64 (38.53–171)
Ki-67**	n (low, high)	17 (3, 14)	9 (9, –)
MGMT	n (M, U)	17 (8, 9)	9 (6, 3)
IDH1**	n (mut, wild)	17 (–, 17)	9 (8, 1)
Subtype	n (classical, proneural, mesenchymal)	17 (9, 4, 4)	–

*Indicates significant difference ($p < 0.01$) between cohorts in this variable; ** Indicates significant difference ($p < 0.001$) between cohorts in this variable.

Patients who were still alive at the end of the study were censored in the Kaplan Meier survival analysis.

2.3. Reagents, barcodes, reagent suppliers and catalogue numbers

Reagents used in the thesis are shown on Table 2.3.1. Sequences of barcodes used for direct RNA sequencing are shown on Table 2.3.2.

Table 2.3.1. List of reagents and kits, reagent suppliers and catalogue numbers

Name	Supplier	Catalogue number
DMEM/Ham F-12 media	Sigma-Aldrich	D8437
100 IU/mL of penicillin, 100 µg/mL of streptomycin	Gibco	15140122
Fetal bovine albumin fraction V (FBS)	Gibco	15260037
1 × minimum essential media	Gibco	11140035
D-Glucose solution	Sigma-Aldrich	G8644
B-27 supplement	Gibco	17504044
N-2 supplement	Gibco	17502048
bFGF supplement	Gibco	PHG0261
EGF supplement	Gibco	PHG0311
DMEM, high glucose media	Gibco Thermo Scientific™	10566016 61965059
Fetal bovine serum	Gibco	10500064
DMEM/F12 media	Thermo Scientific™	10565018
NeuroCult basal media	STEMCELL Technologies	05750
NeuroCult supplement	STEMCELL Technologies	05711
Antibiotic/antimycotic solution	Wisent	450-115-EL
Heparin	STEMCELL Technologies	07980
rhEGF	STEMCELL Technologies	78006
rhFGF	STEMCELL Technologies	78003.2
TRIzol	Invitrogen	15596026
Agilent RNA 6000 Pico kit	Agilent	5067-1513
Dynabeads mRNA DIRECT kit	Invitrogen	61012
Glycogen	Thermo Scientific™	R0551
Pure ethanol (96%)	Vilniaus degtinė	P075
RNase/DNase-free water	Invitrogen	10977-035

Table 2.3.1. Continued

Name	Supplier	Catalogue number
m ⁶ A antibody	Synaptic Systems	202-003
Magna MeRIP m ⁶ A kit	Sigma-Aldrich	1710499
Pierce Protein A/G Magnetic Beads	Thermo Scientific™	88803
SUPERase-In RNase inhibitor	Invitrogen	AM2694
m ⁶ A salt	Sigma-Aldrich	M2780
TRIS-HCl	ROTH	9090.2
Igepal	Sigma-Aldrich	13423
RVC	Sigma-Aldrich	18896
RNA sequencing kit	ONT	SQK-RNA002
Qubit fluorometer DNA HS assay	Invitrogen	Q32851
MinION flow cells	ONT	R9.4.1
EpiQuik m ⁶ A RNA Methylation Quantification kit (Colorimetric)	EpigenTek group	P-9005
DNase I	Thermo Scientific™	EN0521
High-Capacity cDNA Reverse Transcription Kit	Thermo Scientific™	4368814
Power SYBR Green PCR Master Mix	Applied Biosystems	4367659

Table 2.3.2. List of ONT barcodes for dRNA-seq

Oligo name	Barcode name	Sequence (5'-/5Phos-/3')
<i>Oligo A1</i>	BC1	CCTCCCCTAAAAACGAGCCGCATTTGCGTAGTAGGTTTC
<i>Oligo A2</i>	BC2	GAGGCGAGCGGTCAATTTTCGCAAATGCGGCTCGTTTTT AGGGGAGGTTTTTTTTTTT
<i>Oligo B1</i>	BC3	CCTCGTTCGGTTCTAGGCATCGCGTATGCTAGTAGGTTTC
<i>Oligo B2</i>	BC4	GAGGCGAGCGGTCAATTTTGCATACGCGATGCCTAGAAC CGACGAGGTTTTTTTTTTT

2.4. Human cell lines

Glioblastoma stem-like cell line NCH421k (CLS Cell Lines Service GmbH, Eppelheim, Germany, cat. no. 300118) (generously donated by dr. A. Jekabsone) was grown as spheroid suspension in DMEM/Ham F-12 media, supplemented with 100 IU/mL of penicillin, 100 µg/mL of streptomycin, 0.12% fetal bovine albumin fraction V (FBS), 1 × Minimum essential media, 0.8 g/L D-Glucose solution, 0.5 × B-27, 0.5 × N-2, 20 ng/mL bFGF and

EGF. Cell lines were incubated at 37 °C in a humidified atmosphere containing 5% CO₂. Only mycoplasma-free cells were used for all the study's experiments.

The European Collection of Cell Cultures were acquired glioblastoma (U87-MG) (ECACC, cat. no. 89081402) cells, which were grown in high glucose DMEM solution media supplemented with 10% FBS, 100 IU/mL of penicillin, 100 µg/mL of streptomycin.

2.5. RNA extraction and polyA RNA enrichment

This study consisted of different sample groups: 1) LGG, 2) GB, 3) GSCs (NCH421k), 4) U87-MG. Details of each sample group outlined in the table below (Table 2.5.1). Total RNA from the homogenized snap-frozen tissues and cell lines were extracted through TRIzol following the manufacturer's instructions. The quality of isolated RNA was determined using Agilent 2000 Bioanalyzer with “*Agilent RNA 6000 Pico kit*”. The total RNA was stored at – 80 °C until polyA RNA enrichment.

Table 2.5.1. Number of samples in each group

Sample type	GB	LGG	GSC	U87-MG
n	17	9	5	3

GB – glioblastoma; LGG – low-grade glioma; GSC – glioma stem cells (NCH421k).

The “*Dynabeads mRNA DIRECT kit*” was used for the polyA enrichment of 40–180 µg total RNA according to the manufacturer's instructions. Magnetic beads were resuspended in the sample lysate and total RNA was added to allow the polyA tail to hybridize to the oligo (dT)₂₅ on the beads. The complex of the beads/mRNA was washed and eluted. PolyA enriched RNA was precipitated overnight at –80 °C in a precipitation buffer with 100 µg/mL of glycogen and pure 100% ethanol. Precipitated RNA was resuspended in RNase/DNase-free water and analyzed by Agilent 2100 Bioanalyzer and NanoDrop™ 2000 (Thermofisher Scientific).

2.6. Enzyme-linked immunosorbent assay (ELISA)

ELISA was performed to analyze the total polyA RNA m⁶A modification in patient samples according to the manufacturer protocol. The study included 17 samples from GB patients and 9 samples from LGG glioma patients, providing insights into the m⁶A modification patterns in different tumor samples. After total RNA extraction and polyA enrichment, RNA binds to the assays well. Wells were washed multiple times and the capture m⁶A

antibody was added. Wells were washed again, then added detection antibody and enhancer solution. Finally, added color developing solution for color development and measured absorbance. m⁶A standard control was added into the assay wells at different concentrations and then measured. To determine the relative m⁶A RNA methylation status of RNA samples, a calculation for the percentage of m⁶A were calculated using the following formula:

$$m^6A\% = \frac{(\text{Sample OD} - \text{NC OD}) \div S}{(\text{PC OD} - \text{NC OD}) \div P} \times 100\%$$

where: S is the amount of input sample RNA in ng;

P is the amount of input positive control (PC) in ng.

2.7. N6-methyladenine immunoprecipitation (MeRIP-seq) by next-generation sequencing

Before m⁶A immunoprecipitation, polyA RNA was fragmented into 100 nt length fragments. 18 µg of polyA RNA in 20 µL of total volume with 10 × fragmentation buffer (H₂O, TRIS-HCl, pH 7.0; ZnCl₂), in a thermal cycler (Applied Biosystems) set to 94 °C for three minutes. The effectiveness of polyA RNA fragmentation was assessed using an Agilent Bioanalyzer and a 1.5% agarose gel. According to the Dominissini [10] and Meyer [108] group's "*Magna MeRIP m⁶A kit*" protocols, m⁶A immunoprecipitation (MeRIP) was performed. Five µg of m⁶A antibody and 0.125 mg of Pierce Protein A/G Magnetic Beads were combined in 500 µL IP buffer (50 mM Tris-HCl pH 7.5, 150 mM NaCl, 0.1% (vol/vol) Igepal) for six hours at 4 °C. After, the bead-antibody complex twice washed for ten minutes using 1 mL of IP buffer. The mixture of 5 µg of fragmented polyA RNA and 500 µL of IP buffer (with 0.3 U/µL SUPERase-In RNase inhibitor and 2 mM RVC), was set on a bead-antibody complex and incubated for the entire night at 4 °C. Two 10-minute washes of the mixture were performed using 1 mL IP buffer (supplemented with 0.1 U/µL SUPERase-In RNase inhibitor) and 1 mL high salt buffer (50 mM Tris-HCl pH 7.5, 300 mM NaCl, 0.1% (vol/vol) Igepal, and 0.1 U/µL SUPERase-In RNase inhibitor). 100 µL of elution buffer (enriched with m⁶A salt at 6.7 mM) was applied twice to the bead-antibody-RNA complex for one hour at 4 °C. RNA was collected using an overnight ethanol precipitation method at -80 °C using 2.5 vol of 100% ethanol and 1/10 volume of 3 M sodium acetate (pH 5.2).

2.8. MeRIP-seq m⁶A peak calling

Sequencing reads were processed using “MeRIPseqPipe” pipeline v3.1 [156] run within container through Nextflow and Docker container support and contained all of the third-party tools [157]. Briefly, quality control and preprocessing of raw data were evaluated with FastQC. Reads were aligned against Ensembl’s GRCh38 reference genome using SAMtools v1.15.1 [158] and STAR v2.1.3 [159]. Eventually, the peaks and m⁶A enrichment were called with MATK [160] providing input samples as a control. All the computational analysis were performed on the GenomeDK cluster.

Following a quality control of all sequenced samples, the third U87-MG replicate was identified as a severe outlier, therefore, this sample was eliminated from the downstream analysis.

2.8.1. Differential gene expression and methylation of MeRIP-seq

Finally, differential methylation analysis was processed using QNB (Quantile-based Negative Binomial) [161], a statistical approach for differential RNA methylation analysis with count-based sample sequencing data, and widely used package DESeq2 [162], for MeRIP-seq data. Differential expression analysis was performed using featureCounts [163] – a software for quantification of gene expression in MeRIP-seq analysis.

2.9. Direct RNA library preparation and MinION sequencing (dRNA-seq) by Oxford Nanopore Technologies (ONT)

2.9.1. dRNA-seq sequencing library preparation

The RNA sequencing kit was used to generate the sequencing libraries for dRNA-seq. For each sequencing library, 500–1000 ng of enriched polyA were used as input following manufacturer’s protocols (*ver. DRS_9080_v2_revO_14Aug2019* and *DRS_9195_v4_revD_20Sep2023*). There were some modifications in the protocol, and we used Hyeshek Chang [164] and Smith et al. [165] recommendations to devise a barcoded reverse transcription adapter (RTA) to replace the previous RTA, which was the only modification made to this protocol. Except for two patient samples, which were grouped together, all patients’ samples were separated into groups of four. Assess the yield of the library preparation using the Qubit fluorometer DNA HS assay. The remaining eluate was used as dRNA-seq input and loaded into MinION mk1B and mk1C flow cells.

2.9.2. ONT MinION flow cell loading and sequencing

All the sequencing experiments in this thesis used MinION flow cells (R9.4.1). The MinION sequencer was used to insert flow cells and evaluate the number of accessible pores before the sequencing runs. Prior to the start of each sequencing run, MinION flow cells with a minimum of 1100 accessible pores were used (sequencing library volume – 15 μ L, samples concentration range – 108.3–147.2 ng/ μ L). All prepared sequencing libraries loaded into the flow cell through spot on port. Sequencing runs were started and lasted for 72 h each.

2.9.3. Mapping of sequencing data

Sequencing reads generated with a minimum read quality score of 6 were used for mapping and downstream analysis. Using ONT’s Guppy software v5.0.11, Fast5 files were base-called with high accuracy mode by applying a dRNA-seq configuration file (“rna_r9.4.1_70bps_hac.cfg”). To extract fastq files for every barcoded sample, fast5 files were processed using Poreplex software v0.5. Next, resulting FASTQ files generated from sequencing runs aligned to human genome (Ensembl release 105, Genome assembly version: GRCh38) [166] using minimap2 v2.17-r941 [167], and SAMtools [168]. Aligned reads were sorted, merged, and indexed to BAM files with SAMtools.

2.9.4. Differential gene expression and methylation of dRNA-seq

Epinano v1.2.0 [169] was used for identification of m⁶A modifications within RRACH motifs. For gene expression quantification, genome-aligned dRNA-seq reads were processed with featureCounts v2.0.1 [170], using Ensembl gene annotation (release 105) with strand-specific and long-read settings enabled. Methylation counts were normalized and identified as differentially methylated genes ($p < 0.05$ and \log_2 Fold Change > 1) using DESeq2. P values were adjusted by the Benjamini-Hochberg method.

2.10. Quantitative RT-PCR

mRNA level estimation of stemness genes was performed using quantitative real-time reverse transcription PCR (RT-qPCR) on 7500 Fast Real-time PCR detection system (Applied Biosystems). Relative quantification model ($2^{-\Delta\Delta CT}$) was utilized to assess stemness gene expression in NCH421k and U87-MG cell lines. Total RNA was extracted and treated with DNase I to remove any remaining DNA contamination. Copy-deoxyribonucleic acid (cDNA) was synthesized by High-Capacity cDNA Reverse

Transcription Kit. The mRNA expression of stemness genes *SOX2*, *POU5F1*, *MYC*, *PROM1*, *KLF4*, *NANOG*, *GFAP* and housekeeping gene *ACTB* was evaluated. The reaction volume was 12 μ L, with 6 μ L of “Power SYBR Green PCR Master Mix”, 15 ng of each cDNA sample, 0.2 μ M of each primer, and nuclease-free water. Primer sequences showed in Table 2.10.1.

Table 2.10.1. Primers for RT-qPCR

Gene name	Forward, 5'–3'	Reverse, 5'–3'	Amplicon size, bp
<i>SOX2</i>	TGCCTTCATGGTGTGGTC	TTGCTGATCTCCGAGTTGTG	81
<i>POU5F1</i>	AGTGAGAGGCCAACCTGGA	CTCGGACCACATCCTTCTC	104
<i>MYC</i>	CTACCCTCTCAACGACAGC	CTTCTTGTTCCCTCCTCAGA GTC	185
<i>PROM1</i>	TGGATGCAGAACTTGACA ACG	ATACCTGCTACGACAGTC GTG	133
<i>KLF4</i>	CATTACCAAGAGCTCATG CCA	AATTTCCATCCACAGCCGT	221
<i>NANOG</i>	CAGCTACAAACAGGTGAA GAC	TGGTAGGAAGAGTAAAG GCT	144
<i>GFAP</i>	ACCTGCAGATTCGAGAA ACC	CTCCTTAATGACCTCTCCA TCC	113
<i>ACTB</i>	AGAGCTACGAGCTGCCT GAC	AGCACTGTGTTGGCGTA CAG	184

2.11. Silhouette Plot

Silhouette Plot was used for a graphical representation of glioma patients' data consistency and allowed to visually analyze clusters quality using data visualization toolkit “Orange Data Mining” v3.32 [173]. Silhouette score measurement showed how similar an object is to its own cluster when compared to other clusters. Silhouette score around 1 suggested that the data instance is close to the clusters' center, whereas a silhouette score near 0 indicates that the data instance is on the boundary between two clusters.

2.12. m⁶A methylation and stemness score calculations

m⁶A methylation score calculation was performed to aggregate statistical significance of m⁶A modifications across all patients' samples and target RRACH motifs, which aligns with the concept of quantifying m⁶A methylation levels.

$$m^6A \text{ score} = \sum (\chi^2_i \times m^6A \text{ status})$$

where: χ^2_i represented chi-square value of the target RRACH;
m⁶A status – 1 if target RRACH was modified and 0 if target RRACH was unmodified in the patient sample

The single-sample extension of Gene Set Enrichment Analysis (ssGSEA) was used to calculate stemness score across all patients' samples using toolkit "Orange Data Mining". Scores were calculated for gene sets based on individual sample gene expression levels through incorporating the contributions of genes ranked in an ordered expression matrix, with high expression values positively influencing the score.

2.13. Random forest algorithm (Alluvial plot)

The Random Forest algorithm was utilized to visualize the relationships significant clinical characteristics (age, tumor size, tumor location) and total m⁶A methylation score in glioma patients. Alluvial plot was used to illustrate random forest algorithm analysis. The axes were shown as ribbons that change in width and this reflected the movement of patients from one clinical characteristic to another. The size of bands showed patient samples moving, thereby determined the most important connections and trends.

2.14. Nomogram analysis

Nomogram was used for manually obtaining predictions from a regression model using *rms* package v8.0-8. The nomogram had a reference line for reading scoring points (default range 0–100). Total points were added, and the predicted results found at the bottom of the nomogram. The total point for the nomogram consisted of the sum of patients' age, sex, MGMT status, tumor location, tumor size, Ki-67 status, stemness and m⁶A methylation score, and the higher total point predicted the risk score of death. Lengths of the lines in the nomogram corresponded to spans of odds ratios, suggesting importance of clinical characteristics.

2.15. Pathway enrichment analysis

Kyoto Encyclopedia of Genes and Genomes (KEGG) databases were used for functional enrichment analysis of differentially expressed genes from dRNA-seq using *clusterProfiler* v4.4.4 [174]. Parameters used for KEGG enrichment were as follows: Permutations (nPerm): 10000, minimum gene set size (minGSSize): 3, maximum gene set size (maxGSSize) = 1000,

minimum p (p-valueCutoff) = 0.05, organism (Orgdb) = org.Hs.eg.db, pAdjustMethod = Benjamini-Hochberg (BH). Graphs were plotted using ggplot2 (v3.3.6, R-ver. 4.3.3).

2.16. Statistical analysis

All statistical analyses were conducted with R Programming language v4.3.3 [171], GraphPad Prism v6.01 [172] and data visualization toolkit “Orange Data Mining”. Kaplan–Meier survival curves were used to assess patient survival, and statistical differences between groups were evaluated using the log-rank test. Cox proportional hazards regression was applied to estimate hazard ratios and assess the impact of covariates on survival outcomes. The relationship between RRACH motifs, and the probability of the values being modified was used logistic regression model. Pearson correlation was used to evaluate m⁶A methylation level of RRACH motifs and their presence across different glioma patient samples and investigate relationship between stemness-related genes and our selected m⁶A-modified target genes in clusters C1 and C2. Correlation coefficient of $r \geq 0.85$ indicated strong correlation, $r \leq 0.2$ denoted a weak correlation, $r = 0$ reflected no correlation between gene expression levels. Linear regression analysis was utilized for continuous patients clinical characteristics such age, tumor size, and survival time, whereas the Chi-square (χ^2) test was used for MGMT methylation, tumor location, and Ki-67 gene status to evaluate relationship within patient samples. Forest plot for Cox proportional hazards model of target mRNAs expression was performed using *ggforest* package v0.1.0. Differences in all statistical tests were considered significant at * $p < 0.05$, ** $p < 0.01$, *** $p < 0.001$.

3. RESULTS

3.1. The composition of RNA profile from m⁶A epitranscriptome aligned MeRIP-seq in glioblastoma U87-MG and glioma stem cell NCH421k lines

To begin with, we focused on the NCH421k stem cells and U87-MG glioblastoma cell lines, which were utilized for methylated RNA immunoprecipitation sequencing (MeRIP-seq) analysis (Fig. 3.1.1 A, B). RT-qPCR was used to measure the gene expression levels of *SOX2*, *POU5F1*, *MYC*, *PROM1*, *KLF4*, *NANOG*, and *GFAP* in order to confirm stemness. Notably, in our analysis, NCH421k cells exhibited significantly higher expression levels of these stemness-associated genes compared to U87-MG cells (Fig. 3.1.1 C) (see publication “Transcriptome-wide analysis of glioma stem cell specific m6A modifications in long-non-coding RNAs”).

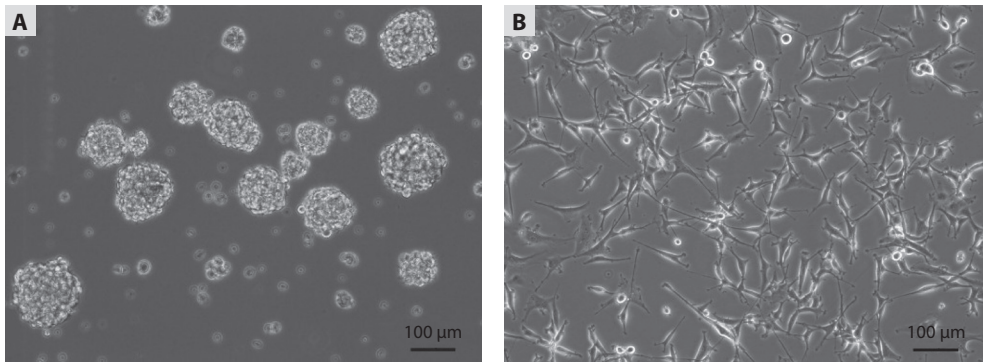


Fig. 3.1.1 (A–B). Phase contrast images of cell cultures used for MeRIP-seq analysis and stemness gene expression

(A) Represents NCH421k stem cells, and (B) glioblastoma U87-MG cell line.

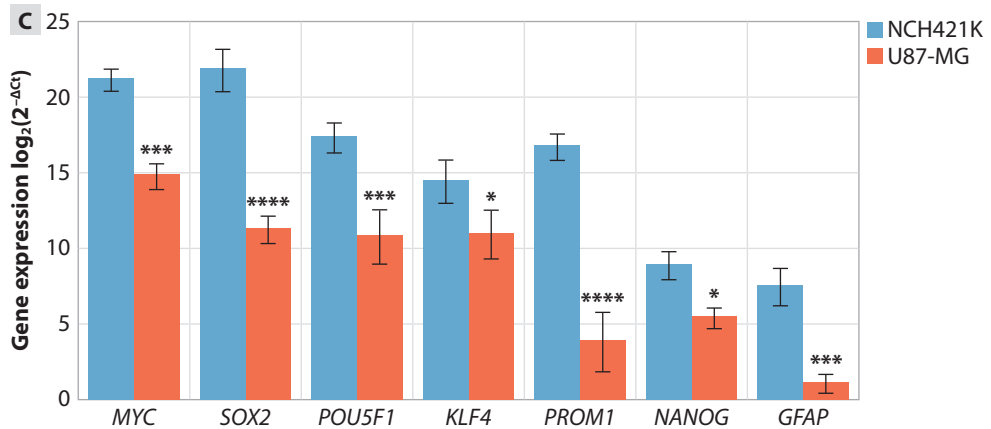


Fig. 3.1.1 (C). Phase contrast images of cell cultures used for MeRIP-seq analysis and stemness gene expression

(C) Stemness gene expression in NCH421K cells as compared to U87-MG cells. Data are presented as means \pm SD. Statistical method: two-way ANOVA followed by Bonferroni's multiple comparisons test. * $p < 0.05$, *** $p < 0.001$, **** $p < 0.0001$.

The epitranscriptome profiles of the many cell types that make up tumor tissues vary greatly [175]. The RNA biotypes (Ensemble) of distinct genes from glioma tumors and cell lines that were identified by MeRIP-seq and dRNA-seq were subjected to bioinformatic analysis in order to assess the capacity of read sequencing to capture m⁶A epitranscriptome diversity utilizing polyA enriched RNA isolated from snap frozen tumor tissue samples and cell lines.

First, pie charts were generated to illustrate the m⁶A modified RNA biotype profile of genes detected by reference genome-aligned MeRIP-seq reads from each sample group and the profile between U87-MG and NCH421k cell lines (Fig. 3.1.2). The majority of identified genes in MeRIP-seq are classified as protein-coding (94.4%), followed by lncRNA (4.2%), transcribed processed pseudogenes (0.2%), transcribed unprocessed pseudogenes (0.7%), transcribed unitary pseudogenes (0.2%), TEC (0.1%) and others (0.2%) (Fig. 3.1.2 A). There were identified 8345 unique genes. RNA biotype profiles were highly similar between samples groups. Sequencing reads from U87-MG cells identified genes belonging to the following biotypes: protein-coding (89.9%), lncRNA (4.4%), transcribed processed pseudogenes (0.2%), transcribed unprocessed pseudogenes (0.7%), transcribed unitary pseudogenes (0.2%), TEC (0.1%) and others (4.5%) (Fig. 3.1.2 B) while NCH421k samples' reads were allocated 89.3% of protein-coding, 4.8% of lncRNA, processed pseudogenes – 0.2%, 0.3% of transcribed processed pseudogenes, 0.2 of transcribed unitary pseudogenes and 0.8% of

transcribed unprocessed pseudogenes, 4.3% – others (Fig 3.1.2 C). The total number of unique genes identified 15444.

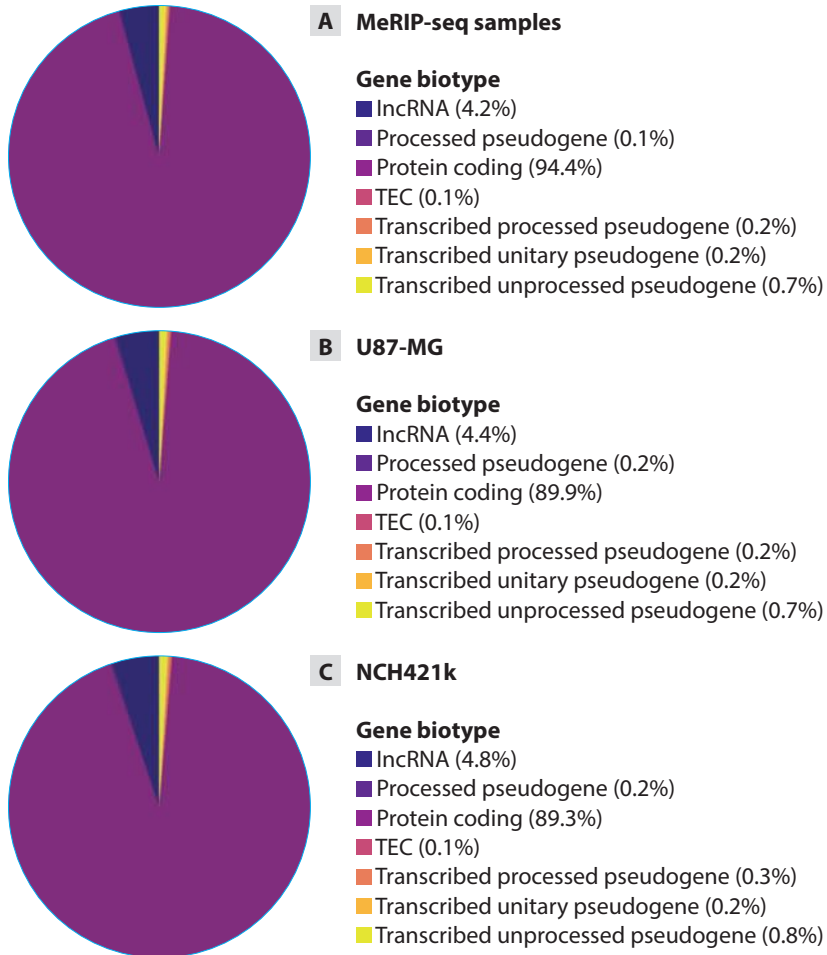


Fig. 3.1.2. RNA biotype composition of gliomas by m^6A epitranscriptome by MeRIP-seq

(A) Pie chart depicting the distributions of gene biotypes of m^6A epitranscriptome in U87-MG and NCH421k samples, (B) U87-MG, (C) NCH421k samples.

In total of 33 986 modified peaks were found among both U87-MG and NCH421k. Notably, cell lines shared 25 964 peaks while 6579 peaks were exclusive to the NCH421k, and 1443 peaks were unique to U87-MG (Fig. 3.1.3 A). Additionally, the distribution of modified sites revealed that 43.1% were located in the 5' region followed by the 3' area (21.4%) and CDS site (21.4%) and others (14.1%) (Fig. 3.1.3 B).

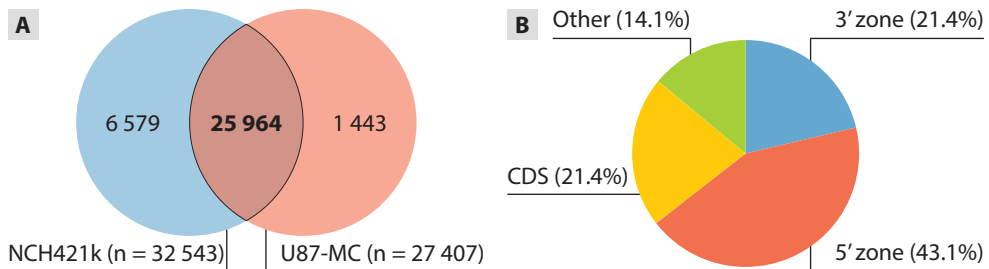


Fig. 3.1.3. *Distribution of MeRIP-seq data*

(A) Venn-diagram of detected cell line specific and common m⁶A peaks after MeRIP-seq, (B) pie chart of the percentage of detected m⁶A peaks in mRNA transcripts by peak localization.

3.2. The composition of RNA profile from m⁶A epitranscriptome aligned dRNA-seq in glioma patient samples

For dRNA-seq pie charts were generated to illustrate the RNA biotype profile of genes detected of m⁶A modification data in glioma patient samples (Fig. 3.2.1). The majority of identified genes in dRNA-seq are classified as protein-coding (96%), followed by rRNA (0.1%), lncRNA (2.9%), processed pseudogenes (0.1%), transcribed processed pseudogenes (0.1%), transcribed unprocessed pseudogenes (0.6%) and transcribed unitary pseudogenes (0.1%). The total number of unique genes identified 10319.

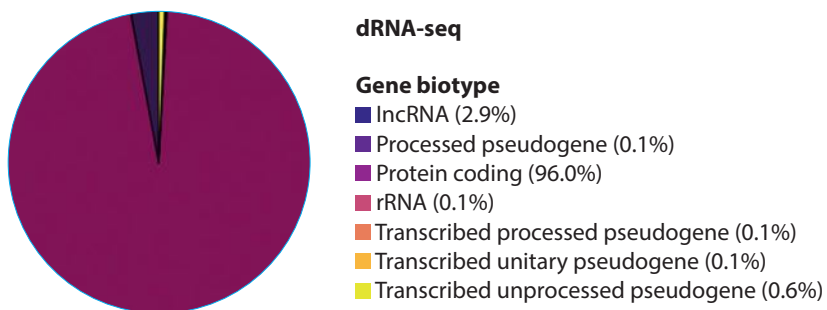


Fig. 3.2.1. *RNA biotype composition of gliomas by epitranscriptome in dRNA-seq*

Pie chart depicting the average of gene biotypes of epitranscriptome in dRNA-seq samples.

In total of 437 839 modified transcripts were found among both GB and LGG. Notably, cell lines shared 185 744 peaks while 239 797 transcripts were exclusive to the GB and 12 298 transcripts were unique to LGG (Fig. 3.2.2 A). Also, the distribution of modified sites revealed that 1.3% were in the 5' region followed by the 3' area (56%) and CDS zone (31%) and others (1.3%) (Fig. 3.2.2 B).

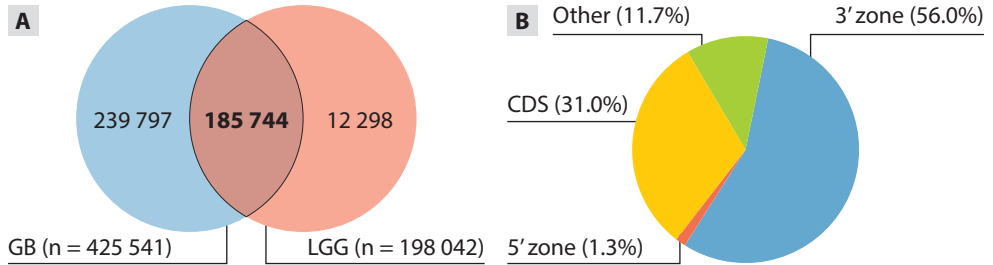


Fig. 3.2.2. Distribution of dRNA-seq RRACH motifs data in glioma patients

(A) Venn-diagram of detected patients specific and common m⁶A transcripts after dRNA-seq, (B) pie chart of the percentage of detected m⁶A transcripts by localization.

In our analysis of LGG patient samples using Nanopore dRNA-seq, we observed a significantly higher m⁶A methylation status across all RRACHs ($p < 0.05$) compared to GB patient samples (Fig. 3.2.3 A). The elevated m⁶A methylation in LGG samples highlight the potential of m⁶A as a biomarker. To validate total m⁶A methylation in glioma samples, we conducted an ELISA method specifically targeting the total m⁶A modification levels in glioma patients polyA RNA. According to the total m⁶A modification assessed by ELISA, it was confirmed that LGG samples exhibit significantly higher m⁶A modification levels compared to GB samples ($p = 0.0049$) (Fig. 3.2.3 B). The average m⁶A methylation in GB samples was found to be 4.55%, while LGG samples demonstrated an average of 12.5%, indicating that LGG has nearly three times higher m⁶A modification levels.

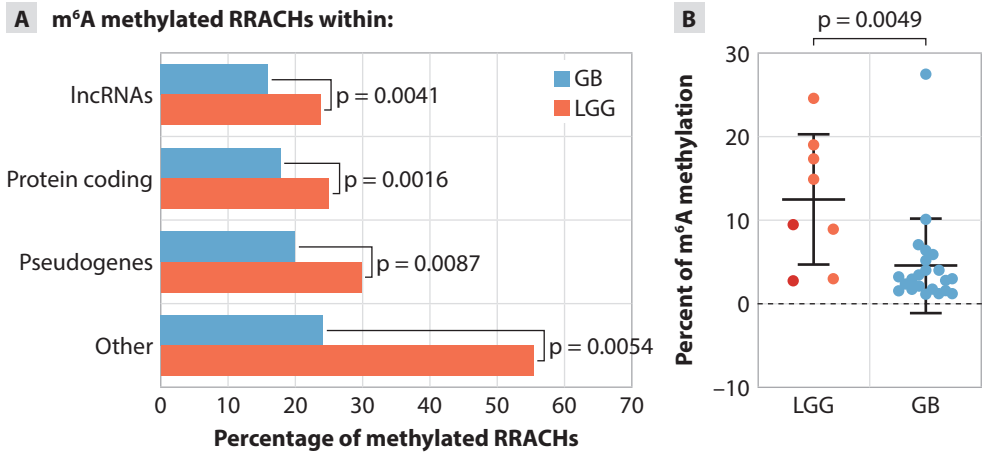


Fig. 3.2.3. Comparison of total m⁶A modification percentages in GB and LGG patient samples

(A) Total polyA RNA m⁶A methylated RRACHs in dRNA-seq by RNA biotype, (B) polyA RNA m⁶A methylation by ELISA.

3.3. Protein-coding RNA m⁶A modification target selection via MeRIP-Seq and dRNA-seq data

3.3.1. Target selection in mRNA in MeRIP-seq data

Two sample groups were sequenced to investigate the most promising diagnostic mRNAs. Sequencing was done from glioblastoma cell line U87-MG and glioma stem cells NCH421k. To find the differentially modified genes between the NCH421k and U87-MG cell lines, we performed a DESeq2 analysis with the reference group set as U87-MG cells. Results of differential gene expression analysis between samples were plotted as volcano plot in Fig. 3.3.1.1. A total of 1570 distinct differentially modified genes were found using a criterion of \log_2 Fold Change (\log_2 FC) > 1 and $p < 0.05$. Of these, 740 genes were hypermethylated, and 830 genes were hypomethylated in NCH421k compared to U87-MG. Our goal was to further refine and identify the most significant genes from this dataset that may be useful indicators linked to gliomas. In order to provide vital information for glioma research and treatment plans, these genes were ranked and examined according to their significance and biological relevance in glioma progression which may serve as diagnostic, and therapeutic targets.

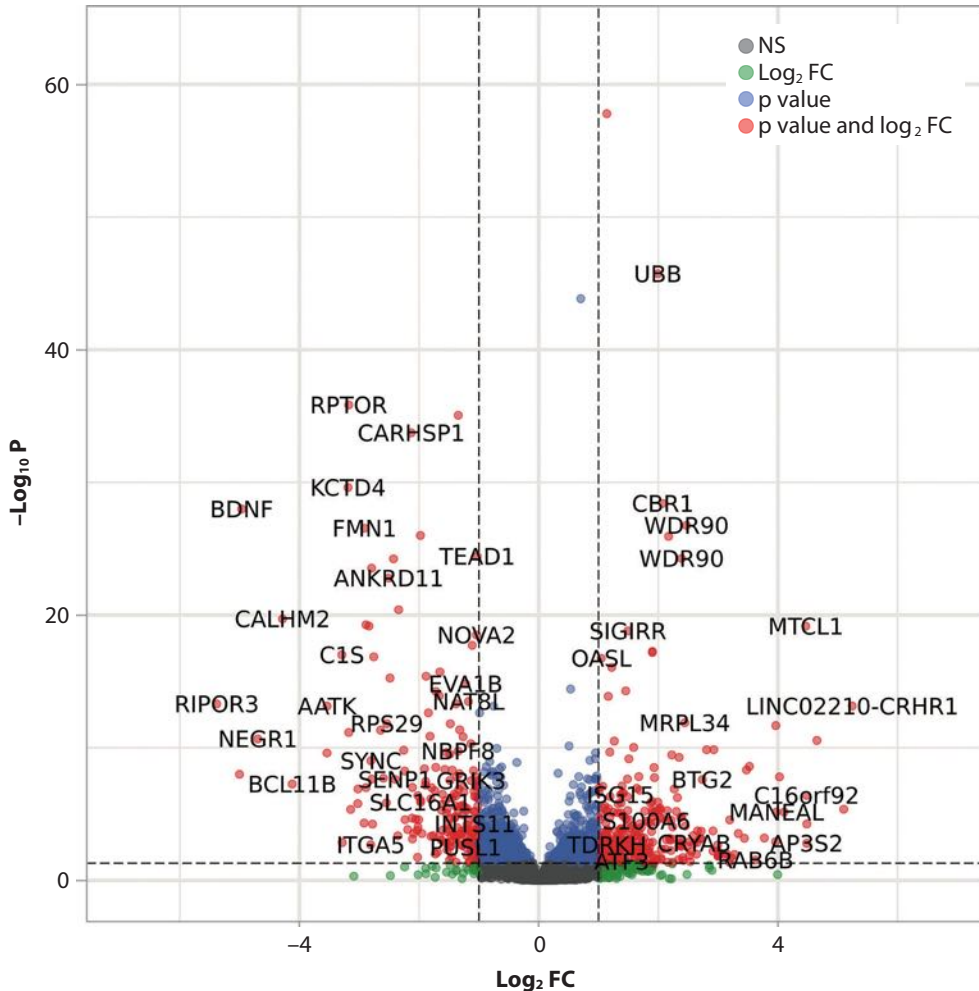


Fig 3.3.1.1. Differences between U87-MG and NCH421k cell lines epitranscriptome via MeRIP-seq (total 14 049 variables)

Volcano plot of differentially modified mRNAs between different sample groups. Horizontal dashed line shows p threshold while vertical $-\log_2$ FC threshold. Red dots color indicates significant modified peaks by p and \log_2 FC thresholds, green – \log_2 FC, blue – p value, and grey – not significant peaks. FC – Fold Change.

To illustrate the relationship between m⁶A methylation and gene expression levels, we produced a four-quadrant plot to show the distribution of differentially expressed mRNAs with statistically significant m⁶A modifications. We applied the same thresholds as DESeq2 analysis \log_2 FC > 1 and $p < 0.05$. In total of 1804 significant unique genes used for four-quadrant analysis, 77 were hypo-methylated downregulated genes, 65 hypo-methylated upregulated genes, 157 hyper-methylated downregulated genes, and

41 hyper-methylated upregulated genes (Fig. 3.3.1.2) were found as a result of the investigation.

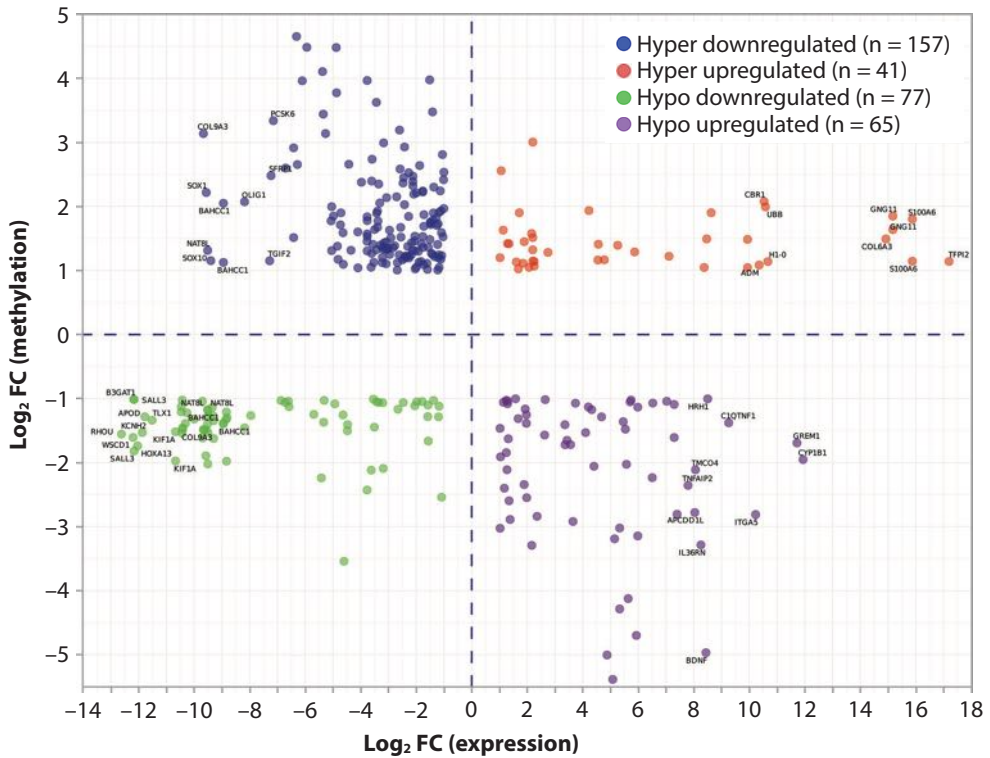


Fig. 3.3.1.2. The four-quadrant plot shows the distribution of differentially expressed statistically reliable mRNAs with m^6A modifications

Red dots color indicates significant hyper modified upregulated genes by p value and log₂ FC thresholds, green – hypo modified downregulated genes, blue – hyper modified downregulated, and purple – hypo methylated upregulated genes. FC – Fold Change.

Since we are focusing on m^6A modifications we decided to examine the hyper-methylated genes (both upregulated and downregulated) in more detail. These genes are interesting because they may reveal new information about the regulation of m^6A methylation and how this may affect gene expression.

3.3.2. Selection of m⁶A-modified mRNA targets in glioma patients dRNA-sequencing data

Glioblastoma (GB) and lower-grade glioma (LGG) patient data from dRNA-seq were referenced with the distinct genes found by MeRIP-seq analysis, which showed m⁶A-modified transcripts. We were able to confirm and examine these genes in relation to patient samples using the dRNA-seq data. Since RRACH motifs, a consensus sequence for m⁶A sites, were where m⁶A modifications are most common, we concentrated our subsequent research on genes that contain these motifs in the patient datasets. We aim to uncover glioma-associated genes with m⁶A modifications by combining the MeRIP-seq and dRNA-seq data, which will help us better understand their possible functions as biomarkers or therapeutic targets in the progression of gliomas. Without using any thresholds, our examination of the dRNA-seq data showed that, across all patients' samples, there were 4340 RRACH motifs linked to hyper-methylated upregulated genes and 9106 RRACH motifs linked to hyper-methylated downregulated genes. We decided to concentrate on the RRACH motifs seen in more than 13 of the 26 patient samples in order to further narrow down our selection. As a result, 569 RRACH motifs linked to hyper-methylated upregulated genes and 988 RRACH motifs linked to hyper-methylated downregulated genes were identified. To find statistically significant RRACH motifs in the hyper-methylated upregulated and hyper-methylated downregulated sites from patients' data we used a logistic regression model. This model found the relationship between RRACH motif, and the probability of the values being modified as well as the output will be interpreted as significant modified RRACHs in glioma patient sample set. Additionally, we were able to assess the Pearson correlation between the methylation level of RRACH motifs and their presence across different patient samples by using this statistical method. We found 212 statistically significant RRACH motifs with this approach. Fig. 3.3.2.1 shows the results in the heat map, which illustrates the arrangement of the RRACH motifs in glioma patients.

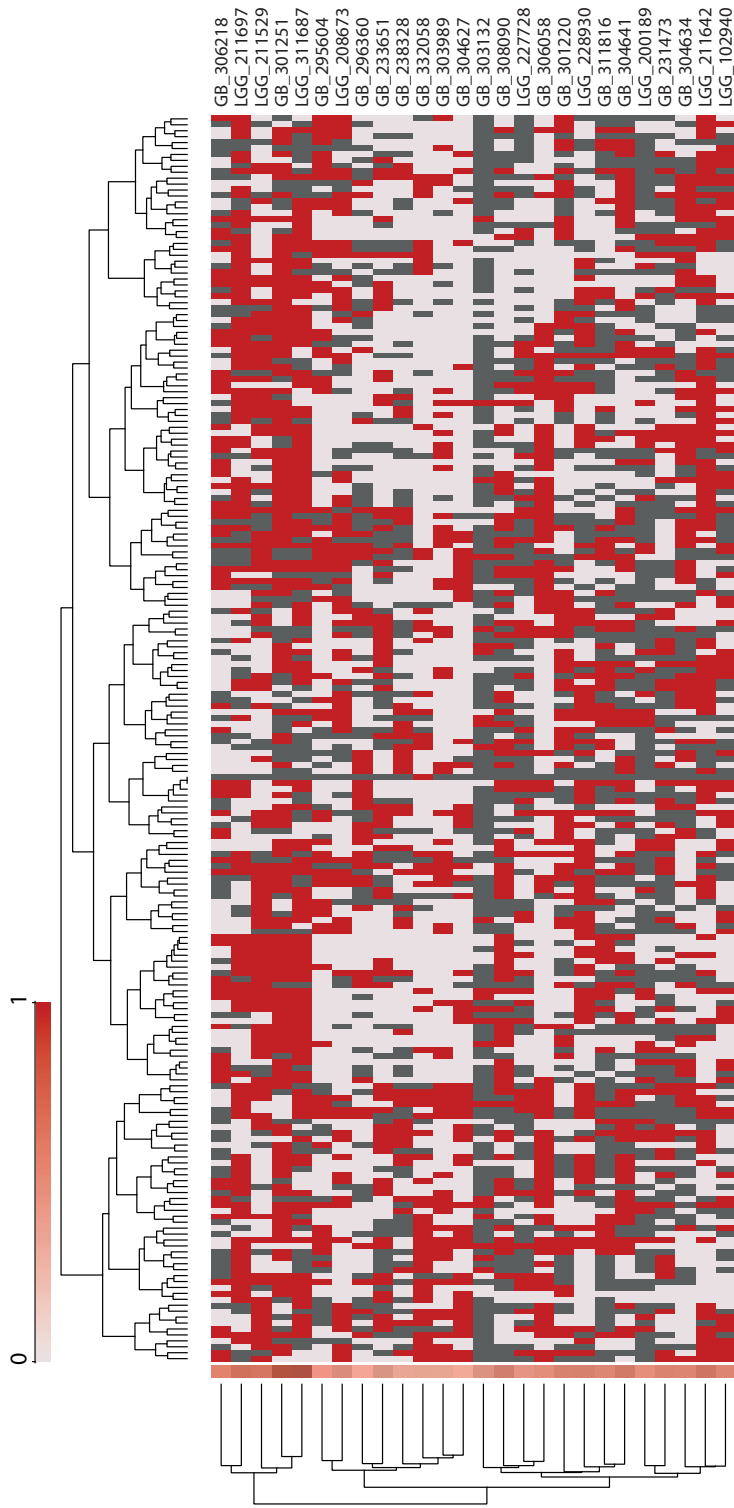


Fig. 3.3.2.1. Heat map of 212 significant methylated RRACH in glioma patients

White color (0) represents unmethylated sites, red (1) modified sites and grey color represents Na values (no information).

We used a silhouette plot to assess if the 212 statistically significant RRACH motifs were appropriate for additional examination and validation in patient samples (Fig. 3.3.2.2). This technique gives an indication of the clustering quality by calculating how well each data point (in this case, each RRACH pattern) fits into its designated cluster. Higher silhouette values, which range from -1 to 1 , denote clear and significant clumping. Using this method, we evaluated the RRACH motifs' separation and cohesiveness across patient samples. When analyzing patient samples, a silhouette plot is essential because it confirms the quality and consistency guaranteeing that the RRACH motifs found are appropriately categorized and appropriate for further investigation. The silhouette plot's findings supported the usage of our dataset for patient sample validation and subsequent research into the therapeutic significance of these motifs by confirming that it is suitable for additional study.

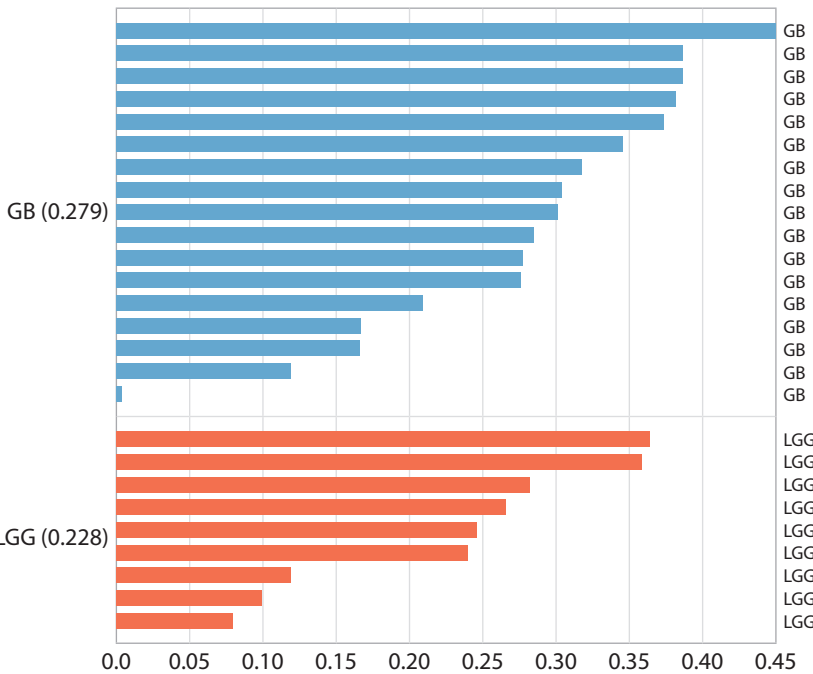


Fig. 3.3.2.2. Silhouette analysis. Separation for glioma patient samples validation applying 212 RRACH motifs

Then, as a further filtering step, we used a Chi-square test to narrow down this list and concentrate on the strongest relationships. We narrowed the list to eight motifs by using the Chi-square test to check for broad correlations between the motifs and variables relevant to gliomas' modifications. This two-step process made sure that our final results are both biolo-

gically significant and statistically sound. After Chi-square test, we selected 8 RRACH motifs, which corresponded to 7 unique genes (Table 3.3.2.1).

Table 3.3.2.1. Significant RRACH sites after two-step filtering

RRACH	The Odds Ratio (OR)	p value	χ^2	p value
AAACA 2129 <i>OS9</i>	2.87	0.010	3.86	0.049
AGACA 1210 <i>PAGR1</i>	2.84	0.012	4.15	0.041
GGACA 2173 <i>OS9</i>	2.24	0.048	8.27	0.004
GGACT 2187 <i>TOB1</i>	3.33	0.002	4.26	0.039
AAACC 3283 <i>PIK3R2</i>	2.50	0.032	6.54	0.011
GAACC 3068 <i>ENSG00000284874</i>	2.40	0.035	4.94	0.026
GGACA 3110 <i>RETREG1</i>	2.24	0.048	7.87	0.005
GGACT 3122 <i>LUC7L3</i>	2.89	0.009	4.66	0.031

Using patients' clinical characteristics, the eight RRACH motifs and the seven distinct genes that correspond to them were thoroughly examined to determine their possible importance and relevance throughout the progression of the disease and patient outcomes. In further analysis and calculations gene *ENSG00000284874* named as *GP1BB*.

3.4. Clustering of glioma patients based on m⁶A epitranscriptomic signatures

We performed an epitranscriptomic analysis in glioma patients after using target selection to identify eight significant modified motifs in MeRIP-seq and dRNA-seq data. First, we examined overall modification levels by pathology in glioma patients after target selection. The findings showed that the glioblastoma and low-grade glioma samples differed significantly. The percentage of selected transcripts that were modified in LGG samples was 80.5%, which was much greater than the 23.6% in GB samples. This suggests that compared to GB samples, LGG samples undergo modifications about 3.4 times more frequently ($p < 0.001$). After, we applied hierarchical clustering analysis to cluster our patients' samples. Two independent clusters were identified that divided glioma patient samples: cluster C1 contained two GB samples and all LGG samples, whereas cluster C2 contained only GB samples (Fig. 3.4.1 A). The distribution of methylation patterns across these clusters was further emphasized using a heatmap analysis, which also showed distinct variations in epitranscriptomic modifications between the two groups (Fig. 3.4.1 B).

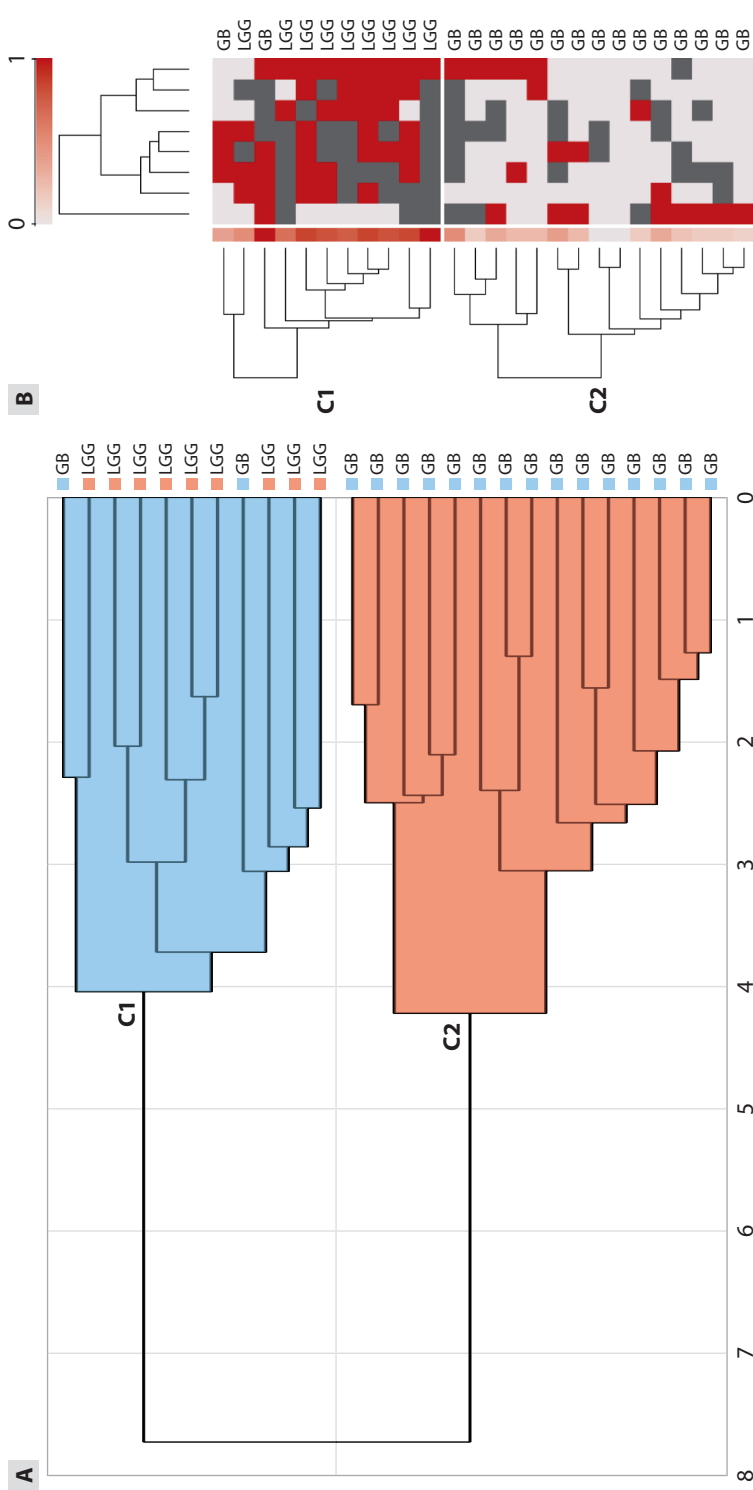


Fig. 3.4.1. Epitranscriptomic data analysis of selected RRACH motifs in glioma patients

(A) Hierarchical clustering analysis shows separation of glioma patient samples, (B) Heatmap shows modification levels in C1 and C2 clusters where 0 represents unmodified, 1 – modified and grey color – no information.

We determined each cluster's modification levels based on the clusters that were evaluated. The modification level in Cluster C2 was much higher at 75% (t-test, $p < 0.001$) than in Cluster C1, which had a modification level of 19.3%. These results highlight the different epitranscriptomic characteristics of the two clusters more strongly. According to our analysis, genes *RETRG1*, *PAGR1*, *OS9*, *PIK3R2*, *GPIBB* and *TOB1* were highly methylated in cluster C1 while gene *LUC7L3* in cluster C2.

To assess cluster separation and identify the ideal number of clusters in our data, silhouette analysis and scoring were performed using the eight RRACH motifs (Fig. 3.4.2). The samples were clearly separated into discrete clusters based on the silhouette analysis. One GB sample, on the other hand, had a negative silhouette score, suggesting that it was either on the border between clusters or maybe misclassified. Despite this, the inclusion of the sample did not affect the overall clustering outcome, and therefore, it was retained in the analysis.

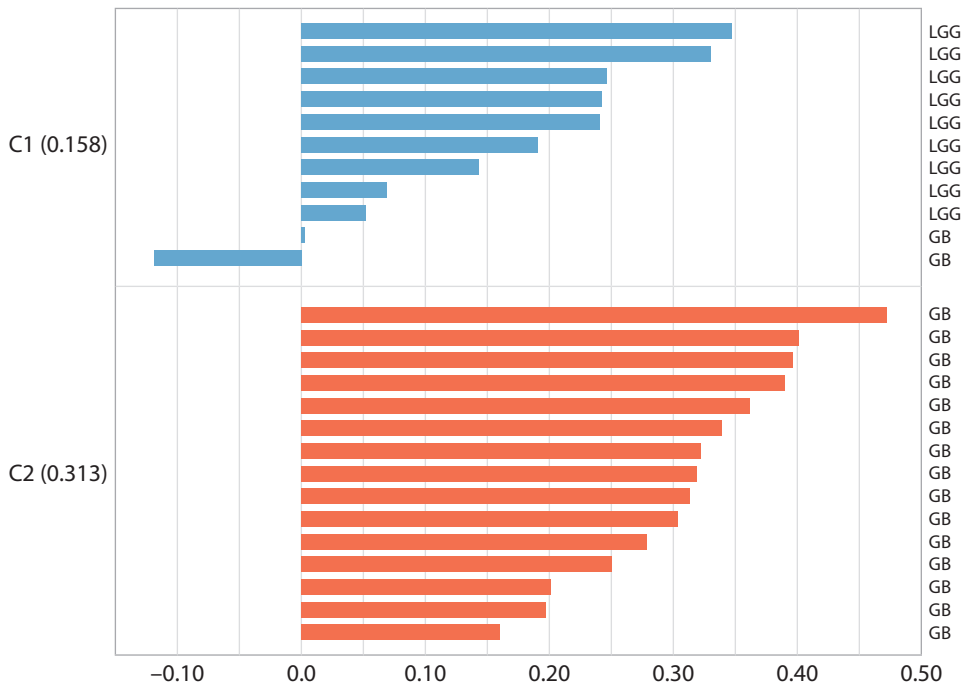


Fig. 3.4.2. Silhouette analysis and scores applying 8 RRACH motifs for clusters

3.4.1. Relationship between mRNA m⁶A methylation and patients' clinical data in combination of RRACH motifs

At first, we decided to check if m⁶A total methylation in all 8 RRACHs has associations with clinical patients' data. We revealed significant differences in survival outcomes between patients with modified and unmodified methylation status ($p = 0.0036$) highlighting the association of m⁶A modification with better prognosis in glioma patients (Fig. 3.4.1.1).

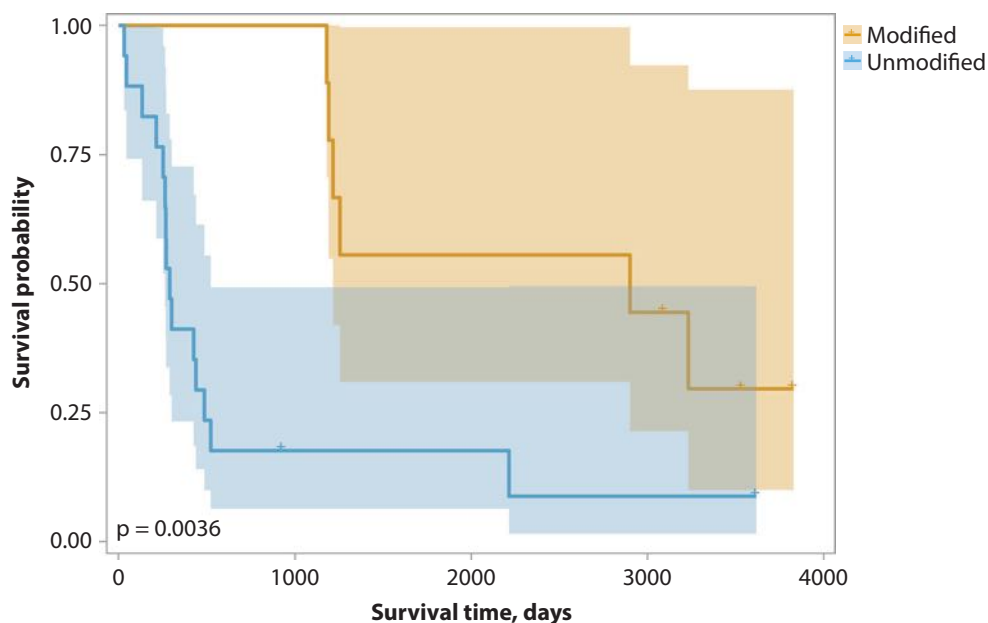


Fig. 3.4.1.1. Kaplan-Meier survival curves of glioma patients' overall survival time (in days) with total modified and total unmodified m⁶A in tumor specimens

m⁶A methylation in the selected promising combined RRACHs showed significant relationships with glioma patients' overall survival ($p = 0.007$) and age ($p = 0.026$). For the continuous variables such as age, tumor size and survival time was used linear regression analysis and for MGMT methylation, tumor location and Ki-67 gene status were used Chi-square Pearson test (Table 3.4.1.1).

Table 3.4.1.1. Associations of glioma patients' clinical data and m⁶A modifications of 8 selected RRACH motifs methylation

	m ⁶ A total methylation		p value
	R-square	χ^2	
Survival, days	8.54		0.007
Age	5.56		0.026
Sex		10	0.997
MGMT		4.32	0.634
Tumor size	13.05		0.074
Ki-67		11.69	0.069
Tumor location		41.56	0.078

m⁶A methylation in the selected promising combined RRACHs in only glioblastoma patients showed significant relationships with glioma patients' overall survival ($p = 0.049$) and tumor location ($p < 0.0001$) (Table 3.4.1.2). Our results imply that the location of the tumor affects the survival time of glioblastoma patients. Some researchers found no association between tumor location and survival [176–178] while others claim that central tumor location associated with worse survival [179], temporal lobe glioblastomas had a statistically significant better survival time [180] or tumors in the right occipitotemporal also associated with poor survival time [181].

Table 3.4.1.2. Associations between clinical data and m⁶A modifications of 8 selected RRACH motifs in glioblastoma patients

	m ⁶ A total methylation		p value
	R-square	χ^2	
Survival, days	4.59		0.049
Age	0.30		0.591
Sex		6.48	0.166
MGMT		4.10	0.393
Subtype		1.23	0.540
Tumor Size	0.04		0.849
Ki-67		7.83	0.098
Tumor Location		34.74	< 0.0001

Additionally, we calculated total m⁶A methylation score to aggregate statistical significance of m⁶A modifications across all patients' samples and target RRACH motifs, which aligns with the concept of quantifying m⁶A methylation levels. m⁶A methylation scores were incorporated into predic-

tions of patients' outcomes (Fig. 3.4.1.2). Results revealed that methylation score had strong significance comparing cluster C1 and C2 ($p = 0.0002$) being higher in cluster C1 (Fig. 3.4.1.2 A). Kaplan-Meier survival curves demonstrated significant differences between low and high methylation scores in glioma patients (Fig. 3.4.1.2 B) suggesting that low m^6A methylation score is associated with a worse survival prognosis in glioma patients ($p = 0.016$). This finding showed that patients with lower levels of methylation may experience reduced survival rates compared to those with higher methylation scores.

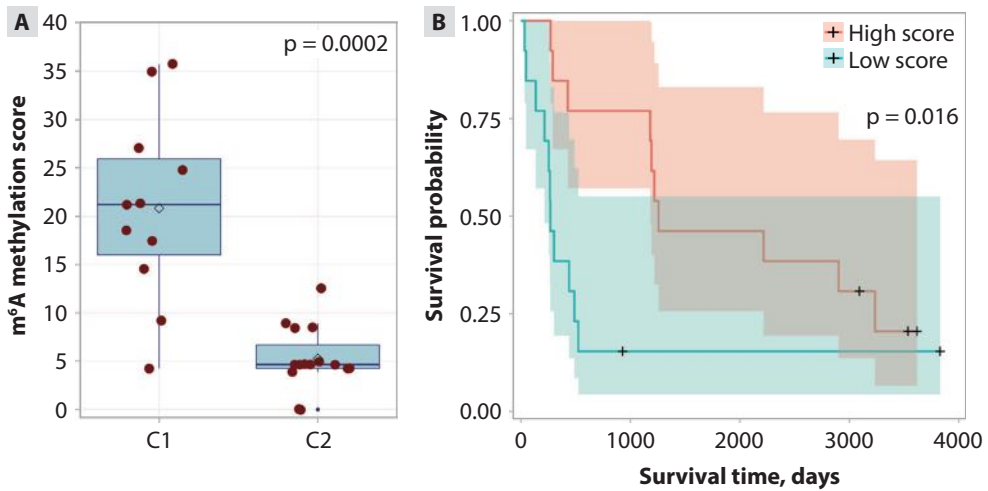


Fig. 3.4.1.2. Total m^6A methylation scores and their association with patient clusters and survival in glioma

(A) Total m^6A methylation score of all target RRACHs in m^6A methylation-based clusters C1 and C2 (t-test, $p = 0.0002$), (B) Kaplan-Meier survival analysis in glioma patients with low and high m^6A methylation scores ($p = 0.016$).

The Random Forest algorithm was utilized to visualize the relationships and transitions on significant clinical characteristics and total m^6A methylation score in glioma patients (Fig. 3.4.1.3). Alluvial plot effectively illustrated how different clinical characteristics interacted and changed across various dimensions, allowing for a comprehensive understanding of underlying patterns. This plot illustrated that most glioma patients in cluster C1 had a similar distribution of age, tumor size, and tumor localization, with the exception of the m^6A methylation score, which was high in the majority of cases. The alluvial plot revealed important insights into the distribution of glioma patients across various clinical factors and total m^6A methylation levels. For instance, it may show that certain cluster is predominantly associated with specific age group or tumor location, suggesting potential

correlations. Additionally, the visualization of methylation level alongside these clinical factors provided a holistic view of how molecular features may relate to clinical outcomes.

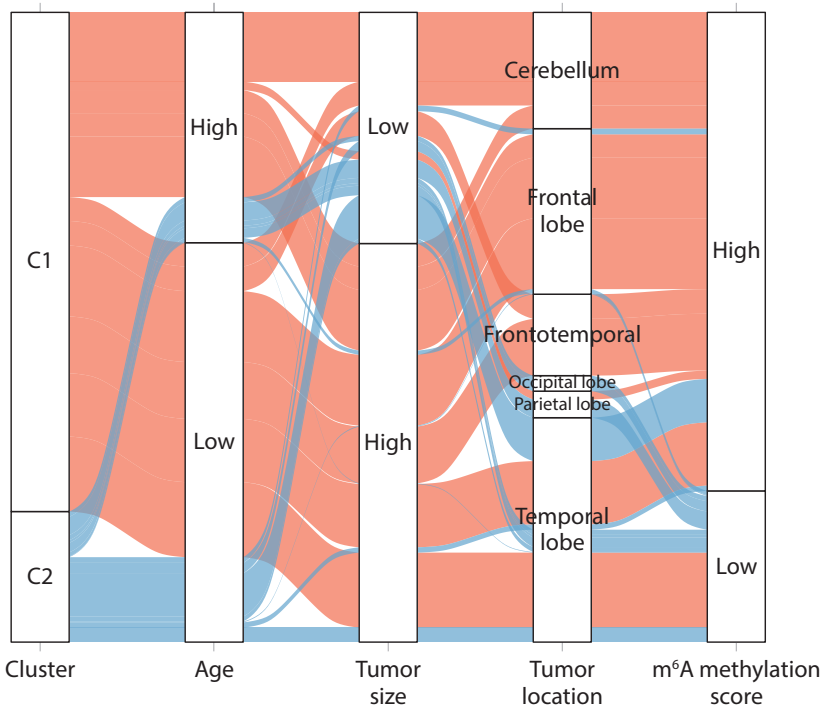


Fig. 3.4.1.3. Alluvial plot showing the changes of cluster, patients' age, tumor size, tumor location and total m⁶A methylation score

We checked total target RRACHs' m⁶A methylation score associations with clinicopathological features (Fig. 3.4.1.4). Interestingly, we noticed that methylation score significantly negatively correlated with patients' age ($p = 0.013$) (Fig. 3.4.1.4 A). There were no significant differences between m⁶A methylation score and tumor size (Fig. 3.4.1.4 B) ($p = 0.5$), pathologies (Fig. 3.4.1.4 C) ($p = 0.189$), patients' gender (Fig. 3.4.1.4 D) ($p = 0.344$), MGMT status (Fig. 3.4.1.4 E) ($p = 0.424$) and Ki-67 status (Fig. 3.4.1.4 F) ($p = 0.179$). Methylation score and tumor location showed significant differences: cerebellum location which had higher methylation scores demonstrated significant relationship with the frontal lobe location ($p = 0.023$), occipital lobe ($p = 0.026$) and temporal lobe ($p < 0.0001$) (Fig. 3.4.1.4 G). Lower frontal lobe showed significant relationship with frontotemporal tumor location ($p = 0.018$) while higher frontotemporal location revealed associations with occipital lobe ($p = 0.021$) and temporal lobe ($p < 0.0001$).

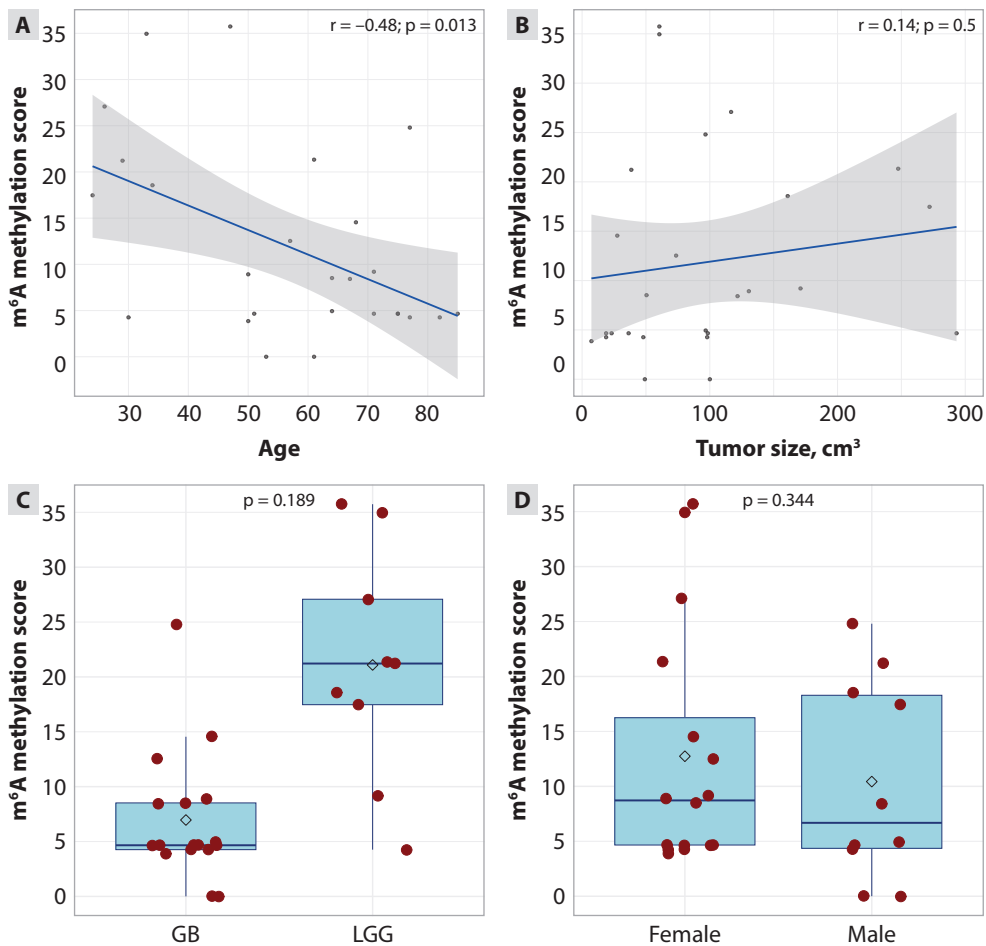


Fig. 3.4.1.4 (A–D). Total m⁶A methylation score associations with patients' clinical characteristics

(A) Total m⁶A methylation score relationship with patients' age ($p = 0.013$), (B) tumor size ($p = 0.5$), (C) pathology ($p = 0.189$), (D) sex ($p = 0.344$).

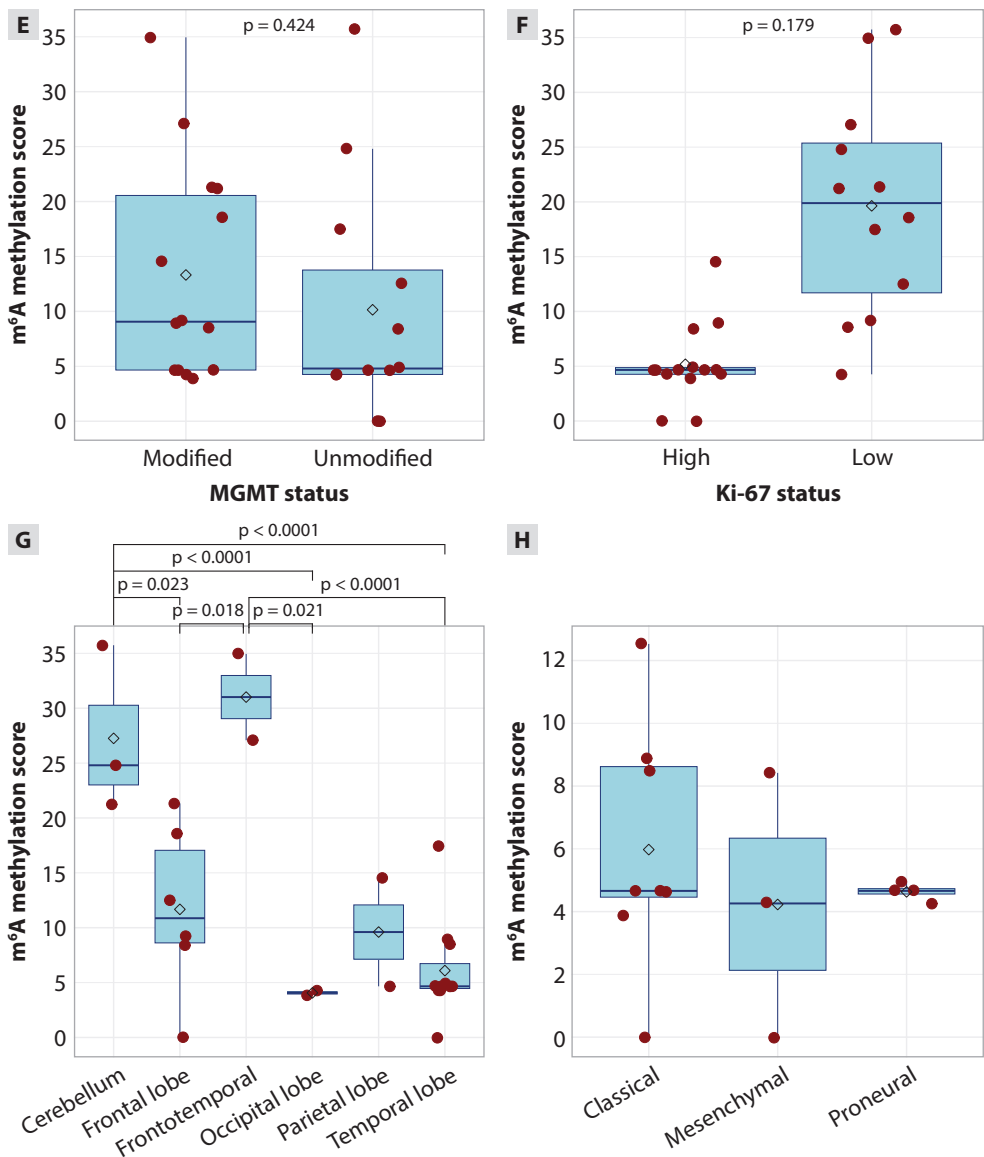


Fig. 3.4.1.4 (E–H). Total m⁶A methylation score associations with patients' clinical characteristics

(E) MGMT status ($p = 0.424$), (F) Ki-67 status ($p = 0.179$), (G) Tumor location, (H) subtypes in C1 cluster samples.

Since the modified target RRACHs were successfully identified (AAACA|2129|OS9, AGACA|1210|PAGRI, GGACA|2173|OS9, GGACT|2187|TOBI, AAACC|3283|PIK3R2, GAACC|3068|GPIBB, GGACA|3110|RETREG1 and GGACT|3122|LUC7L3) in the cohort of glioma patients, the importance of targets and patients' outcomes in the prosper of biomarkers, will be further described individually in more detail.

3.4.2. AAACA|2129|OS9 RRACH m⁶A modification is significantly associated with gliomas survival and Ki-67

Although the OS9 gene has been poorly studied in cancer patients, gene amplification has been observed in patients with osteosarcoma [117]. In the case of gliomas, we decided to evaluate whether the RRACH motif of this gene has associations with clinical data. It has been identified as significantly associated with glioma survival time and the expression of Ki-67 (Table 3.4.2.1).

Table 3.4.2.1. Associations of glioma patients' clinical data and m⁶A modifications in AAACA motif of OS9 gene at 2129 position

	Coefficient	χ^2	p value
Survival time, days	0.71 (HR)		< 0.001
Age	-0.40 (LR)		0.097
Sex		1.38 (df = 1)	0.240
MGMT		1.02 (df = 1)	0.313
Tumor size	0.08 (LR)		0.758
Ki-67		5.40 (df = 1)	0.020
Tumor location		7.54 (df = 5)	0.184

HR – represents Hazard-Ratio; LR – represents Logistic regression.

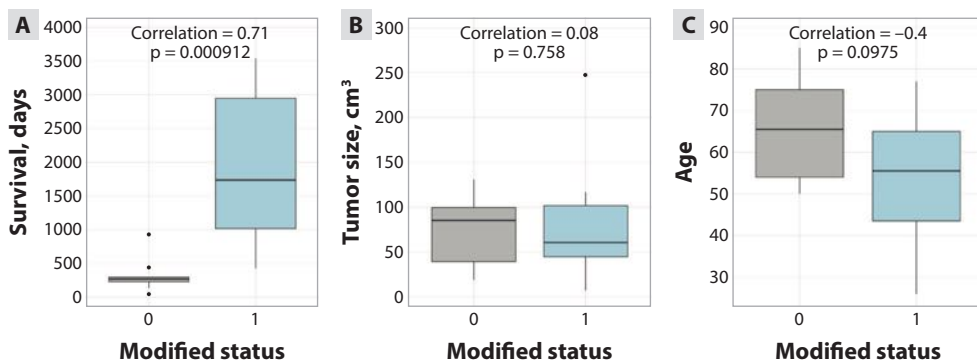


Fig. 3.4.2.1. Box plots of survival time, age, tumor size and m^6A modification status in tumor tissues in AAACA of gene *OS9*

(A) m^6A modification associations with patients' survival time in days, (B) tumor size, (C) patients' age.

According to Fig. 3.4.2.1 A, longer survival time of glioma patients is noted in patients with high m^6A methylation ($p < 0.001$). Although no statistical significance or significant tendency was seen when comparing m^6A methylation with tumor size (Fig. 3.4.2.1 B) however, a clear trend is seen when comparing methylation with patient age which shows that younger patients have most modified AAACA motif in gene *OS9* (Fig. 3.4.2.1 C). m^6A methylation in AAACA motif of *OS9* gene at 2129 position only in glioblastoma patients showed slight tendency with overall survival ($p = 0.059$) to have better survival rates when m^6A modified (Table 3.4.2.2).

Table 3.4.2.2. Associations of glioblastoma patients' clinical data and m^6A modifications in AAACA motif of *OS9* gene at 2129 position

	Coefficient	χ^2	p value
Survival time, days	0.22 (HR)		0.059
Age	-0.009 (LR)		0.867
Sex		0.07 (df = 1)	0.798
MGMT		0.35 (df = 1)	0.554
Subtype		1.75 (df = 3)	0.417
Tumor size	-0.02 (LR)		0.233
Ki-67		0.89 (df = 1)	0.354
Tumor location		5.02 (df = 5)	0.286

HR – represents Hazard-ratio; LR – represents Logistic regression.

3.4.3. AGACA|1210|*PAGRI* RRACH m⁶A modification is significantly associated with gliomas survival and glioblastoma subtypes

It has already been confirmed that *PAGRI* (also known as *PAI*) gene plays a significant role in regulating adipogenesis [182] or is implicated in DNA damage response [119, 183]. In the case of gliomas, we found that the AGACA motif of the *PAGRI* gene is significantly associated with glioma patients' survival (Table 3.4.3.1).

Table 3.4.3.1. Associations of glioma patients' clinical data and m⁶A modifications in AGACA motif of *PAGRI* gene at 1210 position

	Coefficient	χ^2	p value
Survival, days	0.6 (HR)		0.015
Age	-0.43 (LR)		0.094
Sex		0.004 (df = 1)	0.950
MGMT		1.016 (df = 1)	0.314
Tumor size	0.31 (LR)		0.236
Ki-67		3.81 (df = 1)	0.051
Tumor location		9.91 (df = 5)	0.078

HR – represents Hazard-ratio; LR – represents Logistic regression.

Fig. 3.4.3.1 A shows that patients with higher m⁶A methylation had higher survival duration (p = 0.015). A distinct trend is observed when comparing methylation with patient age, indicating that older patients (≥ 61 years old) had the most changed AGACA pattern in gene *PAGRI* (Fig. 3.4.3.1 C), even though there were no statistical significance or tendency when comparing m⁶A methylation with tumor size (Fig. 3.4.3.1 B).

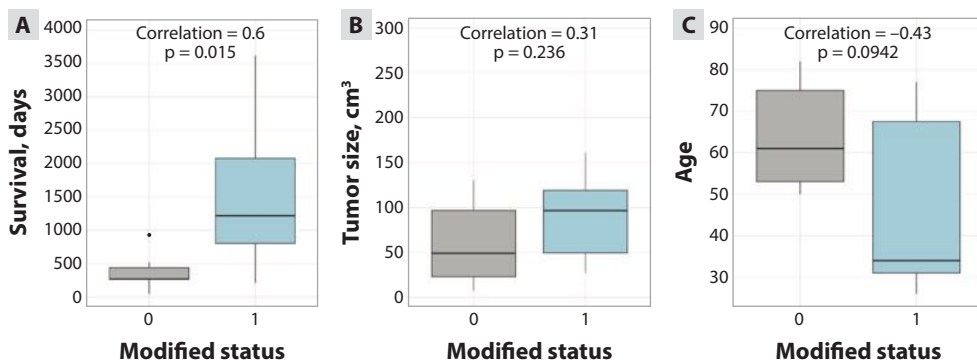


Fig. 3.4.3.1. Box plots of survival time, age, tumor size and m⁶A modification status in tumor tissues in AGACA motif of *PAGRI* gene

(A) m⁶A modification associations with patients' survival time in days, (B) tumor size, (C) patients' age.

m⁶A methylation in the AGACA|1210|*PAGRI* RRACH in only glioblastoma patients showed significant relationships with tumor location ($p < 0.003$) (Table 3.4.3.2). According to our glioblastoma patients we found that tumors in cerebellum location were all modified and associated with better survival prognosis compared to other tumor locations.

Table 3.4.3.2. Associations of glioblastoma patients' clinical data and m⁶A modifications in AGACA motif of *PAGRI* gene at 1210 position

	Coefficient	χ^2	p value
Survival, days	0.64 (HR)		0.574
Age	0.07 (LR)		0.294
Sex		0 (df = 1)	1
MGMT		0 (df = 1)	1
Subtype		1.64 (df = 3)	0.440
Tumor size	0.02 (LR)		0.447
Ki-67		0 (df = 1)	1
Tumor location		16.54 (df = 5)	0.003

HR – represents Hazard-ratio; LR – represents Logistic regression.

3.4.4. GGACA|2173|*OS9* RRACH is strongly associated with glioma patients clinicopathological characteristics

Another particularly noteworthy motif in the *OS9* gene, GGACA, showed strong and significant association with the clinical data of patients (Table 3.4.4.1). GGACA motif of gene *OS9* in 2173 location demonstrated notable features as a biomarker employing m⁶A methylation status and survi-

val, patients' age, and Ki-67. On the other hand, m⁶A methylation of the motif in only glioblastoma patients showed no significant relationships with clinical data (Table 3.4.4.2).

Table 3.4.4.1. Associations of glioma patients' clinical data and m⁶A modifications in GGACA motif of OS9 gene at 2173 position.

	Coefficient	χ^2	p value
Survival, days	0.79 (HR)		< 0.0001
Age	-0.56 (LR)		0.011
Sex		0.102 (df = 1)	0.749
MGMT		0.087 (df = 1)	0.767
Tumor size	0.23 (LR)		0.331
Ki-67		4.375 (df = 1)	0.036
Tumor location		9.643 (df = 5)	0.086

HR – represents Hazard-ratio; LR – represents Logistic regression.

Table 3.4.4.2. Associations of glioblastoma patients' clinical data and m⁶A modifications in GGACA motif of OS9 gene at 2173 position

	Coefficient	χ^2	p value
Survival, days	< 0.01 (HR)		0.999
Age	0.09 (LR)		0.402
Sex		0.598 (df = 1)	0.439
MGMT		0 (df = 1)	1
Subtype			
Tumor size	-0.08 (LR)		0.354
Ki-67		0 (df = 1)	1
Tumor location		0 (df = 5)	1
Subtype (GB)		0.81 (df = 3)	0.668

HR – represents Hazard-ratio; LR – represents Logistic regression.

A strong association was found between m⁶A modification status and survival ($p < 0.0001$) in glioma patients (Fig. 3.4.4.1 A), indicating that patients with modified GGACA motifs survived longer compared to those without. Although tumor size was not associated with methylation ($p > 0.05$) (Fig. 3.4.4.1 B), it is also interesting that younger patients (≤ 61 years old) had higher m⁶A methylation levels (Fig. 3.4.4.1 C).

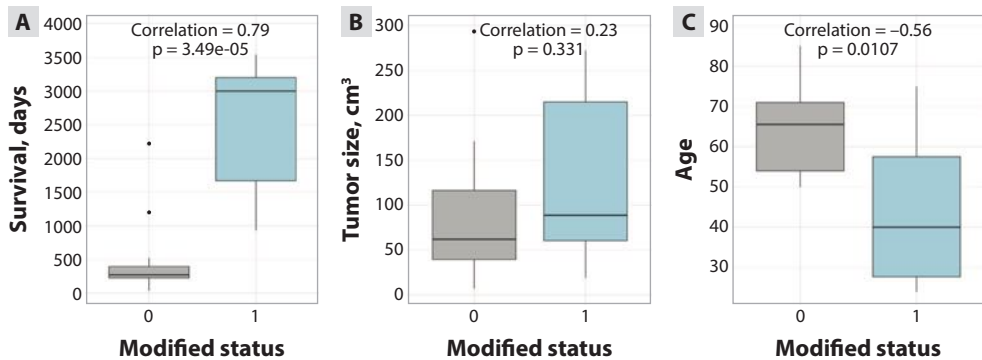


Fig. 3.4.4.1. Box plots of survival time, age, tumor size and m^6A modification status in tumor tissues in GGACA motif of OS9 gene

(A) significant m^6A modification associations with patients' survival time in days, (B) tumor size, (C) patients' age.

3.4.5. Weak link between GGACT|2187|TOB1 RRACH methylation and glioma patients' clinical characteristics

Although the gene plays a significant role in gastric [124], pancreatic [184] and breast cancers [185], unfortunately, the methylation of the GGACT motif in *TOB1* gene has no significant differences with glioma patients' clinical outcome (Table 3.4.5.1).

Table 3.4.5.1. Associations of glioma patients' clinical data and m^6A modifications in GGACT motif of *TOB1* gene at 2187 position

	Coefficient	χ^2	p value
Survival, days	0.36 (HR)		0.081
Age	-0.18 (LR)		0.384
Sex		0.007 (df = 1)	0.935
MGMT		0.076 (df = 1)	0.783
Tumor size	0.31 (LR)		0.135
Ki-67		2.061 (df = 1)	0.151
Tumor location		5.114 (df = 5)	0.402

HR – represents Hazard-ratio; LR – represents Logistic regression.

Although, no correlation found between m⁶A methylation and tumor size (Fig. 3.4.5.1 B) or patient age (Fig. 3.4.5.1 C), we concluded that patients with higher m⁶A modification levels tend to live longer (Fig. 3.4.5.1 A).

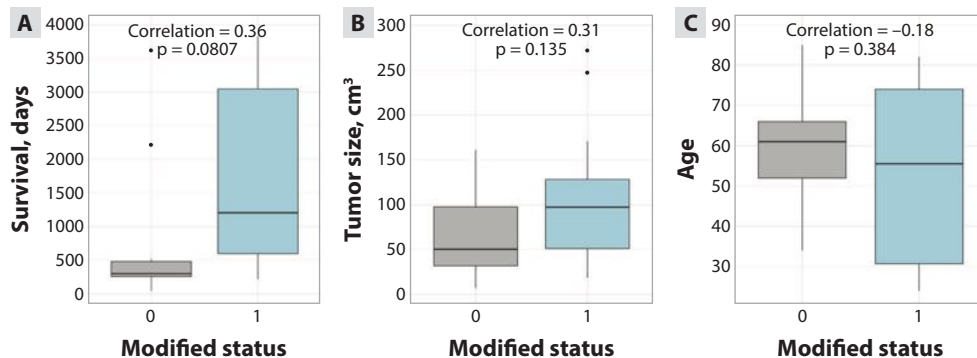


Fig. 3.4.5.1. Box plots of survival time, age, tumor size and m⁶A modification status in tumor tissues in GGACT motif of *TOB1* gene

m⁶A modification associations with (A) patients' survival time in days, (B) tumor size, (C) patients' age.

m⁶A methylation of the motif GGACT in *TOB1* gene in only glioblastoma patients showed no significant relationships with clinical data (Table 3.4.5.2).

Table 3.4.5.2. Associations of glioblastoma patients' clinical data and m⁶A modifications in GGACT motif of *TOB1* gene at 2187 position

	Coefficient	χ^2	p value
Survival, days	0.72 (HR)		0.553
Age	0.07 (LR)		0.164
Sex		0 (df = 1)	1
MGMT		0.27 (df = 1)	0.601
Subtype		0.36 (df = 3)	0.837
Tumor size	0.01 (LR)		0.427
Ki-67		0 (df = 1)	1
Tumor location		2.49 (df = 5)	0.647

HR – represents Hazard-ratio; LR – represents Logistic regression.

3.4.6. Strong link between AAACC|3283|PIK3R2 RRACH methylation and glioma patients'

PIK3R2 gene is poorly studied in the human brain, however preclinical deletion causes tumor regression [133] and reduces invasion [186]. In our case, glioma patients and AAACC|3283|PIK3R2 RRACH methylation are strongly correlated, suggesting that this methylation pattern may be important for the development and features of gliomas (Table 3.4.6.1).

Table 3.4.6.1. Associations of glioma patients' clinical data and m⁶A modifications in AAACC motif of PIK3R2 gene at 3283 position

	Coefficient	χ^2	p value
Survival, days	0.77 (HR)		0.001
Age	-0.67 (LR)		0.009
Sex		0.111 (df = 1)	0.739
MGMT		0.525 (df = 1)	0.469
Tumor size	-0.02 (LR)		0.943
Ki-67		6.541 (df = 1)	0.011
Tumor location		8.919 (df = 5)	0.112

HR – represents Hazard-ratio; LR – represents Logistic regression.

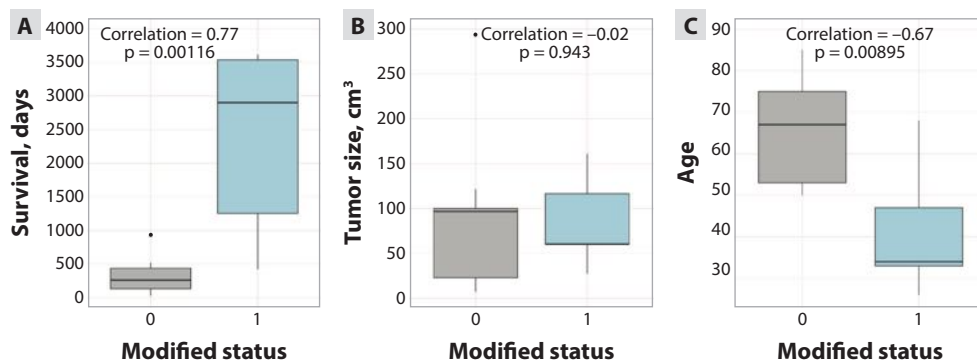


Fig. 3.4.6.1. Box plots of survival time, age, tumor size and m⁶A modification status in tumor tissues in AAACC motif of PIK3R2 gene

m⁶A modification associations with (A) patients' survival time in days, (B) tumor size, (C) patients' age.

While no significant differences between PIK3R2 gene AAACC RRACH motif m⁶A methylation and sex, MGMT status, tumor size and tumor location were found, on the other hand there were strong link between survival time, patients age and Ki-67 gene. Fig. 3.4.6.1 A shows significant difference in survival time according to methylation status implying that

patients with high m⁶A modification level live longer, they are also younger patients (Fig. 3.4.6.1 C). We concluded that smaller tumor size was associated with unmodified m⁶A but not significantly (Fig. 3.4.6.1 C). GB patients and AAACC|3283|PIK3R2 RRACH methylation had no significant tendency when compared with clinical data (Table 3.4.6.2).

Table 3.4.6.2. Associations of glioblastoma patients' clinical data and m⁶A modifications in AAACC motif of PIK3R2 gene at 3283 position

	Coefficient	χ²	p value
Survival, days	0.89 (HR)		0.920
Age	0.02 (LR)		0.841
Sex		0 (df = 1)	1
MGMT		0 (df = 1)	1
Subtype		4.44 (df = 3)	0.108
Tumor size	-0.03 (LR)		0.493
Ki-67		NA (df = 1)	NA
Tumor location		NA (df = 5)	NA

HR – represents Hazard-ratio; LR – represents Logistic regression; NA – not applicable.

3.4.7. GAACC|3068|GP1BB RRACH methylation associated with and glioma patients' clinical outcome

Glioma patients' characteristics such as survival, Ki-67 gene status and GAACC|3068|GP1BB RRACH methylation showed significant associations (Table 3.4.7.1).

Table 3.4.7.1. Associations of glioma patients' clinical data and m⁶A modifications in GAACC motif of GP1BB gene at 3068 position

	Coefficient	χ²	p value
Survival, days	0.47 (HR)		0.047
Age	-0.33 (LR)		0.186
Sex		NA (df = 1)	NA
MGMT		NA (df = 1)	NA
Tumor size	0.34 (LR)		0.162
Ki-67		4.938 (df = 1)	0.026
Tumor location		6.600 (df = 5)	0.252

HR – represents Hazard-ratio; LR – represents Logistic regression; NA – not applicable.

We turned our attention to examining methylation link inside glioma patients of the survival time, age, and tumor size (Fig. 3.4.7.1). Patients who were m⁶A modified survived significantly longer ($p < 0.05$) than those who were unmodified (Fig. 3.4.7.1 A), there is a tendency for larger tumor size to be modified compared to small tumor size (Fig. 3.4.7.1 B) and older patients tend to have low m⁶A modification levels of this gene motif (Fig. 3.4.7.1 C).

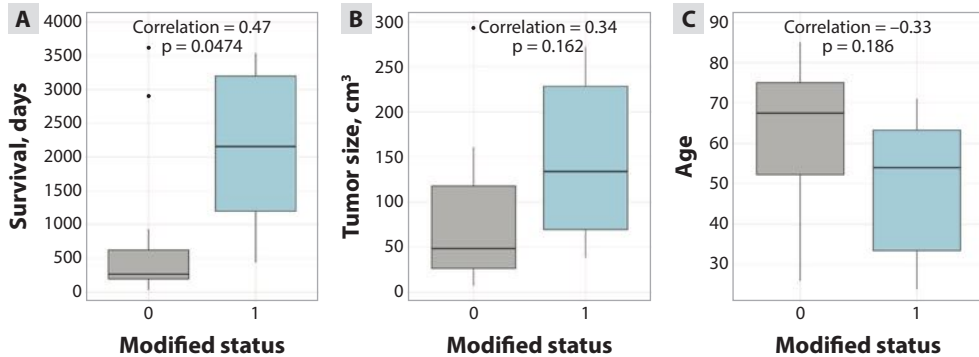


Fig. 3.4.7.1. Box plots of survival time, age, tumor size and m⁶A modification status in tumor tissues in GAACC motif of GP1BB gene

m⁶A modification associations with (A) patients' survival time in days, (B) tumor size, (C) patients' age.

Examining methylation link inside glioblastoma patients with clinical factors we found no significance or tendency in all cohort (Table 3.4.7.2).

Table 3.4.7.2. Associations of glioblastoma patients' clinical data and m⁶A modifications in GAACC motif of GP1BB gene at 3068 position

	Coefficient	χ^2	p value
Survival, days	0.60 (HR)		0.640
Age	-0.04 (LR)		0.674
Sex		0 (df = 1)	1
MGMT		0 (df = 1)	1
Subtype		1.93 (df = 3)	0.382
Tumor size	0.003 (LR)		0.770
Ki-67		NA (df = 1)	NA
Tumor location		NA (df = 5)	NA

HR – represents Hazard-ratio; LR – represents Logistic regression; NA – not applicable.

3.4.8. GGACA|3110|*RETREG1* RRACH is a very promising molecular marker for glioma prognostics

It is already found that *RETREG1* plays a crucial role in reticulophagy and cell death [150, 187]. Therefore, we verified how the *RETREG1* gene GGACA motif methylation associated with glioma patients. GGACA motif of gene *RETREG1* demonstrated notable features as biomarker employing methylation.

It was determined strong relationship between methylation and patients' survival, age, Ki-67 gene status and tumor location (Table 3.4.8.1) indicating that methylation patterns serve as critical biomarker for predicting clinical outcomes.

Table 3.4.8.1. Associations of glioma patients' clinical data and m⁶A modifications in GGACA motif of *RETREG1* gene at 3110 position.

	Coefficient	χ^2	p value
Survival, days	0.61 (HR)		0.004
Age	-0.56 (LR)		0.010
Sex		0.087 (df = 1)	0.769
MGMT		NA (df = 1)	NA
Tumor size	0.03 (LR)		0.896
Ki-67		12.098 (df = 1)	< 0.001
Tumor location		15.238 (df = 5)	0.009

HR – represents Hazard-ratio; LR – represents Logistic regression; NA – not applicable.

For instance, it was shown that younger patients tend to have higher m⁶A methylation levels than older ones ($p = 0.010$) (Fig. 3.4.8.1 C) as same as better survival prognosis were noted in glioma tumors with high m⁶A methylation (Fig. 3.4.8.1 A) ($p = 0.004$). Tumor size did not reveal differences in m⁶A methylation ($p > 0.05$) (Fig. 3.4.8.1 B).

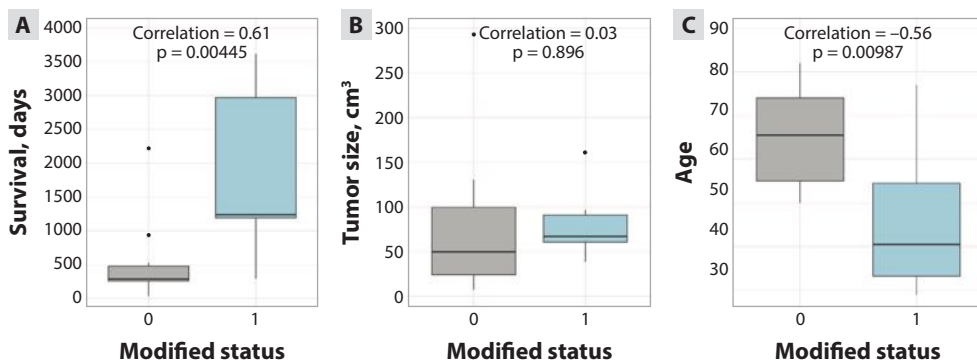


Fig. 3.4.8.1. Box plots of survival time, age, tumor size and m^6A modification status in tumor tissues in GGACA motif of *RETREG1* gene

m^6A modification associations with (A) patients' survival time in days, (B) tumor size, (C) patients' age.

m^6A methylation in the GGACA|3110|*RETREG1* RRACH in only glioblastoma patients showed significant relationships with tumor location ($p < 0.042$) and Ki-67 gene ($p = 0.029$) (Table 3.4.8.2).

Table 3.4.8.2. Associations of glioblastoma patients' clinical data and m^6A modifications in GGACA motif of *RETREG1* gene at 3110 position

	Coefficient	χ^2	p value
Survival, days	0.68 (HR)		0.623
Age	0.02 (LR)		0.784
Sex		0 (df = 1)	1
MGMT		0.33 (df = 1)	0.568
Subtype		2.29 (df = 3)	0.319
Tumor size	0.002 (LR)		0.880
Ki-67		4.75 (df = 1)	0.029
Tumor location		NA (df = 5)	0.042

HR – represents Hazard-ratio; LR – represents Logistic regression; NA – not applicable.

These findings had significant and relevant implications for diseases such as cancer, neurological disorders, and irregularities of the sensory and motor neurons characterized by disturbed reticulophagy [187].

3.4.9. Weak link of GGACT|3122|LUC7L3 RRACH in glioma patients' clinical data

The methylation analysis of GGACT motif in gene *LUC7L3* showed no significant differences in glioma patients (Table 3.4.9.1).

Table 3.4.9.1. Associations of patients' clinical data and m⁶A modifications in GGACT motif of *LUC7L3* gene at 3122 position

	Coefficient	χ^2	p value
Survival, days	-0.42 (HR)		0.064
Age	0.43 (LR)		0.061
Sex		1.019 (df = 1)	0.313
MGMT		0.247 (df = 1)	0.619
Tumor size	-0.09 (LR)		0.701
Ki-67		0.247 (df = 1)	0.619
Tumor location		8.014 (df = 5)	0.156

HR – represents Hazard-ratio; LR – represents Logistic regression.

Comparing patients by m⁶A modification status did not significantly alter overall survival rates, according to our analysis of the association between survival time and m⁶A modification (Fig. 3.4.9.1 A) as same as in tumor size (Fig. 3.4.9.1 B). It was a clear trend in relation to patient age, indicating that older people were more likely to display changed m⁶A patterns than younger people (Fig. 3.4.9.1 C).

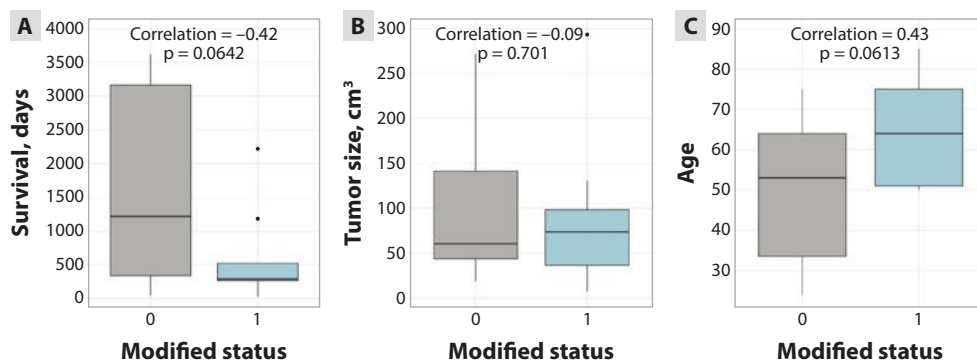


Fig. 3.4.9.1. Box plots of survival time, age, tumor size and m⁶A modification status in tumor tissues in GGACT motif of *LUC7L3* gene

m⁶A modification associations with (A) patients' survival time in days, (B) tumor size, (C) patients' age.

Analyzing GGACT motif of gene *LUC7L3* in glioblastomas revealed a strong association between modification and glioblastoma subtypes ($p = 0.027$). The complete lack of modified m⁶A in the mesenchymal subtype could contribute to its aggressive phenotype (Table 3.4.9.2).

Table 3.4.9.2. Associations of glioblastoma patients' clinical data and m⁶A modifications in GGACT motif of *LUC7L3* gene at 3122 position

	Coefficient	χ^2	p value
Survival, days	0.81 (HR)		0.735
Age	-0.003 (LR)		0.953
Sex		0.69 (df = 1)	0.406
MGMT		1.24 (df = 1)	0.265
Subtype		7.22 (df = 3)	0.027
Tumor size	0.006 (LR)		0.516
Ki-67		0.60 (df = 1)	0.437
Tumor location		7.36 (df = 5)	0.118

HR – represents Hazard-ratio; LR – represents Logistic regression.

We turned our attention to examining stemness in glioma patients after finishing the analysis of the epitranscriptomic data. In order to do this, patients' stemness analysis we conducted a thorough stemness score calculation, using accepted practices to assess the differences in stemness of glioma patients.

3.5. Unraveling stemness: a deep dive into glioma patients' stemness scores

Increased research has shown that stem cells are essential for drug resistance, carcinogenesis, and progression [115, 188]. Establishing stemness scores simplifies the development of customized therapeutics, helps stratify patients according to their individual characteristics, and allows for a greater knowledge of cellular behavior or targeted therapies – all of which improve patient outcomes [189]. Thus, we performed a single-sample gene enrichment analysis (ssGSEA) method [190], which assigns scores to gene sets based on gene expression in an individual sample. We used a dataset of glioma stemness-related genes prepared by Malta et al. 2018 [191] which includes twenty-one stemness genes. Stemness score of each patient was calculated for 17 GB samples and 9 LGG samples. Based on the studies already described it has been established that glioblastomas have a statistically higher stemness score compared to low-grade gliomas [192]. The distribution of stemness scores were analyzed across m⁶A methylation-based patient clusters C1 (represents LGG cluster and includes 2 GB samples) and C2 (all glo-

blastomas) got through m⁶A methylation clustering analysis. Our analysis of the stemness score showed that GB samples mean is higher than LGG samples mean, although the result was not statistically significant ($p = 0.408$) (Fig. 3.5.1 A). However, a Kaplan–Meier survival analysis revealed a significant difference in survival between patients with high and low stemness scores within these m⁶A-defined clusters ($p = 0.0061$), with higher stemness scores being associated with poorer overall survival (Fig. 3.5.1 B).

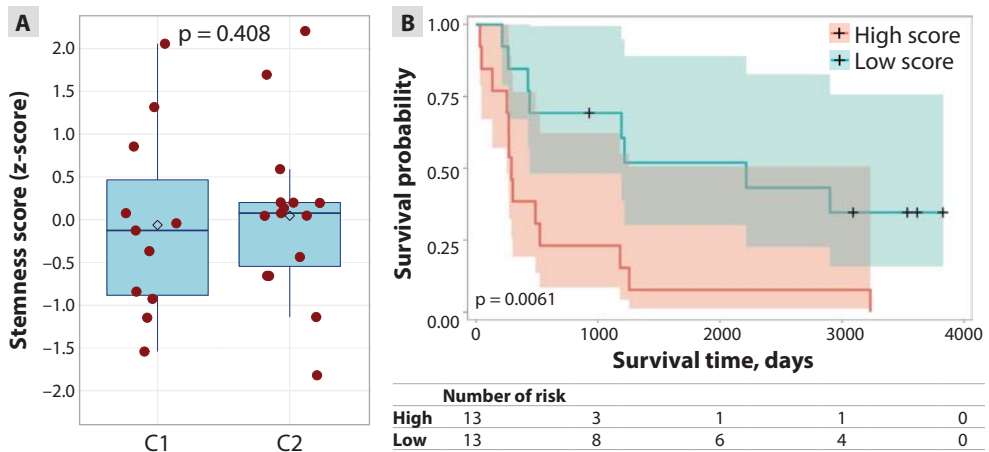


Fig. 3.5.1. Distribution and survival rates of stemness score in glioma patients

(A) Stemness score distribution in cluster C1 and C2 (t-test, $p = 0.408$). (B) Kaplan-Meier analysis in glioma patients by high and low stemness score ($p = 0.006$). Horizontal line in the boxes shows median, quadrate – mean.

According to the median cut-off of the stemness score (0.046), 26 glioma patients were divided into low ($n = 12$) and high stemness score groups ($n = 14$). We used Chi-square test to investigate the correlation between stemness score and clinicopathological features. We did not find that stemness score significant correlated with patients' clinical data (Fig. 3.5.2). Interestingly, we noticed a tendency that the occipital lobe to have a higher stemness score compared to frontal lobe ($p = 0.06$) (Fig. 3.5.2 G). Also, interesting results are shown in Fig 3.5.2 H, where we can see a tendency that classical type of glioblastomas are likely to have higher stemness score compared to proneural and mesenchymal subtypes ($p = 0.09$, $p = 0.06$ respectively). Although the results are not statistically significant due to the possible small number of sample size, they provide useful insights for further research into gliomas.

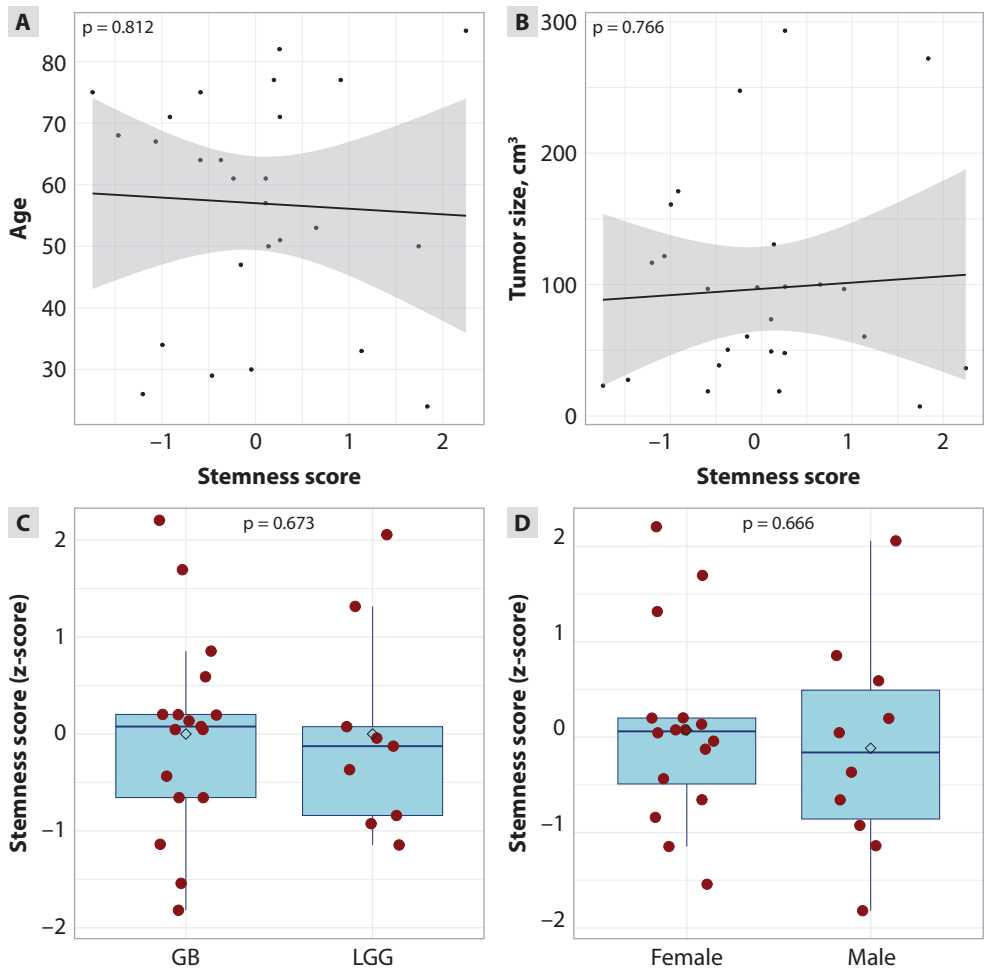


Fig. 3.5.2 (A–D). Correlation between stemness score and clinicopathological features. The distribution of stemness score in glioma patients

(A) age, (B) tumor size, (C) pathology, (D) gender. Horizontal line in the boxes shows median.

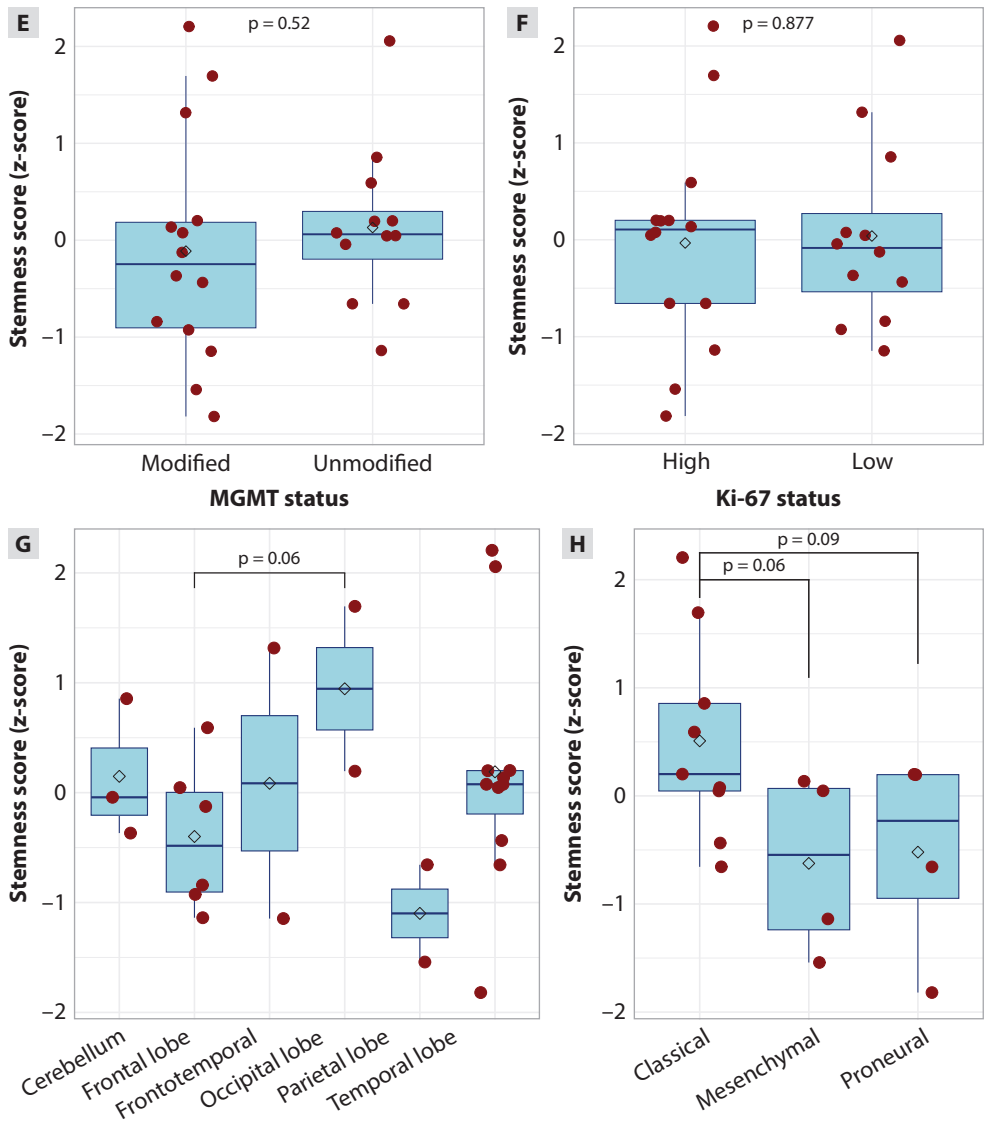


Fig. 3.5.2 (E–H). Correlation between stemness score and clinicopathological features. The distribution of stemness score in glioma patients

(E) MGMT status, (F) Ki-67 status, (G) tumor location, (H) glioblastoma subtypes. Horizontal line in the boxes shows median.

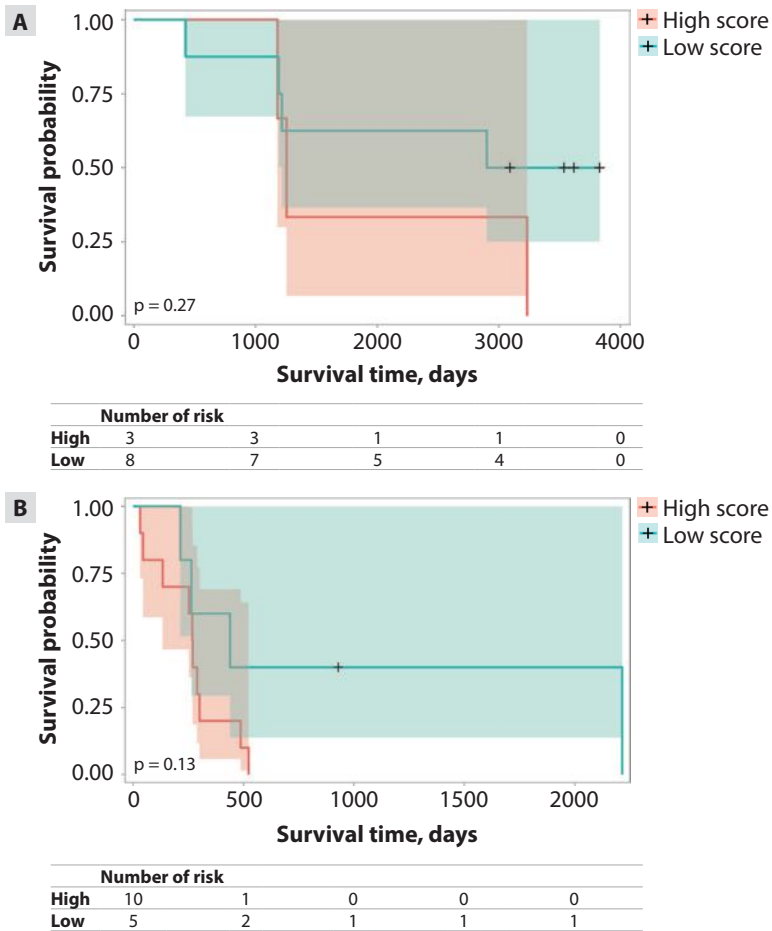


Fig. 3.5.3. Kaplan-Meier survival curves of patients' overall survival time with low and high stemness score

m⁶A methylation-based clusters (**A**) C1, (**B**) C2.

Next, we revealed a Kaplan-Meier analysis between patients' stemness score and survival time (Fig. 3.5.3). Survival analysis including cluster C1 did not reveal significant different patient survival between low and high stemness score groups ($p = 0.27$) (Fig. 3.5.3 A) as same as cluster C2 ($p = 0.13$) (Fig. 3.5.3 B). Although gliomas are highly heterogeneous and there are many factors that affect prognosis, a low stemness score is often linked to better chemotherapy responses, but it does not ensure superior survival results [193]. Combining LGG and GB samples together, there is a substantial relationship between stemness score and survival time, indicating that stemness scores are crucial for comprehending the overall progression of gliomas. The lack of relevance within individual groups, cluster C1 and C2,

emphasized how complicated the biology of gliomas is and how other tumor-specific characteristics must be considered when determining prognosis. These findings can serve as a foundation for further research. Additionally, as stemness scores might not always be enough for risk stratification, this emphasized the significance of individualized approaches for glioma treatment [194].

We wanted to take a closer look at the stemness genes that were used to calculate the stemness score, so we performed additional analysis using the expression of stemness markers in sequenced patients. 17 out of 21 stemness-related genes were included in analysis. We found that stemness-related genes precisely separate patients into two different clusters according to pathology using stemness markers for ssGSEA (Fig. 3.5.4 A). Except for two glioblastoma cases, most of the samples in cluster C1 are low-grade glioma samples. Cluster C2, on the other hand, only contains samples of glioblastoma. This clustering demonstrates how stemness markers can be used to differentiate between different glioma groups and emphasizes how important they are for comprehending the pathogenic variability of gliomas. Next, the distribution of the clusters based on stemness-related markers is shown using the Principal Component Analysis (Fig. 3.5.4 B). PCA enables an accurate representation of how glioma patients' samples cluster together based on their stemness profiles by lowering the dimensionality of the dataset. Both clusters are shown by this approach, emphasizing the distinction between glioblastoma and LGG samples.

Interesting, that m⁶A methylation and stemness score effectively categorizing patients according to their pathology. This approach allowed us to identify groups that aligned with the underlying pathology, proving the robustness for patient stratification. Notably, the clustering highlighted the importance of m⁶A methylation and stemness as crucial markers in pathology classification.

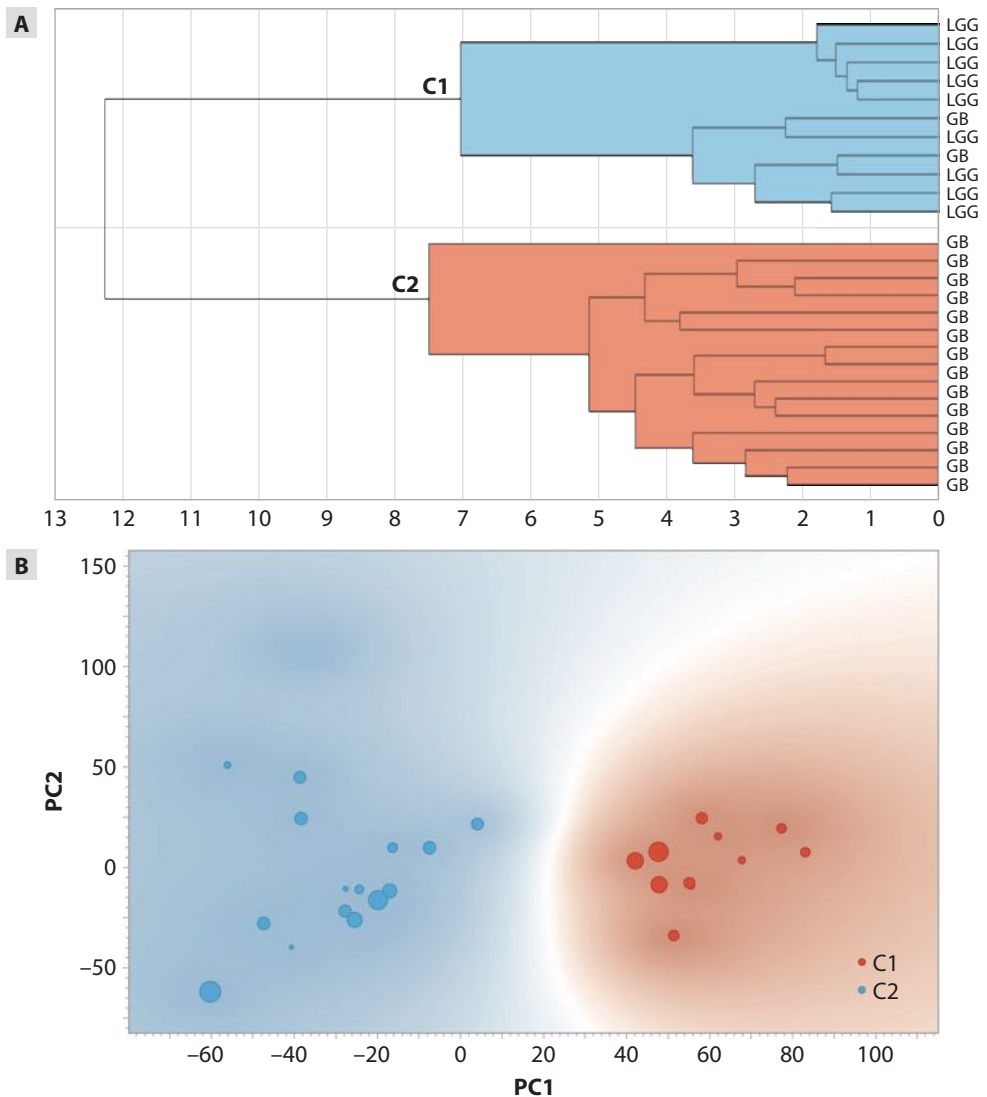


Fig. 3.5.4. Stemness score analysis based on stemness-related markers

(A) Hierarchical clustering analysis shows separation of glioma patient samples. (B) PCA shows the distribution of stemness score in C1 and C2 clusters. The size of circle represents stemness score value.

Furthermore, we used to develop a nomogram by integrating the stemness score, total m⁶A methylation level and clinical characteristics of glioma patients (Fig. 3.5.5). According to performed nomogram, the most important clinical factors were Ki-67 status, tumor location, pathology, and patients' age. It was particularly important to emphasize that nomogram-based model

had certain limitations and provided prognosis at diagnosis not at evaluation [195]. Also, limited sample size may bring bias in reliability of the risk prediction. For the nomogram to be sufficiently accurate, it should be performed on a large sample set.

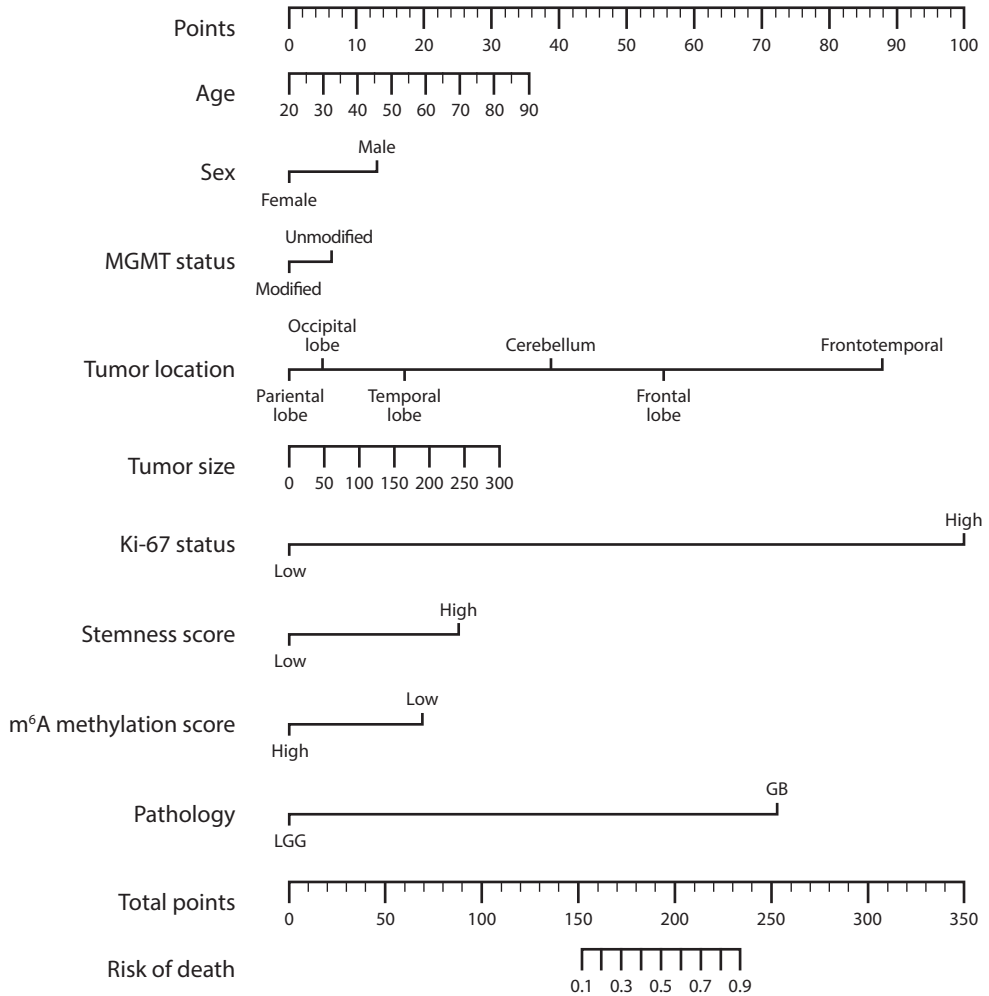


Fig. 3.5.5. *Nomogram for predicting risk of death for individual glioma patient*

3.6. Analysis of expression levels in target genes

We shifted our focus to investigating target genes expression inside the glioma patients after finishing the analysis of the stemness. In order, we conducted a thorough gene expression analysis, using accepted practices to assess the clusters' differences in expression patterns. The approach gives us

a better understanding of the gliomas behind the observed clustering and enable us to investigate the potential effects of epitranscriptomic changes on gene expression. We sought to identify significance in the pathophysiology of gliomas by combining gene expression and patients' clinical data.

Our starting point was to look at the target gene expression in patients' samples clusters classified after m⁶A methylation. We aimed to examine expression patterns of the target genes collectively and estimate potential impact on analyzed samples. The expression of the 7 target genes shown into a heatmap (Fig. 3.6.1 A). In addition, box plot analysis showed clear tendency to have higher combined target genes expression levels in the glioblastomas cluster C1 compared to C2 cluster (Fig. 3.6.1 B).

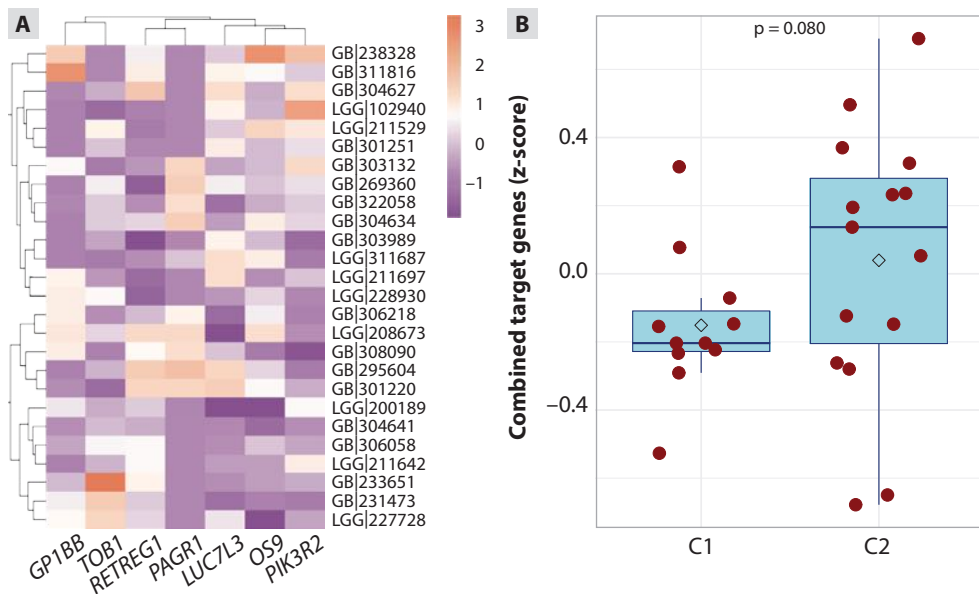


Fig. 3.6.1. Target gene expression patterns in glioma patients

(A) Heatmap of target genes in all patients, (B) box plot of target genes expression in C2 and C1 samples. Horizontal line in the boxes shows median, quadrates – mean.

The Kaplan-Meier survival analysis (Fig. 3.6.2 A) indicated that there were no significant differences in survival between glioma patients with high and low combined gene expression levels ($p > 0.05$). Additionally, the analysis did not reveal any tendency for survival differences based on the combined gene expression levels only in C2-glioblastomas cluster (Fig. 3.6.2 B).

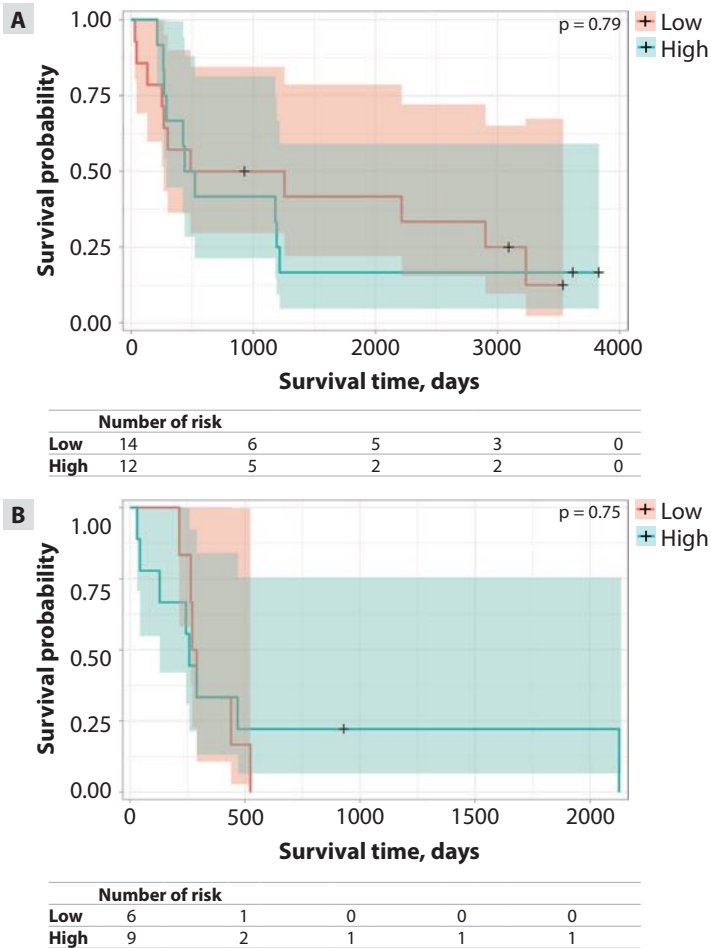


Fig. 3.6.2. Kaplan-Meier survival curves of patients' overall survival time with low and high combined target genes

(A) all glioma patients and (B) glioblastomas only.

Since we were unable to identify any significant associations between combined target gene expression levels in glioma patients, it is crucial to look at each gene separately. For that reason, we looked more deeply and accurately at possible relationships between m⁶A methylation-based clusters and stemness-related gene expression levels.

Our results showed that target gene *PIK3R2* had significant differences in clusters ($p < 0.019$) contained higher gene expression levels in cluster C1 (Fig. 3.6.3). There is a tendency to have higher *PAGRI* gene expression levels in cluster C2 ($p = 0.051$).

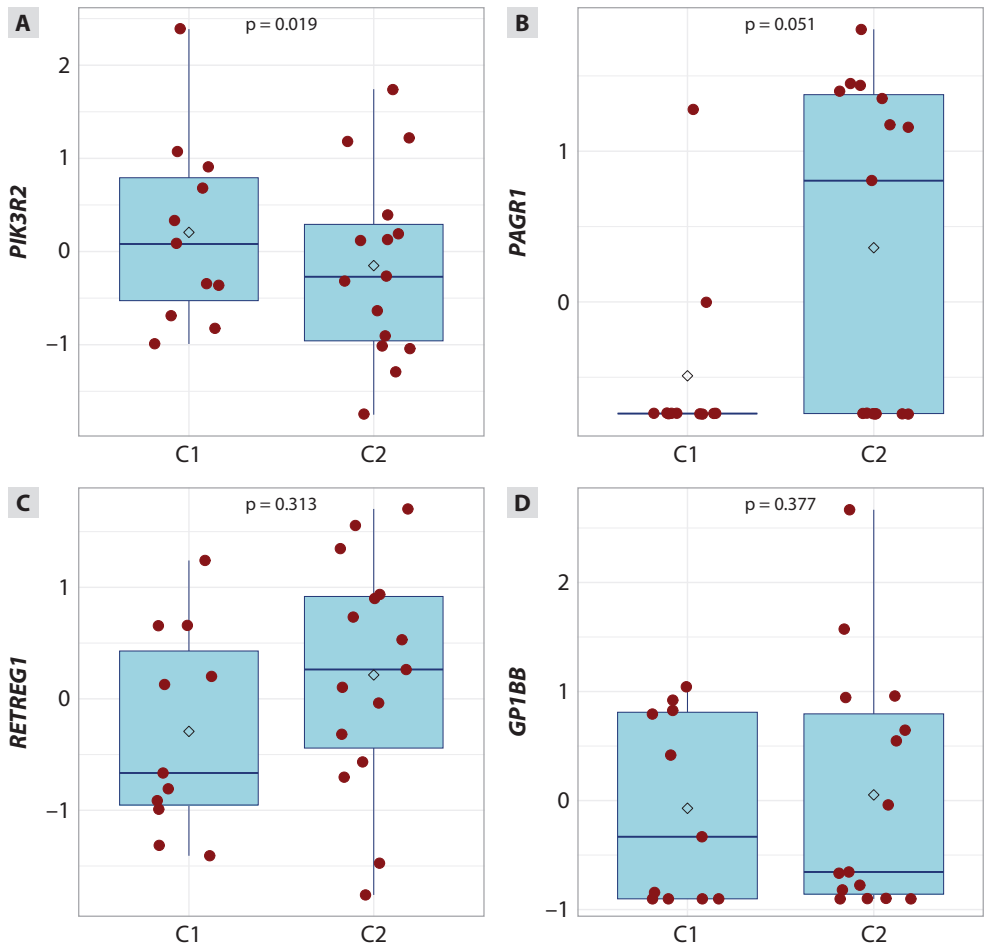


Fig. 3.6.3 (A–D). Individual target gene expression patterns in clusters (z-score)

Horizontal line represents median, quadrate – mean.

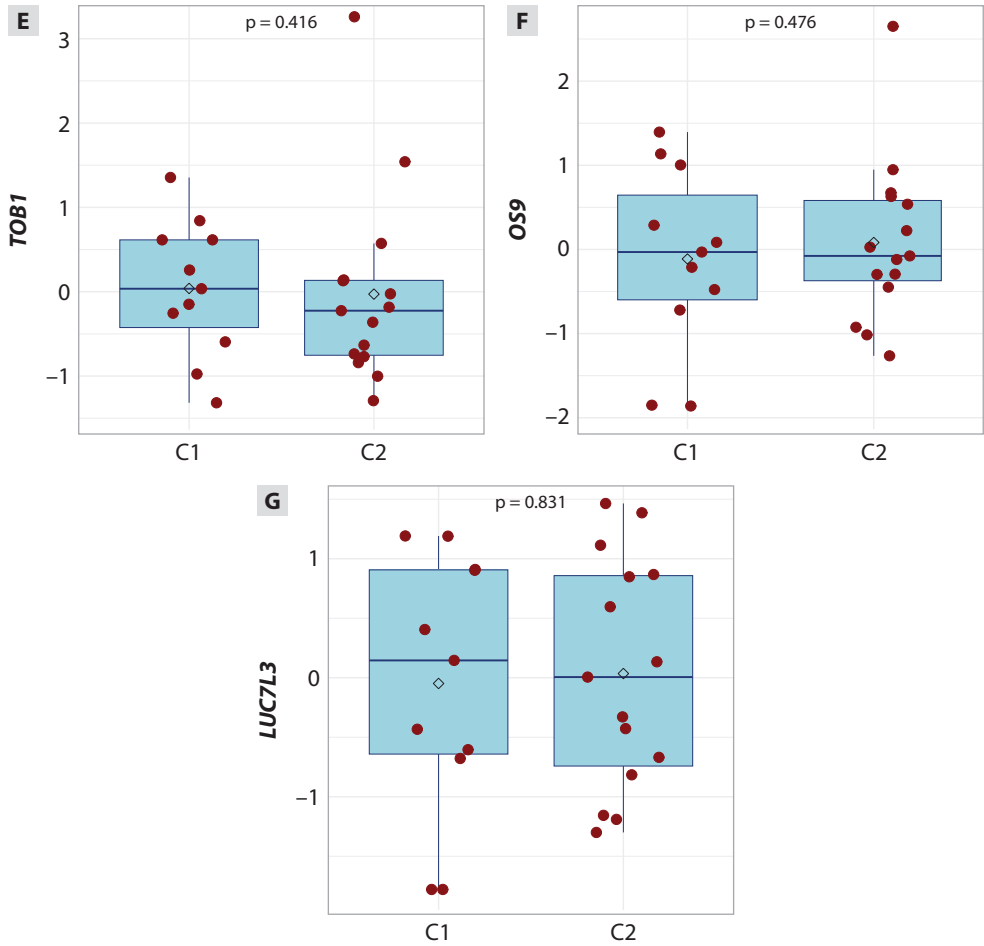


Fig. 3.6.3 (E–F). Individual target gene expression patterns in clusters (z-score)

Horizontal line represents median, quadrate – mean.

Subsequently, we conducted a correlation analysis to investigate relationship between stemness-related genes (used for stemness score calculation) and our identified target genes in cluster C1 (Fig. 3.6.4 A) and cluster C2 (Fig. 3.6.4 B). We expected to reveal significant correlations with certain target genes showing associations with specific stemness-related genes. The results revealed significant correlations, with target genes showing positive or negative associations with specific stemness-related genes. In cluster C1, the target genes *PIK3R3*, *TOB1*, *GP1BB*, *RETREG1* had strong statistically positive significant correlation ($p < 0.05$) with the stemness genes *EZH2*, *HIF1A*, *LGR5* and *PROM1*, respectively. Also, *GP1BB* target gene had a strong, statistically significant negative correlation with the *CD34* stemness gene, and *RETREG1* target gene had a moderate, statistically significant negative correlation with the *TWIST1* stemness gene ($p < 0.05$). Additionally, cluster C2 which only contains glioblastoma samples showed that *PIK3R3* target gene had a strong positive statistically significant correlation with the stemness-related genes *CD34* and *KDM5B* ($p < 0.05$), and the *GP1BB* target gene had also a positive statistically significant correlation with the *LGR5* stemness-related gene ($p < 0.05$). We also see a trend for the target gene *LUC7L3* to have a moderate positive correlation with the *CD34* stemness gene ($p = 0.06$), as well as the *PIK3R3* target gene with the *TWIST1* stemness gene ($p = 0.05$) and *GP1BB* to have a negative correlation with the *CD44* gene ($p = 0.06$).

In this analysis, we identified significant correlations between our selected target genes and stemness-related genes. Stemness is a hallmark of cancer stem cells which are known to drive tumor initiation, therapy resistance, recurrence, or progression of gliomas [196, 197]. The associations found suggest that our target genes may play a role in preserving the stem-like characteristics, which may have an impact on tumor aggressiveness. This association also suggests that our target genes could be used as therapeutic targets to interfere biomarkers, which could slow the growth of tumors and increase the effectiveness of treatment.

3.6.1. Target gene expression relations to epitranscriptomic data

Although it has long been known that RNA modifications stabilize RNA molecules and guarantee their accurate function [198]. Changes in RNA modification patterns which are frequently caused by variations in protein expression can disrupt the balance and result in the irrational activation or suppression of protein synthesis [199, 200]. Such dysregulation highlights the carcinogenic potential of epitranscriptomic changes by driving tumorigenic effects, such as uncontrolled growth of cells, invasion, or self-renewal [201–

203]. At first, we checked combined gene expression with total m⁶A methylation relations by Chi-square analysis which showed no significant differences in glioma patients (coefficient = 0.009, p = 0.926), then in cluster C1 (coefficient = 2.507, p = 0.113) and cluster C2 (coefficient = 0.601, p = 0.435). Exploring the relationship between total m⁶A modifications and gene expression we did not find any significant or direct correlations which suggested that total level of methylation across the transcriptome may not directly predict gene expression changes in a straightforward manner. However, it became crucial to concentrate on particular genes which could distinguish scenarios in methylation to be more prominent in the regulation of genes.

3.6.2. Individual target genes' expression relations to patients' clinical data in clusters

Pearson Chi-square test was used to assess individual target gene expression with patients' clinical data stratified by clusters to explore how specific gene expression patterns associated with clinical factors (Table 3.6.2.1).

According to our results, we found significant relationship between *RETREG1* gene expression and MGMT status (p = 0.034) and tumor location (p = 0.027) in cluster C1. In gene *GP1BB* there were significant associations with stemness score in cluster C2 which showed that high gene expression associated with high stemness score (p = 0.044). Also, *TOBI* gene showed significance relationship with patients' age in cluster C1 and *PAGRI* gene – glioblastomas' subtype (p = 0.004).

Table 3.6.2.1. Associations of glioma patients' clinical data and individual target gene expression in clusters

	<i>LUC7L3</i>				<i>RETREG1</i>			
	C1		C2		C1		C2	
	χ^2	p value	χ^2	p value	χ^2	p value	χ^2	p value
Survival time, days	1.21	0.415	0.84	0.356	1.42	0.657	1.16	0.796
Age	0.55	0.077	-0.31	0.245	-0.32	0.339	-0.17	0.549
Sex	2.75	0.097	0.10	0.751	0.74	0.391	0	1
MGMT	0	1	0.06	0.809	4.482	0.034	0.63	0.426
Subtype	2.04	0.361	0.27	0.874	2.04	0.361	3.28	0.194
Location	3.61	0.462	4.06	0.255	11	0.027	1.38	0.709
Tumor size	0.162	0.635	0.10	0.735	0	1	0.10	0.751
Ki-67	< 0.01	0.924	< 0.01	1	0	1	0.74	0.388
Stemness score	-0.15	0.668	0.04	0.881	0.74	0.391	0	1

Table 3.6.2.1. Continued

	<i>OS9</i>				<i>PIK3R2</i>			
	C1		C2		C1		C2	
	χ^2	p value	χ^2	p value	χ^2	p value	χ^2	p value
Survival time, days	0.92	0.909	0.56	0.305	4.93	0.140	1.15	0.806
Age	2.23	0.136	0	1	0	1	0	1
Sex	2.75	0.097	0	1	0	1	0	1
MGMT	0.16	0.689	0	1	< 0.01	0.953	0.06	0.809
Subtype	2.04	0.361	0.27	0.874	1.39	0.497	3.45	0.178
Location	3.61	0.462	1.38	0.709	3.08	0.545	1.38	0.709
Tumor size	0	1	0	1	< 0.01	0.953	0	1
Ki-67	< 0.01	0.924	0	1	0	1	0.44	0.509
Stemness score	2.75	0.097	0.84	0.360	0	1	0.03	0.855
	<i>GP1BB</i>				<i>TOBI</i>			
Survival time, days	1.45	0.628	0.38	0.104	2.15	0.326	1.11	0.858
Age	0	1	0	1	4.65	0.031	1.64	0.201
Sex	0	1	0	1	0	1	0.10	0.751
MGMT	0.74	0.391	0.63	0.426	0	1	0	1
Subtype	2.04	0.361	0.77	0.680	2.03	0.361	1.27	0.529
Location	3.61	0.462	1.38	0.709	8.31	0.081	2.28	0.517
Tumor size	2.75	0.097	0	1	0.16	0.687	0.10	0.751
Ki-67	0	1	0	1	0	1	0	1
Stemness score	0.74	0.391	4.05	0.044	0.74	0.391	0	1
	<i>PAGRI</i>							
Survival time, days	< 0.001	0.999	1.55	0.449				
Age	0.86	0.35	0.05	0.809				
Sex	0	1	0.10	0.751				
MGMT	0	1	0	1				
Subtype	11	0.004	0.27	0.875				
Location	6.52	0.164	1.38	0.709				
Tumor size	0	1	0.55	0.460				
Ki-67	0.75	0.387	0	1				
Stemness score	0	1	0.03	0.855				

Finally, Cox's proportional hazard analysis was performed with set off all targeted protein-coding mRNAs to evaluate numerical changes in mRNAs expression related to all glioma patients' survival. The significant impact on glioma patients' survival time had an expression of *LUC7L3*, *OS9* and *TOB1* genes (Table 3.6.2.2). The most effective mRNA for the shift of patients' baseline hazard of survival was *OS9* indicating the strongest relationship between *OS9* gene expression and increased risk of death (8.9-fold increase) which means gene is the most associated with a poor survival.

Table 3.6.2.2. Cox's proportion hazard importance of target mRNA expression in gliomas for patients' survival

	Coefficient	Effect	p value
<i>LUC7L3</i>	-0.41	Decrease 0.6 times	0.031
<i>RETREG1</i>	0.10	Increase 1.1 times	0.637
<i>OS9</i>	2.19	Increase 8.9 times	0.0006
<i>PIK3R2</i>	0.38	Increase 1.5 times	0.47
<i>GP1BB</i>	0.03	Increase 1.03 times	0.87
<i>TOB1</i>	-1.07	Decrease 0.35 times	0.030
<i>PAGRI</i>	-0.04	Decrease 1 times	0.86

To display the Hazard ratios linked to our target gene expression levels we performed a forest plot analysis (Fig. 3.6.2.1). The forest plot analysis revealed distinct patterns of gene expression changes, with three genes showing statistically significant alterations. The most pronounced change was observed in *OS9*, which exhibited a substantial upregulation (8.9-fold increase, $p = 0.0006$). Two genes showed significant downregulation: *TOB1* (0.35-fold decrease, $p = 0.030$) and *LUC7L3* (0.6-fold decrease, $p = 0.031$). The following genes showed no statistically significant changes ($p > 0.05$): *PIK3R2*: 1.5-fold increase ($p = 0.47$), *RETREG1*: 1.1-fold increase ($p = 0.637$), *GP1BB*: 1.03-fold increase ($p = 0.87$) and *PAGRI*: no substantial change ($p = 0.86$). These results highlight the potential of target genes as biomarkers for targeted therapies and personalized treatment interventions in glioma management.

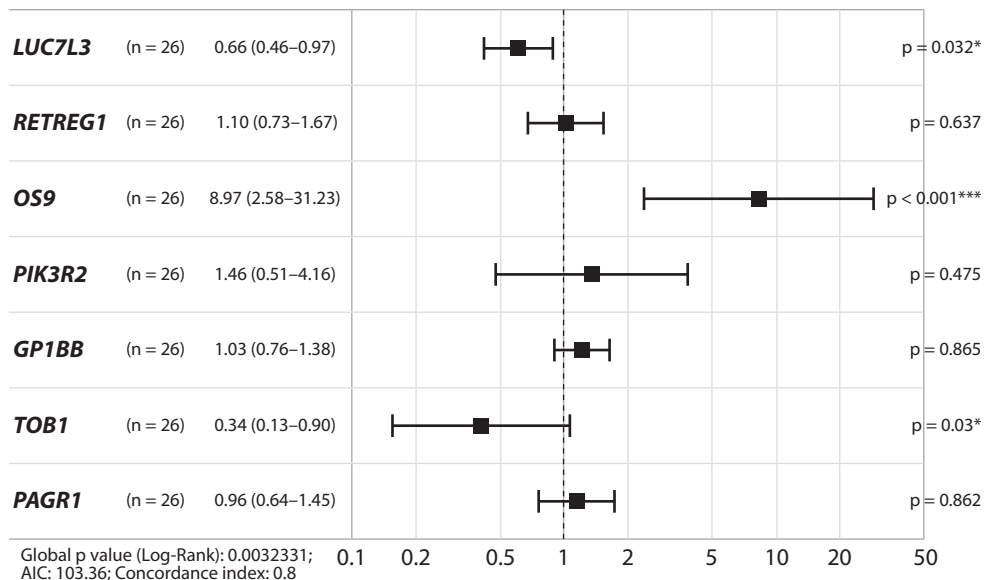


Fig. 3.6.2.1. Forest plot of hazard ratios showing the survival-associated of target protein-coding RNAs in glioma patients

The end of the whiskers shows the 95% confidence.

3.7. mRNA signaling pathways related to stemness in m⁶A methylation-based clusters

Signaling pathways play a crucial role in regulating stemness, which contribute to self-renewal, differentiation, and survival in glioma stem cells. They are complex and comprise molecular signals and regulatory elements associated with glioma stemness [204]. Glioma tumors are glial cell-derived and have unique cellular and molecular features that are frequently caused by dysregulated signaling pathways [205]. Additionally, glioma cells have the ability to control cell communication by manipulating the information sent to the target cells, interacting with the receptor to produce particular biological effects including cytoskeleton alterations and cell proliferation, and promoting angiogenesis and glioma growth [206]. To analyze signaling pathways is essential particularly in addressing challenges such as heterogeneity, therapy resistance, and recurrence in gliomas and monitoring of stemness-related signaling pathways could help predict tumor development and progression [207].

Scientists have already identified signaling pathways that are associated with stem cell properties. Every stemness-related pathway involves stemness markers. Wnt/ β -catenin signaling pathway enhancing tumor stemness and includes stemness markers such as *CD24*, *PROM1*, *CD44*, and *ALDH1* [208], Notch signaling pathway – *CD133*, *Notch1*, *Notch3*, *JAG1*, *JAG2* [209–211]. Pathway JAK/STAT includes variety of ligands and receptors, hormones, interleukins, and interferons [212]. Proteins JAK1-3 and TYK2 are activated by phosphorylation upon ligand attachment to receptors and that recruits the STAT family proteins [213]. As same as Notch and Wnt signal pathways, JAK/STAT promotes stem cell self-renewal and neurogenesis [214]. Tumor-initiating effect of this pathway in glioblastoma describes its function in stem cells regulation [215]. The transforming growth factor (TGF)- β -activated JAK/STAT pathway promotes the ability to self-renew and inhibited the differentiation of glioma-initiating cells obtained from patient tumors in a glioblastoma model, which facilitated the formation of tumors [215, 216]. It has been suggested that activation of the HH signaling pathway (Hedgehog) supports proliferation and stemness in stem cells in various types of cancer including gliomas [217–219]. NF- κ B signaling pathway mediates the tumorigenesis of glioma [220] while PI3K/AKT is crucial for stem cells population maintaining [221] where overexpression and/or mutation of EGFR leads to activation of pathway and patients have poor prognosis [222, 223].

Here, we decided to check signaling pathways associated with m⁶A methylation-based clusters C1 and C2. We conducted KEGG (Kyoto Encyclopedia of Genes and Genomes) analysis to delve deeper into biological significance (Fig. 3.7.1).

After performing KEGG pathways analysis, top 15 most enriched signaling pathways were found for cluster C1 (Fig. 3.7.1 A) and cluster C2 (Fig. 3.7.1 B). Notably, cluster C2 consists of GB patients, revealed a significant enrichment of stemness-associated pathways JAK-STAT and PI3K-Akt which are crucial for maintaining the self-renewal and aligns with the aggressive glioblastomas' nature and tumor progression. The presents of stemness-related pathways suggest that GB cells in cluster C2 may exhibit enhanced tumor-initiating potential, resistance to therapy and ability to adapt to tumors microenvironmental conditions. This enrichment indicated that GB patients are likely to have a poor prognosis compared to LGG (cluster C1) which often links to aggressive tumor behavior.

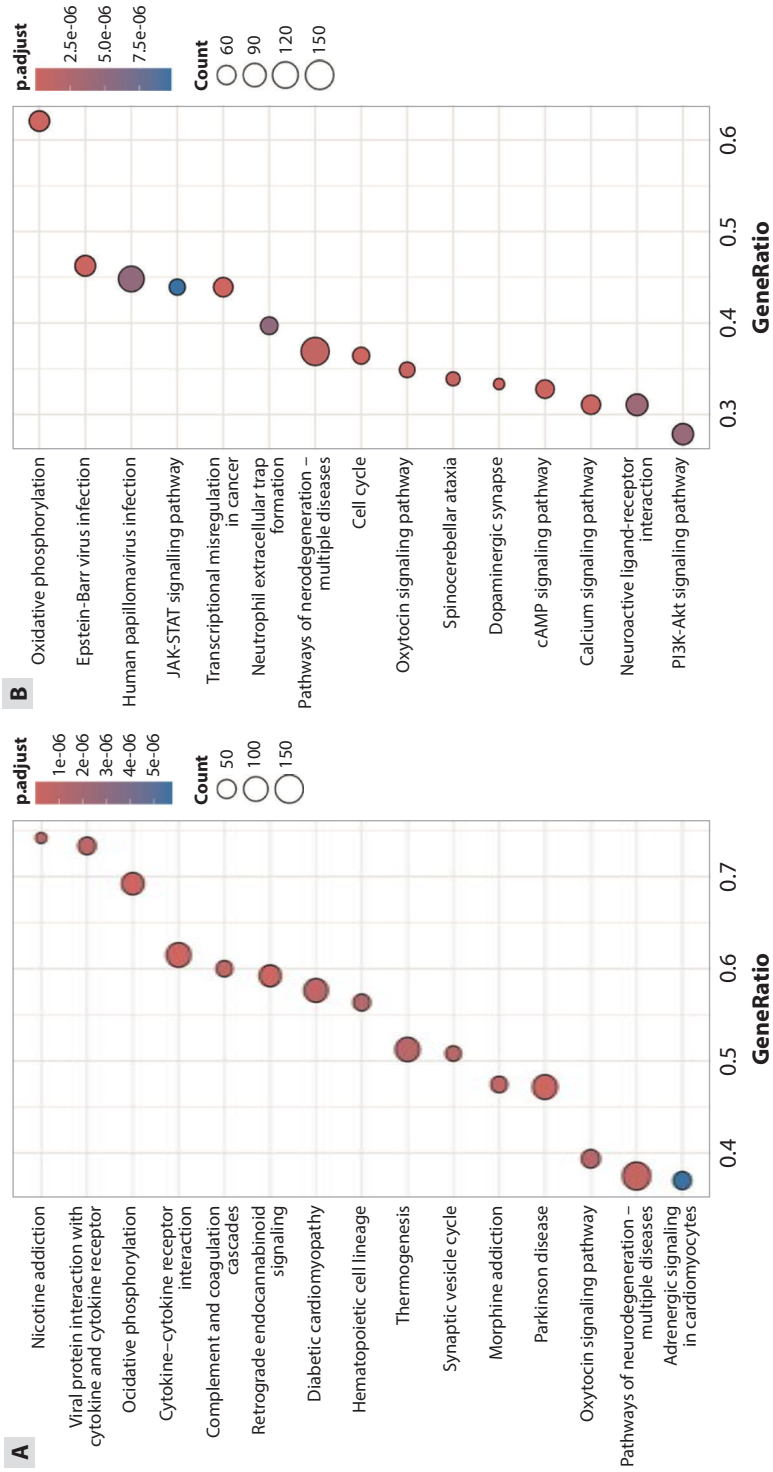


Fig. 3.7.1. Visualization of the top 15 most enriched signaling pathways was performed in *m⁶A* methylation-based clusters

(A) C1 cluster and (B) C2 cluster. The size of the dots indicates the number of genes enriched. The larger the dots, the more genes are enriched in the function. Color of the dots represents the corrected p value.

In cluster C2, the Gene Set Enrichment Analysis (GSEA) results show that both JAK-STAT and PI3K-Akt signaling pathways are positively regulated (Fig. 3.7.2). Results highlighted that molecular mechanisms driving the malignancy of GB in cluster C2 and also underscore the poor prognosis associated with glioblastoma compared to cluster C1. These pathways could serve as potential targets to disrupt the aggressive behavior of glioblastomas and should deserve more attention in further research.

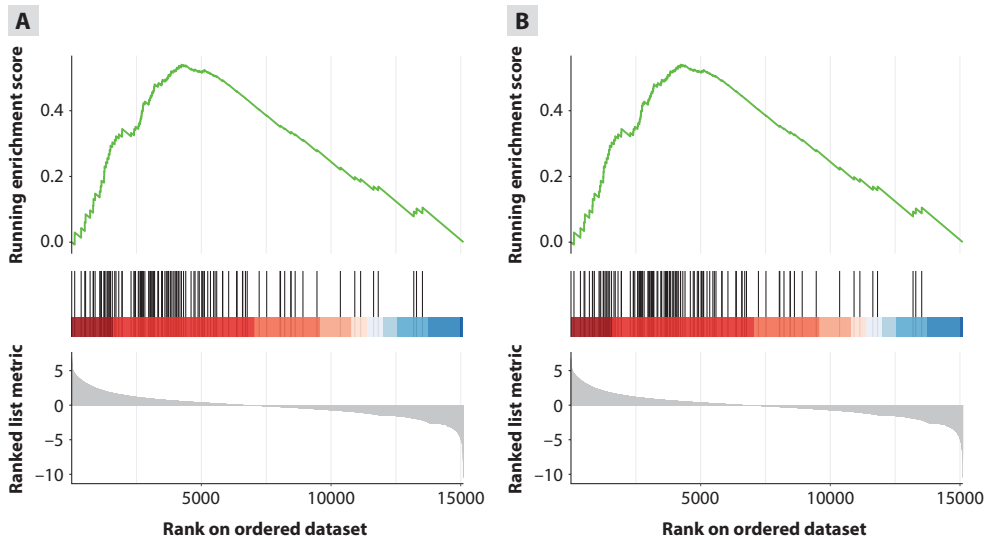


Fig. 3.7.2. Gene set enrichment analysis (GSEA) of significant stemness-related pathways in glioblastomas cluster C2

(A) Represents gene set enrichment analysis of JAK-STAT signaling pathway. (B) PI3K-Akt signaling pathway. In a ranked list of all the genes found in the dataset, the GSEA algorithm determines an enrichment score that indicates the level of overrepresentation at the top of the list of genes included in a gene set. Red color indicates high genes expression or positive enrichment scores. Genes associated with a particular gene set are enriched at the top of the ranked list, suggesting they are upregulated. Blue color represents low genes expression or negative enrichment scores. Those genes are frequently at the bottom of the ranked list, indicating they are downregulated.

Fig. 3.7.3 represents genes involved in stemness-related pathways. Gene-concept network visualize the relationships between core enriched genes and pathways identified after GSEA analysis. The plot focused on genes which contributing most significantly to the enrichment in the stemness-related pathways.

This analysis highlights the complexity of stemness-related pathways, as the same genes can be involved in multiple functional pathways. Results provides important insights into molecular mechanisms underlying stemness

and could be useful in locating possible cancer therapeutic intervention targets in future studies [224–226].

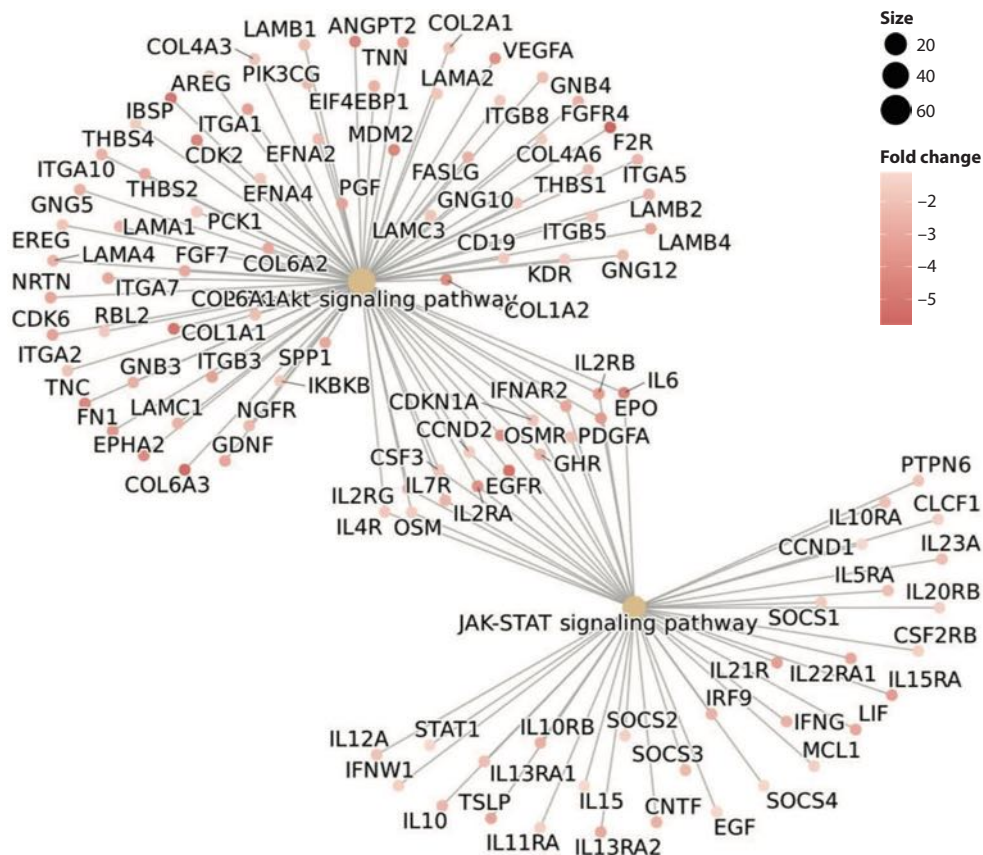


Fig. 3.7.3. Network plot of enriched PI3K-Akt and JAK-STAT signaling pathways in glioblastomas cluster C2 supported with only core enriched genes displayed

Investigation of m⁶A methylation-based clusters has indicated striking enrichment of stemness-related signaling pathways in GB cluster C2 when compared to C1 cluster. The weight of this enrichment confirms the fact that positive activation of stemness-related pathways in GB cluster C2 is consistent with the aggressive and poor prognosis of GB patients. Furthermore, the findings of this study shows that GB related tumors is related to therapy resistance and recurrence which is also described by other researchers [227, 228]. By blocking these pathways, it is possible to produce new ways to treat the patient that can be more effective especially in GB, since the current treatment does not work properly [224, 226].

DISCUSSION

Although many researchers looking for innovative biomarkers in gliomas which could provide insights into glioma tumor biology and potential therapeutic targets, however, glioma, especially glioblastoma, still causes concerns. Despite the understanding of biology, gliomas remain highly resistant to any therapy due to late detection, difficult treatment, and tumor aggressiveness [229, 230]. Even with the challenges including genetic heterogeneity or tumor microenvironmental, there are several options applied for gliomas treatment [231, 232]. The standard of care for diagnosed GB patients involves total/subtotal surgical resection, radiotherapy, immunotherapy, and adjuvant chemotherapy [233], however the standard treatment at some points can be out of luck. Therefore, future research efforts must focus on target identification to reveal approaches to regulate tumor microenvironment or target specific molecules [234].

Glioma-initiating cells (or called glioma stem cells) are the hallmark of relative resistance to treatment in glioblastoma and became extremely tempting for novel treatment therapies against this disease [235, 236]. GSCs represent only a small part of the tumor bulk mass but at the same time participate in many important processes that the growth of the tumor progresses [237]. GSCs promote the development of the initial damage by inducing the differentiation of cancer cells, which have the ability to multiply rapidly. Even when transplanted into the brains of mice, GSCs induce the development of tumors phenotypically similar to the donor tissue [237]. Recent studies have shown a role for GSCs in promoting tumor invasiveness, especially in subpopulations expressing certain, already validated, stemness markers [238, 239]. Meta-analyses have shown that expression of certain stemness genes correlates with poor survival in patients with higher tumor progression, especially in patients with glioblastomas but not grade II and III gliomas, while higher expression levels of other stemness markers correlate with worse survival in patients with only grade II or grade III gliomas [240]. Thus, glioma stem cells are given as the instance of high-throughput experiments, which could be used to discover the molecules targeting such cells [241]. Moreover, converting the enthusiasm for experimental therapies into having successful clinical outcomes led the scientists to a great deal of trouble. Despite the fact that detaining GSC activity is an issue, it is still possible to prevent the therapy-induced phenotype conversion that feeds the remaining tumor of its GSC population and also favors recurrence [236, 242].

m⁶A modification plays another exceptionally key role in gliomas. Recent studies have shown m⁶A modification role in affecting cell survival,

proliferation, invasion [243], and the mRNA m⁶A methylation was observed to have a crucial role in glioma stem cells, which could be key to initiating the tumor and lead to the resistance of a therapy [244]. There is a lot of research on the regulators of m⁶A modifications (called *writers*, *readers*, and *erasers*). It has already been confirmed that modulators such as *METTL3*, *ALKBH5*, *FTO* – maintaining GSC stemness whose downstream targets are *Sox2*, *SSEA1*, *FOXMI*, *ADAM19*, *EPHA3*, *KLF4* [102, 202, 245] and the expression levels in glioblastomas are quite high [246]. There is some contradictory research where the levels of certain m⁶A writers in GB are lower and thus the anti-cancer properties of m⁶A regulators are evident [106, 247]. Contradictions indicate that m⁶A-related methylation might have a complicated impact on the process of GB formation and development. Despite the thorough study of the contributions of m⁶A modification to glioma or GSCs regulation, there is no or little consistent and clear information on the specific modes of actions in the processes or targets.

In this dissertation, we tried to demonstrate mRNA m⁶A modification profile in GSCs and glioma tumors which could help to assess the associations with tumorigenicity and to select GSC specific m⁶A mRNR molecules that could be potential clinical markers and therapeutic candidates. This study may be useful in clinical practice to develop new GB treatments targeting GSCs. Since focus of the dissertation was m⁶A modifications, for this purpose, we identified modified peaks in glioma stem cells compared to glioblastoma cell lines, whose expression was up- and down-regulated. Genes that were modified in GSCs were analyzed in glioma patients using a logistic regression model and chi-square test. Since our modification data in glioma patients was binary, we chosen logistic regression model which designed to model binary outcomes and allowed us to estimate the probability of patient being modified based on the presence of specific RRACH motifs. We identified 8 significant RRACH motifs in glioma samples and, according to hierarchical clustering analysis, samples were classified according to pathology. Target RRACHs were described in detail and the associations of these motifs with clinical characteristics of the patients were evaluated. We interpreted the identified motifs as stemness-related since the genes were selected from the epitranscriptome profile of glioma stem cells.

Our results including 8 GSC specific m⁶A modified RRACHs validated the existing research papers suggesting that a lower m⁶A modification level promotes tumorigenesis and glioblastoma cell growth. Lower-grade gliomas are likely to have higher m⁶A modified compared to glioblastomas which lead to better survival prognosis [248]. For instance, lower m⁶A modification levels in *ADAM19* or *FOXMI* mRNAs regulate GSC self-renewal [8, 202]. mRNAs *FTO* and *ALKBH5* are the two primary demethylases that are critical

for lowering the level of m⁶A methylation and necessary for keeping the GSC to a self-renewing and tumorigenic state. A highly expressed in GSCs *ALKBH5* gene has been shown to be responsible for their proliferation and self-renewal abilities [249]. The reduction in m⁶A levels by the force of higher demethylases activity allows the oncogenic mRNAs to be retained and thus the tumor grows and becomes more severe [243]. A study conducted on nineteen m⁶A highly methylated mRNAs in gliomas highlighted *IGF2BP3* as the most obviously affected gene. Additional research revealed that glioma patients with *IGF2BP3* overexpression had a strikingly lower chance of survival as compared to the ones who had low *IGF2BP3* levels [243, 250]. Likewise, m⁶A modified demethylases *FTO* and *ALKBH5* are very crucial in controlling the growth and invasion of lung cancer cells by the removal of methyl groups, thus affecting the stability and translation efficiency of mRNA [251], *METTL3* and *METTL14* directly target mRNA *MYC*, which repressing differentiation [252]. Thus, the mRNA m⁶A methylation can activate or inhibit various processes in cancer depending on the analyzed target or cellular context.

It was revealed some important associations of the analyzed RRACH motifs with the clinical characteristics of the patients together and individually in each RRACH. The clinical factors associated with target gene methylation identified as age, tumor location, overall survival, Ki-67 gene status, and GB subtype. Although our analysis showed a significant association between the overall and individual GGACA motif methylation in the *OS9* gene, AAACC in the *PIK3R2* gene, GGACA motif in the *RETREG1* gene, and age, it would be misleading to assume that m⁶A methylation is related to the age of the patients. Employing univariate and multivariate Cox analysis, it was determined that an increased age and higher m⁶A risk scores were independent, negative prognostic factors for the glioma patients [253]. It was concluded in an earlier examination that age was also an independent risk factor for GB, and that growing old can lead to less favorable survival outcomes [254]. It has not been confirmed how m⁶A methylation is related to tumor location yet. This study showed a unique significant association between m⁶A methylation and tumor location. High methylation level was associated with central tumor locations in the cerebellum and frontotemporal lobes compared to other tumor locations. The main lobes where glioblastomas are localized are the frontal and temporal lobes [255]. Corr et al. [256] review showed that there is a lack of prospective studies analyzing the prognostic, anatomical, and radiological characteristics of GB, which would facilitate the determination of tumor recurrence, focusing on an individualized treatment and monitoring strategy. It was demonstrated a non-significant trend in GB tumor samples from the cerebellum region of the brain compared to other locations

[257]. On the other hand, low-grade glioma tumors are more frequently found brainstem region and tend to have better prognosis compared to glioblastomas [258]. Considering the location of tumors in the brain, the main lobes where gliomas are localized are the frontal and temporal lobes and associated with a poor patients' outcome which was also emphasized by other researchers. Aggressive glioma tumors mostly occur in the temporal lobe and affect adolescents and adults while survival time is about 10.3 month [259]. Interestingly, MGMT methylated status and low Ki67 status were correlated with GB in the frontal lobe compared to those in other locations. Whereas temporal lobe was associated with MGMT unmethylated status [260]. For precise diagnosis, prognosis, treatment planning, and the advancement of neuro-oncology research, tumor location analysis is crucial. Glioblastomas have strong tumor heterogeneity and plasticity; therefore, it is challenging to accurately identify molecular subtypes [261–265]. Our finding outcome was in line with the finding that proneural subtype associated with a better prognosis in GB patient more than classical and mesenchymal [7, 266]. m⁶A methylation associations with glioblastoma subtypes have not yet been investigated. Interestingly, we highlighted that m⁶A methylation at the *LUC7L3* GGACT RRACH motif is detected in 78% of all classical GB tumors which was associated with poor GB patient prognosis. In addition, two glioblastoma patients who were assigned to cluster C1, which was dominated by LGG, based on overall target gene methylation, had high m⁶A scores, one of the classical type and the other of the mesenchymal type, and both patients had better survival prognosis. Controversial results, provide new insights into the m⁶A methylation profile in gliomas, but it should be investigated by applying functional and sequencing approaches in more depth.

In our study, we identified m⁶A modified RRACH motifs in glioma patients' samples: AAACA|2129|*OS9*, AGACA|1210|*PAGRI*, GGACA|2173|*OS9*, GGACT|2187|*TOBI*, AAACC|3283|*PIK3R2*, GAACC|3068|*GP1BB*, GGACA|3110|*RETREG1* and GGACT|3122|*LUC7L3*, as potential mRNA candidates related to GSCs.

Both *OS9* AAACA and *OS9* GGACA mRNA RRACHs were highly methylated in LGG tumor tissues and showed better prognosis compared to GB patients whose tumors were unmethylated. Endoplasmic reticulum-associated degradation (ERAD) and ER-to-Golgi transport are two cellular mechanisms that have been linked to *OS9*, a protein that was first discovered to be elevated in osteosarcomas [117, 267]. In the case of osteosarcoma, where its amplification may contribute to tumor growth and progression, its correlation with cancer is especially noteworthy. It has been demonstrated to interact with proteins involved in several cellular processes, including those that could be implicated in the development of cancer. Since many oncogenic

processes can result in protein misfolding and stress responses inside the endoplasmic reticulum, *OS9*'s relationships and functions may specifically impact how cells manage misfolded proteins, which is a crucial factor in the context of cancer [268–270]. An interesting study was conducted applied luciferase experiments where novel long non-coding RNA (lncRNA) *ENST00000480739* positively regulated *OS9* by activating the transcription level of the *OS9* promoter, and overexpression of *ENST00000480739* lncRNA markedly boosted both the mRNA and protein levels of *OS9*. It was also demonstrated that *ENST00000480739* may target the expression of hypoxia-inducible factor-1 α (HIF-1 α) by upregulating *OS9* [271]. Furthermore, phase II research were performed where 17 patients with recurrent IDH1/2 wild-type glioblastoma who had not yet received bevacizumab. Oral, selective antagonist of G protein-coupled receptor *ONC201*, which causes apoptosis in tumor cells via *AKT/ERK* pathway inactivation, were given to glioblastoma patients every three weeks. With an *OS9* of 53%, the median overall survival was 41.6 weeks [272]. Although, *OS9* mRNA shows potential impact in tumor growth, apoptosis and development of cancer, further studies would be necessary to fully clarify the role in gliomas.

A potential implication in neurodevelopmental of *PAGRI* mRNA was observed in the human fetal cerebral cortex at the 16p11.2 locus. The mRNA *PAGRI* is mentioned as one of the transcripts expressed in progenitor cells of the developing cortex [273]. Well-written study evaluated that *PAXIP1-PAGRI* directly is the source for the attachment of cohesin to chromatin. As cohesin not only participates in the regulation of genome stability but also takes part in controlling gene expression, it is now noticeably clear that it is an important factor in preventing oncogenesis [274]. A typical example can be cohesin mutations that causes chromosomal instability, which is a characteristic of cancer [275, 276]. *PAXIP1-PAGRI* might be responsible for changing the structure of chromatin and thus make cohesin much easier to come on. It is a pity that cancer often is accompanied by the disorganization of chromatin, which not only brings improper gene expression but also leads to cancer progression. If *PAXIP1-PAGRI* can effectively regulate chromatin, then some conclusions can be drawn about a new role of this protein in the brain, suggesting implications for neural processes [274]. Additionally, mRNA *PAGRI* expression correlated with smaller tumor size, low Ki-67 status and had better relapse-free survival in breast cancer, meaning that *PAGRI* serve as a potential prognostic indication [277]. Remarkably interesting phenomenon, mRNA *FoxM1*, when it comes to the activation of the *ASPM* promoter *PAGRI*, is indispensable in the regulation of glioblastoma cells: activation in Hs683 glioblastoma cell line and suppression in U87-MG [278]. As such,

PAGRI is a form of the ASPM protein that causes the general control mechanism to be activated and allowed into the promotion of the cell cycle.

Afterwards, the GGACT motif in the *TOBI* gene is highly m⁶A methylated in all LGG and in those GB patients who had a good survival prognosis. The information uncovered by the new research that controlling expression of mRNA *TOBI* in glioblastoma U87-MG cells through *ERN1* inhibition proving that endoplasmic reticulum stress is a main factor of cancer growth and *TOBI* gene plays a role in the process [122]. These findings are in good agreement with the information on mRNA *TOBI* biological involvement and its function in controlling cell proliferation [279–281]. Down-regulation of pro-oncogenic *TOBI* is linked to reduction of cell proliferation driven on by inhibition of *ERN1* enzymatic activity [282–284]. We can state, *TOBI* is a multifunctional gene that contributes to controlling the tumor cell proliferation and invasion. *TOBI* gene has only just begun to be intensively analyzed in glioma patients and the reviewed m⁶A methylation profile of this gene provides new insights for further studies as a potential marker for glioma patients.

Like the previously mentioned motifs, the *PIK3R2* AAACC RRACH also exhibited prominent levels of m⁶A methylation in LGG patients compared to glioblastomas. More recently, studies have shown that *PIK3R2* could serve as a prognostic marker for several cancers [135]. It was discovered that *PIK3R2* expression levels were linked to tumor growth being higher in later stages of breast and colon malignancies [186]. Our results unfortunately show the opposite trend. The expression levels were higher in C1 LGG-based cluster. This may have occurred due to the small sample size, glioblastomas abnormal expression, large necrotic and hypoxic regions in GB tumor, which could suppress *PIK3R2* expression, while less aggressive LGG had sufficiently high expression of this gene due to the less malignant phenotype. Also, in glioblastomas, the PI3K/AKT/mTOR pathway is often hyperactivated due to mutations or amplifications, such as loss of the EGFR or PTEN genes. This may reduce the dependence of *PIK3R2* expression on pathway activation [285]. However, high expression levels of *PIK3R2* were associated with better prognosis of rectum adenocarcinoma, had protective effect on prognosis for breast cancer and head and neck squamous cell carcinoma [135]. *PIK3R2* mRNA was believed to control tumor progression in Isabel Cortés et al. [186] investigation of colorectal and breast malignancies, where *PIK3R2* expression levels were also increased in over half of the tumor samples. *PIK3R2* may act variously in different kind of cancers. This finding highlights the complexity of *PIK3R2* mRNA in gliomas and underscores the need for further research to understand the specific roles of *PIK3R2* in glioma progression.

Precise insights of mRNA *GP1BB* in cancer are unknown. Decreased mRNA expression of the gene *GP1BB* was observed in prostate cancer patients, which showed associations with better survival rates [286]. The same results were observed in colorectal cancer, where RNA-seq analysis was performed [287]. According to GTEx database *GP1BB* mRNA shows the highest median expression on brain cortex, however, Blanco-Luquin team in 2022 [288] was the first to describe *GP1BB* as a potential marker of cell fate in neurogenesis but there is no further research developed. Based on our findings, the mean expression of the *GP1BB* mRNA was higher in GB patients compared to LGG. We found that all C1 clusters' LGG patients had m⁶A modification in the brain cortex in RRACH GAACC in the *GP1BB*, the gene expression was downregulated compared to cluster C2 and associated with better survival prognosis. Although further studies should be performed to confirm.

There are some studies describing *RETREG1* mRNA role in cancer progression. This gene induces tumorigenesis in hepatocellular carcinoma [289], human esophageal squamous cell carcinoma [290], overexpressed in colon cancer and showed tumor suppressive properties [149, 291] and colorectal cancer by showing poor prognosis [292]. There are no studies on the association of *RETREG1* gene with glioma tumors. However, we found high m⁶A methylation levels in LGG patients compared to GB. m⁶A demethylation occurs during tumor progression which leads to increased gene expression.

According to all analyzed m⁶A target RRACHs, *LUC7L3* showed the opposite trend and was heavily methylated in GB compared to LGG and the expression of the gene did not differ from low-grade gliomas. A year ago, *LUC7L3* became a potential marker for hepatocellular carcinoma; it was revealed that high expression levels indicate worse clinical features and associated with enriched cell proliferation-related pathways [154].

As of right now, no precise information about m⁶A changes of seven target genes specific to GSCs is available. Although m⁶A modifications are known to have essential functions in a number of cellular processes, their particular effects have not yet been fully clarified, and research in this area is still in its early stages.

Moreover, it is necessary to emphasize several factors limiting the results. The small sample size is one of the study's main weaknesses. Glioblastomas are extremely heterogeneous in both genetic and epigenetic levels [293]. Small sample numbers may not fully represent the range of variability within glioblastomas and lower statistical power. To validate and expand these findings, larger cohort studies are required. In this study we used Nanopore technology sequencing, and the depth of the sequencing was another

limitation. A lack of sequencing depth can decrease the sensitivity and as a result there is a risk of missing of biologically key features [294]. Finally, the research into m⁶A RNA modifications faced challenges associated with m⁶A detection capacity. The m⁶A detection computational pipelines have yet not fully developed or optimized. This fact has implications on the accuracy of and number of RRACHs identified for m⁶A modification on the epitranscriptome.

Despite weak points and limitations, this study expands unique insights of mRNA alterations in glioma patients. Certainly, further studies are required to confirm or rebut specific mRNAs association with patients' clinical characteristics. Although, the revealed association of target genes may improve the prognosis of glioma patients. Eventually, this study provides a basis for further studies on m⁶A mRNAs methylation.

CONCLUSIONS

1. Epitranscriptomic m⁶A profiling of mRNA in glioma stem cells NCH421k revealed higher methylation level compared to glioblastoma U87-MG cells. 8 glioma stem cells specific transcripts of 7 genes were selected through integration of m⁶A methylation patterns with glioma patient data: *OS9*, *PAGRI*, *TOBI*, *PIK3R2*, *GP1BB*, *RETREG1*, and *LUC7L3*.
2. Clustering analysis based on set of 8 glioma stem cells specific m⁶A transcripts stratified patients into low grade glioma and glioblastoma clusters. The methylation level of m⁶A modified transcripts was 3.4 times higher in LGG compared to GB, which indicated the potential association of m⁶A modifications with gliomagenesis.
- 2.1 Glioma stem cells specific summed m⁶A methylation level and m⁶A score was significantly associated with patients' clinical characteristics – age and overall survival, while in glioblastoma patients – tumor location and overall survival. The set of stemness-related target mRNAs m⁶A modified RRACHs in the cohort of glioma patients were identified as follows: AAACA|2129|*OS9*, AGACA|1210|*PAGRI*, GGACA|2173|*OS9*, GGACT|2187|*TOBI*, AAACC|3283|*PIK3R2*, GAACC|3068|*GP1BB*, GGACA|3110|*RETREG1*, and GGACT|3122|*LUC7L3*). Identified significant associations of m⁶A mRNA set with patients' clinical characteristics are proposing suitability of the target transcripts for glioma stratification and prognosis.
3. Analysis of individual glioma stem cells specific m⁶A modified transcripts revealed associations with patients' age, Ki-67 index and overall survival in GGACA|2173|*OS9*, AAACC|3283|*PIK3R2*; Ki-67 index and overall survival in GAACC|3068|*GP1BB* RRACH motif; patients' survival in AAACA|2129|*OS9* and AGACA|1210|*PAGRI* RRACHs, and finally overall survival, age, Ki-67 status and tumor location in GGACA|3110|*RETREG1* showing the importance of site-specific m⁶A methylation in glioma pathogenesis.

PRACTICAL RECOMMENDATIONS

As glioblastomas are highly heterogeneous tumors, the number of samples should be expanded to increase statistical power. A larger sample size would allow for more reliable evaluation of epitranscriptome and transcriptome results.

Nanopore sequencing is a powerful technology for detecting m⁶A modifications, but to obtain deep results, the sequencing depth should be increased by sequencing each patient individually. This would provide more profound and comprehensive results.

Functional studies (e.g., knockdown or overexpression studies) of target genes with m⁶A should be performed to confirm the role of the modifications in gliomagenesis, including effects on cell proliferation, differentiation, or response to therapy. It would also be beneficial to integrate multidisciplinary studies such as multi-omics approaches to understand how m⁶A modifications affect glioma biology and reveal complex regulatory networks.

Lastly, confirm m⁶A modifications in target genes (*OS9*, *PAGR1*, *TOB1*, *PIK3R2*, *GP1BB*, *RETREG1* and *LUC7L3*) using additional methods. LC-MS/MS (Liquid Chromatography-Tandem Mass Spectrometry), m⁶A-SAC-Seq (Selective Alkyl Chemical Labeling Sequencing), DART-Seq (Deamination Adjacent to RNA Modification Targets) or m⁶A-CLIP (Crosslinking and Immunoprecipitation) combining these methods could validate m⁶A modifications.

SANTRAUKA

IVADAS

Piktybiniai galvos smegenų navikai gliomos yra labiausiai paplitęs centrinės nervų sistemos navikų (CNS) tipas, atsirandantis dėl glijos ląstelių [1]. Standartinė gliomomis sergančių pacientų priežiūra ir prognozė labai skiriasi. Glioblastoma (GB) yra labiausiai paplitęs piktybinis smegenų navikas, kurio sergančiųjų 5 metų išgyvenamumas yra apie 7,2 proc. Glioblastomų gydymo standartas yra chirurginis naviko pašalinimas, po kurios taikoma radioterapija ar temozolomido chemoterapija, tačiau GB heterogeniškumas, infiltracinis pobūdis, kraujo-smegenų barjero apsauga vis dar kelia iššūkius GB gydymo strategijoms [1, 2]. Atsparumą visoms prieinamoms gydymo terapijoms skatina stiprus DNR pažaidų atstatymas ir gliomą sukeliančių ląstelių gebėjimas atsinaujinti [1].

Daugėja mokslinių tyrimų ir įrodymų apie naviką inicijuojančias gliomos kamienines ląsteles (GKL), kurios pasižymi tam tikromis savybėmis susijusiomis su GB atsparumu gydymui ir naviko ataugimu [3, 4]. Tam tikras kamienines ląsteles galima identifikuoti naudojant jau validuotus, ląstelių paviršiaus žymenis *CD133*, *CD44* ar *A2B5*, o tyrimai rodo daug žadančius rezultatus gliomomis sergančiuose pacientuose [3]. Todėl labai svarbu atsižvelgti ir nukreipti dėmesį į GKL, ieškant specifinių taikinių prieš šias atsparias ląsteles.

iRNR molekulių m⁶A (N6-metiladenozino) modifikacijų vaidmuo gliomose įgauna tyrimų pagreitį. Jau yra įrodyta, kad m⁶A yra dinaminis ir grįžtamas modifikavimas [5, 7, 85], kritinis GB kamieninių ląstelių tumorogenezėje ir savaiminiame atsinaujinime [8]. Taip pat žinoma, kad m⁶A modifikuotos iRNR dalyvauja ląstelėse vykstančiuose procesuose, tokiuose kaip diferenciacija, atsakas į DNR pažeidimą, ląstelių augimas ar atsakas į stresą [8, 9]. Iki šiol atlikti m⁶A (N6-metiladenozino) modifikacijų tyrimai gliomos kamieninėse ląstelėse rodo, kad ši modifikacija galėtų būti perspektyvus taikynys nukreiptas į gliomos kamienines ląsteles. Technologijų pažanga padėjo tvirtą pagrindą epitranskriptomikos sričiai, siekiant apibūdinti m⁶A iRNR vaidmenį vėžio biologijoje, įskaitant gliomas. Sukurti didelio našumo sekoskaitos metodai, tokie kaip MeRIP-sek [10] ir Oksfordo nanoporų sekavimo sistemos [11] suteikė naujų, daug žadančių įžvalgų apie m⁶A modifikacijų aptikimą gliomose, pakankamai dideliu tikslumu. Šiame darbe kaip tyrimo medžiaga buvo naudojamos gliomos kamieninės ląstelės, II ir IV laipsnio astrocitiniai gliomos navikai siekiant atrasti galimus, naujus su gliomogeneze susijusius biožymenis. Molekulinių biožymenų atranka leido atrinkti reikš-

mingiausiu taikinius gliomos kamieninėse ląstelėse ir validuoti juos gliomos navikų audiniuose nurodant prognostiškai svarbių transkriptų rinkinį. Ši disertacija parodė ne tik gliomos kamieninių ląstelių ir gliomos navikinių audinių sekvenavimo galimybes, bet ir atskleidė gliomos epitranskriptomo bei transkriptomo pokyčius, atrandant kliniškai reikšmingus iRNR taikinius.

Darbo tikslas: nustatyti gliomoms specifines iRNR N6-metiladenozino modifikacijas gliomos kamieninėse ląstelėse ir navikuose, siekiant atrinkti naujus, kliniškai reikšmingus gliomų molekulinis žymenis.

Darbo uždaviniai:

1. Nustatyti gliomos kamieninių ląstelių (NCH421k) iRNR N6-metiladenozino (m^6A) iRNR modifikacijų profilį lyginant su glioblastomos ląstelėmis (U87-MG) ir atrinkti potencialias, m^6A metilintas iRNR, susijusias su gliomos kamienišku ir progresavimu.
2. Apibūdinti iRNR molekulių rinkinį su būdingomis m^6A epitranskriptominėmis modifikacijomis, susijusiomis su gliomos patogenezė ir paciento prognoze.
3. Ištirti gliomos kamieninėms ląstelėms specifinius m^6A metilintus iRNR transkriptus gliomos navikuose, siekiant įvertinti jų poveikį naviko patologijai bei pacientų klinikinėms charakteristikoms.

Tyrimo išskirtinumas ir reikšmė. Cheminės m^6A modifikacijos iRNR molekulėse tyrimai yra visiškai nauji. Jau šiek tiek žinoma apie jų funkcinę svarbą, tačiau reikšmingų rezultatų vis dar trūksta. Dėmesys iRNR modifikacijoms yra ypač intriguojantis, nes jos tarnauja kaip baltymų transliacijos substratai. m^6A modifikacijų pokyčiai tam tikruose piktybiniuose navikuose gali sustiprinti tam tikro iRNR pogrupio, iš kurių daugelis yra onkogenai, transliaciją. Glioblastomos (GB), agresyvaus ir gydymui atsparaus pirminio smegenų auglio, atveju m^6A pokyčių gliomos kamieninėse ląstelėse (GSC) ir naviko audiniuose tyrimai yra nauja ir reikšminga tyrimų kryptis. Ji yra ypač svarbi ne tik RNR biologijos, bet ir vėžio kamieninių ląstelių bei neuroonkologijos sankirtoje, suteikdama daug perspektyvų. Tyrimai rodo, kad m^6A modifikacijos potencialiai galėtų būti taikynys gliomų atveju. Terapinis epitranskriptomo modifikacijų reguliavimas gliomos kamieninėse ląstelėse galėtų padėti kontroliuoti jų augimą, atsinaujinimą ir naviko vystymąsi. Terapinis gliomos kamieninių ląstelių reguliavimas padeda kontroliuoti jų augimą, atsinaujinimą ir naviko vystymąsi. Šioje disertacijoje pirmą kartą buvo analizuojami m^6A modifikuotos ir su kamieniškumu susijusios iRNR skirtingus gliomos laipsnius turinčiuose navikų audiniuose. Be to, šis tyrimas suteikia įžvalgų apie atrinktų iRNR molekulių rinkinį tinkamą ateities tyrimams, siekiant sukurti prognostinius ir diagnostinius glioblastomos gydymo metodus, nukreiptus į gliomos kamienines ląsteles. Labai svarbu pabrėžti, kad pacientų m^6A metilinimo duomenys buvo deponuoti viešoje GEO

duomenų saugykloje (GSE282642). Mūsų žiniai, tai yra pirmieji m⁶A metilimo duomenys pacientų navikuose, prieinami viešai. Šio tyrimo reikšmė apima ne vien gliomos biologiją. m⁶A modifikacijų tyrimas ląstelėse gali padėti suprasti, kaip iRNR modifikacijos veikia ląstelių elgesį piktybiniuose smegenų navikuose ir gali atskleisti panašius mechanizmus kitų rūšių navikuose.

Tyrimo planas. Disertacinio darbo tyrimas buvo suskirstytas į dvi dalis: 1) potencialių m⁶A modifikuotų iRNR molekulių paieška gliomos prognozei ir diagnozei, naudojant gliomos kamienines ląsteles (NCH421k) lyginant su glioblastomos ląstelėmis (U87-MG); 2) potencialių m⁶A modifikuotų iRNR validavimas gliomos kooperaciniuose audiniuose.

MEDŽIAGOS IR METODAI

Mėginių rinkimas ir etika. Lietuvos sveikatos mokslų universiteto ligoninės Kauno klinikose (Kaunas, Lietuva) Neurochirurgijos skyriuje 2002–2020 m. buvo surinkti 16 glioblastomos (GB) ir 9 difuzinės astrocitomos (LGG) naviko audiniai. Gliomų diagnozė buvo patvirtina patologų. Tyrimui pritarė Kauno regioninis biomedicininis tyrimų etikos komitetas (P2-9/2003 ir BE-2-3) ir buvo atliktas griežtai laikantis Helsinkio deklaracijos. Prieš mėginių surinkimą, visi tyrime dalyvaujantys pacientai davė raštišką sutikimą dalyvauti tyrime. Po chirurginių navikų pašalinimo, audiniai buvo užšaldyti skystame azote (–196 °C).

Pacientų klinikinių charakteristikų atranka. Iš visų nagrinėjamų pacientų klinikinių charakteristikų, į analizę buvo įtraukti: amžius, lytis, išgyvenamumo laikas (dienomis), naviko vieta, naviko dydis, Ki-67 geno statusas, MGMT geno metilimo statusas, glioblastomų potipiai. Pacientai, kurie tyrimo pabaigoje vis dar buvo gyvi – cenzūruojami Kaplan-Meier išgyvenamumo analizėje.

Žmogaus ląstelių linijos. NCH421k kamieninės ląstelės (dovana iš dr. A. Jekabsonės) buvo auginamos kaip sferoidinė suspensija DMEM/Ham F-12 terpėje (Sigma-Aldrich, kat. Nr. D8437), papildyta 100 IU/ml penicilinu ir 100 µg/ml streptomycinu (Gibco, kat. no. 15140122), 0,12 proc. vaisiaus galvijų albumino serumu (FBS) (Gibco, kat. nr. 15260037) ir D-gliokozės tirpalu (Sigma-Aldrich, kat. nr. G8644), taip pat B-27 (Gibco, kat. nr. 17504044), N-2 (Gibco, kat. nr. 17502048), bFGF ir EGF (Gibco, kat. nr. PHG0261 ir PHG0311, atitinkamai). Glioblastomos U-87MG ląstelių linija buvo įsigyta iš Europos ląstelių kultūrų kolekcijos (ECACC, kat. nr. 89081402). Ląstelės buvo auginamos didelės gliukozės koncentracijos tirpalo terpėje DMEM (Gibco, kat. nr. 10566016), papildytoje 10 proc. FBS (Gibco,

kat. nr. 06050). Ląstelių linijos buvo inkubuojamos drėgnoje atmosferoje su 5 proc. CO₂ ir 37 °C temperatūra. Visiems tyrimo eksperimentams buvo naudojamos ląstelės be mikoplazmos.

RNR išskyrimas ir poli A gryninimas. Šį tyrimą sudarė skirtingos imties grupės: 1) LGG, 2) GB ir 3) GKL. Visuminė RNR iš homogenizuotų, greitai užšaldytų audinių ir ląstelių linijų buvo išskirta naudojant TRIzol reagenta pagal gamintojo instrukcijas (Invitrogen, kat. nr. 15596026). Išskirtos RNR kokybė buvo nustatyta naudojant Agilent 2000 bioanalizės prietaisą ir „Agilent RNA 6000 Pico“ rinkinį (Agilent, kat. nr. 5067-1513). Visuminė RNR buvo laikoma –80 °C temperatūroje iki poli A RNR gryninimo. poli A gryninimui naudotas „Dynabeads mRNA DIRECT“ rinkinys (Invitrogen, kat. nr. 61012). 40–180 µg visuminės RNR panaudota poli A gryninimui pagal gamintojo instrukcijas kiekvienam mėginiui. Magnetinės dalelės buvo resuspenduojamos mėginio lizate su visumine RNR, kad poli A uodegėlė galėtų hibridizuotis su oligo (dT)25. poli A praturtinta RNR išsodinta per naktį –80 °C temperatūroje išsodinimo buferyje su 100 µg/ml glikogeno (Thermo Scientific™, kat. nr. R0551) ir grynu 100 proc. etanolium (Vilniaus degtinė, kat. nr. P075). Gauta poli A RNR buvo resuspenduota švariame vandenyje be RNazių/DNazių (Invitrogen, kat. nr. 10977-035), o kokybė patikrinta naudojant Agilent 2100 Bioanalyzer ir NanoDrop™ 2000 (ThermoFisher Scientific) analizatorius.

Su fermentais susijęs imunisorbentinis tyrimas ELISA. ELISA buvo atlikta siekiant išanalizuoti bendrą poliA RNR m⁶A modifikacijų lygį pacientų mėginiuose pagal. Tyrimas buvo atliktas naudojant gamintojo protokolą. Į tyrimą buvo įtraukta 17 mėginių iš glioblastoma sergančių pacientų ir 9 mėginiai iš žemesnio laipsnio gliomos pacientų. Po visuminės RNR išskyrimo ir ir poliA gryninimo, RNR pridedama į lėkštelių šulinėlius. Šulinėliai buvo plaunami kelis kartus ir pridedamas m⁶A antikūnas. Šulinėliai vėl buvo plaunami, tada pridedami aptikimo antikūnai ir stipriklio tirpalas. Galiausiai pridėtas spalvos ryškinimo tirpalas spalvai sukurti ir išmatuota absorbcijai. m⁶A standartinė kontrolė buvo pridėta į tyrimo šulinėlius skirtingomis koncentracijomis ir išmatuota.

N6-metiladenino imunoprecipitacija (MeRIP-sek) pagal naujos kartos sekoskaitą. Prieš m⁶A imunoprecipitaciją, poli A RNR buvo fragmentuojama į 100 nt dydžio fragmentus: 18 µg poli A RNR 20 µl viso fragmentacijos buferio tūrio, 94 °C 3 minutes termocikleryje (Applied Biosystems). Poli A RNR suskaidymo efektyvumas buvo įvertintas naudojant Agilent bioanalizatorių ir 1,5 proc. agarozės gelį. Vadovaujantis Dominissini [10] ir Meyer [108] mokslininkų grupių protokolais, ir „Magna MeRIP m⁶A“ rinkiniu (Sigma-Aldrich, kat. nr. 1710499) buvo atlikta imunoprecipitacija (MeRIP).

MeRIP-sek m⁶A metilintų pikų analizė. Atlikus visų sekvenuotų mėginių kokybės kontrolę, trečiasis U87-MG replikatas buvo nustatytas kaip rimtas nuokrypis nuo normos, todėl šis mėginys buvo pašalintas iš tolimesnių analizių. Gautos sekos buvo apdorojamos naudojant įvairius bioinformatikinius įrankius („MeRIPseqPipe“ *pipeline* [156], *Nextflow* [157]). Nuskaitymai buvo suderinti ir prijungti prie GRCh38 referentinio genomo.

Genų raiška ir MeRIP-sek m⁶A metilinimas. Galiausiai, metilinimo analizė buvo apdorota naudojant QNB [161] ir DESeq2 [162], o genų raiškos analizė atlikta naudojant *featureCounts* [163]. Atlikus visų sekvenuotų mėginių kokybės kontrolę, trečiasis U87-MG ląstelių mėginys buvo pašalintas iš analizės, dėl netinkamos mėginio kokybės.

RNR sekoskaitos bibliotekų paruošimas naudojant Oksfordo nanoporų technologiją (ONT). Sekoskaitai atlikti ir bibliotekoms paruošti buvo naudojamas RNR sekos nustatymo rinkinys (ONT, SQK-RNA002). Kiekvienai sekoskaitos sudarymo bibliotekai buvo naudojama 500–1000 ng praturtintos poli A RNR pagal gamintojo protokolus (ver. DRS_9080_v2_revO_14Aug2019 ir DRS_9195_v4_revD_20Sep2023). Protokole įvedėme vieną pakeitimą, panaudojome Hyeshik Chang [164] ir Smith ir kt. [165] sukurtus atvirkštinės transkripcijos barkodus (RTA), kuriais pakeitėme ankstesnį RTA. Išskyrus 2 pacientų mėginius, kurie buvo sugrupuoti kartu, kiti likę pacientų mėginiai buvo barkoduojami grupėse po 4 vienai leidimo celei, glioblastomos kamieninės ląstelės sekvenuojamos kiekviena atskirai. Bibliotekų paruošimo išėiga įvertinta Qubit rinkiniu (Qubit fluorometer DNA HS assay (Invitrogen, kat nr. Q32851)) ir mėginiai įvedami į MinION mk1B ir mk1C srauto celes sekvenavimui.

MinION srauto celių paleidimas ir sekoskaita. Visuose eksperimentuose buvo naudojamos R9.4.1 celės. Prieš pradėdant kiekvieną sekoskaitą, buvo patikrinamas celių aktyvumas ir naudojamos tos, kurių aktyvių porų skaičius siekė 1100 ir daugiau. Visos paruoštos bibliotekos perkeliamos į celes ir sekoskaita paleidžiama 72 valandoms.

Nanopore technologijos sekoskaitos duomenų apdorojimas. Sekoskaitos nuskaitymai, buvo sukurti su minimaliais 6 skaitymo kokybės balais. Naudojant *ONT Guppy* programinę įrangą (versija v5.0.11), *Fast5* failai buvo apdoroti dideliu tikslumu, taikant dRNR-sek konfigūracijos failą („rna_r9.4.1_70bps_hac.cfg“), Poreplex programinė įranga (versija 0.5) buvo naudojama atskirti naudotus barkodus. Gautos sekos prilygintos žmogaus genomo sekoms (*Ensembl release 105*, *Genome assembly*, versija GRCh38) naudojant *minimap2* (versija 2.17-r941) [167] ir *SAMtools* įrankius [158].

ONT genų ekspresija ir m⁶A metilinimas. Epinano programinė įranga (versija 1.2.0) [169] buvo panaudota identifikuoti m⁶A modifikacijas mole-

kulių transkriptuose (RRACH). *FeatureCounts* [163] panaudota su genomu suderintų sekoskaitos duomenų genų ekspresijos skaičiavimams.

Kiekybinė tikro laiko PGR analizė. Kamieniškumo žymenų (*SOX2*, *POU5F1*, *MYC*, *PROM1*, *KLF4*, *NANOG*, *GFAP* ir *ACTB*) kiekybinė tikro laiko PGR analizė gliomos kamieninėse ir glioblastomos ląstelėse buvo atlikta naudojant 7500 greitąjį realaus laiko PGR aptikimo sistemą („Applied Biosystems“). Kamieniškumo genų raiškai NCH421k ir U87-MG ląstelių linijose įvertinti naudotas santykinis kiekybinio įvertinimo modelis ($2^{-\Delta CT}$). Bendra RNR buvo išskirta ir apdorota DNase I („Thermo Fisher Scientific“, kat. nr. EN0521), kad būtų pašalintas bet kokios likusios DNR priemaišos.

Silueto diagrama. Diagrama buvo naudojama gliomos pacientų duomenų nuoseklumui įvertinti. Silueto balo matavimai parodė, kiek paciento mėginys panašus į kitus, tai pačiai grupei priskiriamus mėginius, lyginant su kitomis grupėmis. Jei balas arti 1, reiškia, kad mėginys yra glaudžiai susijęs su savo grupe, nei balas arti 0 – mėginys yra tarp dviejų grupių ribos.

m⁶A metilinimo ir kamieniškumo balų skaičiavimas. m⁶A metilinimo balo apskaičiavimas buvo atliktas siekiant apibendrinti m⁶A modifikacijų statistinį reikšmingumą visuose pacientų mėginiuose ir tiksliniuose RRACH motyvuose. Kamieniškumo balai kiekvienam pacientui buvo nustatomi naudojant genų praturtinimo analizę (angl. *ssGSEA*). Balai buvo apskaičiuoti remiantis individualių mėginių genų raiškos lygiais, įtraukiant genų, išdėstytų raiškos matricoje, indėlių.

Atsitiktinių medžių klasifikatoriaus algoritmas. Šis algoritmas buvo naudojamas vizualizuoti reikšmingų klinikinių charakteristikų (amžiaus, naviko dydžio, naviko vietos) ir bendro m⁶A metilinimo balo ryšius glioma sergantiems pacientams. Aliuvinė diagrama buvo naudojama algoritmo analizei iliustruoti. Ašys buvo pavaizduotos kaip juostelės, kurių plotis kinta, ir tai atspindėjo pacientų judėjimą nuo vienos klinikinės charakteristikos prie kitos. Juostų dydis rodė pacientų mėginių judėjimą, taip nustatant svarbiausius ryšius ir tendencijas.

Nomogramos analizė. Nomograma buvo naudojama regresinio modelio prognozių gavimui naudojant „rms“ paketą (v8.0-8, R-ver. 4.3.3). Nomogramoje buvo atskaitos linija vertinimo taškams nuskaityti (numatytasis diapazonas 0–100). Bendras taškų skaičius buvo sudėti, o numatyti rezultatai pateikti nomogramos apačioje. Bendrą nomogramos taškų skaičių sudarė pacientų amžiaus, lyties, MGMT būsenos, naviko vietos, naviko dydžio, Ki-67 indekso būsenos, kamieniškumo ir m⁶A metilinimo balo suma, o didesnis bendras taškų skaičius prognozavo mirties rizikos balą.

Signalinių kelių analizė. Kioto genų ir genomų enciklopedijos (KEGG) duomenų bazės buvo naudojamos signalinių kelių nustatymui. Analizei naudota *clusterProfiler* paketas (ver.4.4.4). Analizės parametrai: permuta-

cijos ($nPerm$): 10 000, minimalus genų rinkinio dydis ($minGSSize$): 3, maksimalus genų rinkinio dydis ($maxGSSize$) = 1000, minimali p reikšmė ($p-valueCutoff$) = 0.05, organizmas ($Orgdthb$) = org.Hs.eg.db, metodas: Benjamini-Hochberg (BH). Grafikai paruošti naudojant *ggplot2* paketą (ver. 3.3.6).

Statistinė analizė. Visa statistinė analizė buvo atliekama naudojant R programavimo kalbą (versija 4.3.3) [171], GraphPad Prism (versija v6.01) [172], ir mašininio mokymosi ir vizualizavimo paketą „Orange Data Mining“ (versija 3.32) [173]. Pacientų išgyvenamumui įvertinti naudotos Kaplan-Meier išgyvenamumo kreivės, o statistiniai skirtumai tarp grupių įvertinti naudojant log-rank testą. Rizikos santykiams įvertinti ir kovariantų poveikiui išgyvenamumo rezultatams įvertinti taikyta *Cox* proporcinė regresijos analizė. Ryšiui tarp RRACH motyvų ir modifikavimo verčių tikimybės nustatyti naudotas logistinės regresijos modelis. Pearsono koreliacija naudota RRACH motyvų m^6A metilinimo lygiui ir jų buvimui skirtinguose gliomos pacientų mėginiuose įvertinti bei ryšiui tarp su kamieniškumo funkcijomis susijusių genų ir mūsų atrinktų m^6A modifikuotų taikinių genų C1 ir C2 klasteriuose tirti. Koreliacijos koeficientas $r \geq 0,85$ rodė stiprią koreliaciją, $r \leq 0,2$ – silpną koreliaciją, $r = 0$ neatspindėjo koreliacijos tarp genų raiškos lygių. Tiesinės regresijos analizė buvo naudojama pacientų klinikinėms charakteristikoms, tokioms kaip amžius, naviko dydis ir išgyvenamumas, o Chi kvadrato (χ^2) testas buvo naudojamas MGMT metilinimo, naviko vietos ir Ki-67 indekso ryšiui su pacientų mėginiais vertinti. Skirtumai laikyti patikimais * $p < 0,05$, ** $p < 0,01$, *** $p < 0,001$.

REZULTATAI

RNR m^6A epitranskriptomo sudėtis gliomos kamieninėse NCH421k ir glioblastomos U87-MG ląstelėse, taikant MeRIP-sek analizę. NCH421k gliomos kamieninės ląstelės ir glioblastomos U87-MG ląstelės buvo panaudotos RNR m^6A metilinimo imunoprecipitacijos analizei MeRIP-sek. Tikro laiko PGR, naudojant *SOX2*, *POU5F1*, *MYC*, *PROM1*, *KLF4*, *NANOG* ir *GFAP* genus, buvo atliktas įvertinti genų raiškos lygius, NCH421k ląstelių kamieniškumui patvirtinti. Mūsų analizėje NCH421k ląstelės pasižymėjo žymiai didesniu šių su kamieniškumu susijusių genų ekspresijos lygiu, palyginti su U87-MG ląstelėmis (žr. publikaciją „Transcriptome-wide analysis of glioma stem cell specific m^6A modifications in long-non-coding RNAs“).

Skirtingų genų RNR biotipai iš ląstelių linijų buvo identifikuoti naudojant bioinformatikinę analizę, siekiant įvertinti m^6A modifikacijos įvairovę.

Nustatyta, kad dauguma identifikuotų genų priklausė baltymus koduojantiems genams (94,4 proc.), inkRNR (4,2 proc.), transkribuotiems apdorotiems pseudogenams (0,2 proc.), transkribuotiems neapdorotiems pseudogenams (0,7 proc.), transkribuotiems pirminiams pseudogenams (0,2 proc.), TEC (regionai turintys poli A požymių ir galintys rodyti baltymus koduojančius genus, tačiau eksperimentiškai nepatvirtinti) (0,1 proc.) ir kiti (0,2 proc.). Iš viso buvo identifikuoti 33 986 m⁶A modifikuoti pikai tarp U87-MG ir NCH421k ląstelių linijų. 25 964 modifikuoti pikai persidengė tarp ląstelių linijų, 6579 – unikalūs NCH421k ląstelėms, 1443 – U87-MG. 43,1 proc. pikų buvo 5' regione, 21,4 proc. 3' regione, CDS – 21,4 proc. ir 14,1 proc. kitose vietose.

RNR m⁶A epitranskriptomo sudėtis gliomomis sergančiuose pacientuose, taikant Nanopore RNR-sek. Dauguma nustatytų genų priklausė baltymus koduojantiems – 96 proc., inkRNR (2,9 proc.), apdorotiems pseudogenams (0,1 proc.), transkribuotiems apdorotiems pseudogenams (0,1 proc.), transkribuotiems neapdorotiems pseudogenams (0,6 proc.) ir transkribuotiems pirminiams pseudogenams – 0,6 proc.. Iš viso rasti 437 839 m⁶A modifikuoti transkriptai, iš kurių 239 797 unikalūs glioblastomoms, o 12 298 – LGG. 56 proc. transkriptų buvo nustatyti 3', 1,3 proc. 5' regionuose, CDS – 31 proc. ir 1,3 proc. – kituose. Vertinant bendrą modifikavimo lygį tarp GB ir LGG grupių, pastebėta, kad vidutiniškai LGG pacientai turėjo beveik 3 kartus didesnę m⁶A modifikacijos lygį, lyginant su GB pacientais.

Baltymus koduojančių, m⁶A metilintų RNR atranka naudojant MeRIP-sek ir dRNR-sek duomenis. Skirtingai metilinti genai GKL buvo identifikuoti naudojant DESeq ir keturių kvadrantų analizę MeRIP-sek duomenyse. Ši analizė atrinko reikšmingai metilintus genus, kurie koreliavo su genų raiška GKL lyginant su U87MG. Iš viso 198 genai buvo naudojami tolimesnėje analizėje, kurie buvo metilinti ir turėjo padidėjusią arba sumažėjusią raišką gliomos kamieninėse ląstelėse. Identifikuoti genai buvo ieškomi gliomos pacientų mėginiuose. Kadangi dRNR-sek m⁶A metilintos vietos vertinamos pagal RRACH motyvus, dėmesys buvo sutelktas į visus ieškomų genų motyvus, taikant taisyklę, kad 13 ir daugiau pacientų turi informacijos apie identifikuotus genus iš MeRIP-sek analizės. Surasti reikšmingus RRACH motyvus pacientų mėginiuose, buvo pritaikytas logistinės regresijos modelis, nustatyti ryšį tarp motyvų ir modifikavimo tikimybės. Išvestis buvo interpretuojama kaip reikšmingai modifikuoti RRACH motyvai pacientų mėginiuose. Iš viso buvo rasti 212 metilintų motyvų pacientuose. Kaip antrinį motyvų filtravimo metodą panaudojome Chi kvadrato testą, kad sutelktume dėmesį į stipriausius ryšius. Atrinkome 8 reikšmingiausių RRACH motyvus, kurie atitiko 7 unikalius genus gliomomis sergančiuose pacientuose.

Gliomomis sergančių pacientų klasifikavimas pagal m⁶A epitranskriptomines žymes. Atsižvelgiant į nustatytus 8 RRACH motyvus, pastebėjome, kad LGG pacientuose m⁶A metilinimo dažnumas pagal buvo 3,4 karto didesnis nei GB pacientuose. Pritaikant hierarchinę klasterinę analizę, buvo rasti du nepriklausomi klasteriai, suskirstę pacientus pagal patologiją: C1 klasteryje dominavo LGG ir buvo priskirti 2 GB mėginiai, kai tuo tarpu, C2 klasteryje – visos glioblastomos, o metilinimo dažnumas klasteryje C1 buvo beveik 4 kartus didesnis lyginant su C1.

Ryšys tarp analizuojamų RRACH motyvų ir pacientų klinikinių charakteristikų. Visų pirma patikrinome bendras, sumuotų visų taikinių motyvų, sąsajas su pacientų klinikinėmis charakteristikomis. Nustatyta, kad pacientai, kurie buvo m⁶A metilinti, turėjo geresnę išgyvenamumo prognozę ($p = 0,0036$). Buvo pastebėtas reikšmingas ryšys tarp bendro motyvų metilinimo ir amžiaus gliomos pacientuose. Tai pat, matomos tendencijos su naviko dydžiu, Ki-67 geno statusu bei naviko lokacija. Tik glioblastomos mėginuose, nustatytas ryšys tarp metilinimo ir išgyvenamumo ($p = 0,049$) ir naviko lokalizacijos ($p < 0,0001$). Apskaičiavus bendrą visų taikinių motyvų m⁶A modifikavimo įvertį, nustatėme reikšmingą ryšį tarp klasterių C1 ir C2 ($p = 0,0002$), o išgyvenamumo kreivė parodė, kad mažesnę m⁶A modifikacijos įvertį turintys pacientai išgyvena trumpiau ($p = 0,016$). m⁶A modifikacijos įvertis parodė reikšmingas sąsajas tarp metilinimo ir amžiaus, bei naviko lokacijos. Nustatyti taikiniai motyvai gliomomis sergančiuose pacientuose, buvo detaliau aprašyti ir išanalizuoti, kreipiant dėmesį į kiekvieną motyvą atskirai.

AAACA|2129|OS9 RRACH motyvo m⁶A modifikacijos susiję su gliomų išgyvenamumu ir Ki-67 geno statusu. Buvo nustatytas reikšmingas metilinimo skirtumas tarp AAACA OS9 geno ir išgyvenamumo ($p < 0,001$) bei Ki-67 geno statuso ($p = 0,020$) gliomose. Matoma tendencija, kad jaunesni pacientai turi labiau modifikuotą AAACA motyvą OS9 gene ($p = 0,098$). Vertinant tik glioblastomas, pakankamai reikšmingą tendenciją rasta tarp motyvo metilinimo ir išgyvenamumo ($p = 0,059$), kai modifikaciją turintys GB pacientų išgyvenamumas buvo geresnis.

AGACA|1210|PAGRI RRACH motyvo m⁶A modifikacijos reikšmingai susijusi su gliomų pacientų išgyvenamumu ir potipiais glioblastomose. Buvo nustatyta, kad AGACA motyvo PAGRI gene m⁶A modifikacija reikšmingai susijusi su pacientų išgyvenamumu. Tie pacientai, kurie turėjo modifikuotą adeniną išgyveno ilgiau, nei tie, kurie neturėjo ($p = 0,015$). Nors statistinio patikimumo neužfiksuota, tačiau matomos tendencijos AGACA motyve su pacientų amžiumi ($p = 0,094$), Ki-67 geno statusu ($p = 0,051$) ir naviko vieta ($p = 0,078$). Glioblastomų atžvilgiu, buvo matoma reikšminga sąsaja tarp metilinimo ir naviko vietos ($p = 0,003$).

GGACA|2173|OS9 RRACH motyvas stipriai susijęs su gliomomis sergančių pacientų klinikinėmis charakteristikomis. Geno *OS9* GGACA motyvas parodė potencialias žymens savybes. Metilinimas reikšmingai siejosi su gliomų pacientų išgyvenamumu ($p < 0,0001$), pacientų amžiumi ($p = 0,011$) ir *Ki-67* geno statusu ($p = 0,036$). Taip pat fiksuojama ir tendencija su naviko vieta ($p = 0,086$). Deja, glioblastomos mėginiuose reikšmingų sąsajų ar tendencijų nenustatyta.

Silpnas ryšys tarp GGACT|2187|TOB1 RRACH motyvo metilinimo ir gliomomis sergančių pacientų klinikinių savybių. Nors reikšmingų sąsajų tarp metilinimo ir pacientų klinikinių charakteristikų nenustatyta, tačiau matoma tendencija pacientams, turintiems metilintą adeniną gyventi ilgiau ($p = 0,081$).

Stiprus ryšys tarp AAACC|3283|PIK3R2 RRACH motyvo metilinimo ir pacientų, sergančių gliomomis. Nors reikšmingų skirtumų nepastebėta tarp *PIK3R2* geno AAACC motyvo metilinimo ir lyties, MGMT statuso, naviko dydžio ir naviko vietos, tačiau nustatėme reikšmingas sąsajas su pacientų išgyvenamumu ($p = 0,001$), amžiumi ($p = 0,009$) ir *Ki-67* geno statusu ($p = 0,011$). Tačiau tik glioblastomos pacientuose reikšmingų sąsajų nenustatėme.

GGACA|3110|RETREG1 RRACH motyvas labai perspektyvus molekulinis žymuo gliomų prognozei. *RETREG1* geno GGACA motyvas parodė puikias kaip molekulinio žymens savybes, sutelkiant dėmesį į m^6A metilinimą. Buvo nustatytas stiprus ryšys tarp metilinimo ir pacientų išgyvenamumo ($p = 0,004$), pacientų amžiaus ($p = 0,010$), *Ki-67* geno statuso ($p < 0,001$) ir naviko vieta ($p = 0,009$), o tai rodo, kad metilinimo lygis yra gali tarnauti kaip žymuo prognozuojant klinikinius rezultatus. Pavyzdžiui, nustatyta, kad metilinti navikai dažniau būna jaunesniems pacientams, kaip ir geresnis išgyvenamumas. m^6A metilinimas šiame motyve ir tik glioblastomų pacientuose parodė reikšmingą ryšį su *Ki-67* statusu ($p = 0,029$) ir naviko vieta ($p = 0,042$).

Silpnas ryšys tarp GGACT|3122|LUC7L3 RRACH motyvo metilinimo ir gliomų pacientų klinikinių faktorių. GGACT motyvo metilinimo analizė gene *LUC7L3* neparodė reikšmingų sąsajų su pacientų klinikinėmis charakteristikomis. Remiantis atlikta išgyvenamumo analize ir m^6A modifikacijos lygiu motyve matoma aiški tendencija pacientams išgyventi trumpiau, kurių GGACT motyvas turi metilintą adeniną ($p = 0,064$). Ta pati tendencija matoma amžiuje ($p = 0,061$), rodanti, kad vyresniems pacientams dažniau pasireiškia metilinimas nei jaunesniems. Analizuojant geno *LUC7L3* GGACT motyvą glioblastomose, nustatytas stiprus ryšys tarp modifikacijos ir glioblastomos potipių ($p = 0,027$). Visiškas modifikuoto m^6A trūkumas mezenchiminiame potipyje gali prisidėti prie GB agresyvaus fenotipo.

Kamieniškumo vertinimas. Gliomomis sergančių pacientų kamieniškumo balas. Vis daugiau tyrimų rodo, kad kamieninės ląstelės yra atsparumo vaistams, kancerogenežės ir progresavimo pagrindas [115, 188]. Nustačius kamieniškumo balą kiekvienam pacientui, galime gauti papildomos informacijos apie individualias pacientų savybes, ląstelių elgesį arba galimas individualias tikslines terapijas, o vis tai gali padėti pagerinti pacientų išgyvenamumą [189]. Taigi, atlikome vieno mėginio genų praturtinimo analizę (ssGSEA) [190], kuri genų rinkiniams priskiria balus pagal genų raišką atskiram mėginiui. Mes panaudojome su gliomų kamieniškumu susijusių genų duomenų rinkinį, kurį pristatė Malta ir kt. 2018 metais [191]. Jame yra 21 su kamieniškumu susijęs genas. Kiekvieno paciento kamieniškumo balas buvo apskaičiuotas ir, remiantis jau aprašytas tyrimais, nustatyta, kad glioblastomos turi aukštesnį kamieniškumo balą lyginant su žemo laipsnio gliomomis [192]. Kamieniškumo balų pasiskirstymas buvo išanalizuotas atskiruose pacientų klasteriuose, gautuose po m^6A metilino analizės (žr. skyrių „*Gliomomis sergančių pacientų klasifikavimas pagal m^6A epitranskriptomines žymes*“). Analizė parodė, kad C2 (glioblastomų) kamieniškumo balo vidurkis buvo didesnis nei C1 klasteryje. Įvertinus išgyvenamumą, nustatyta, kad žemą kamieniškumo balą turintys pacientai išgyvena geriau ($p = 0,0061$). Nors ir neradome statistiškai reikšmingų skirtumų su pacientų klinikinėmis charakteristikomis, pastebėjome tendenciją, kad navikai iš pakaušio skilties turėjo aukštesnį kamieniškumo balą nei priekinės skilties ($p = 0,06$). Taip pat labai įdomi tendencija matoma, kad klasikinio tipo glioblastomos turėjo didesnę kamieniškumo balą lyginant su pronerviniu ir mezenchiminiu potipiais ($p = 0,09$, $p = 0,06$, atitinkamai). Nors rezultatai nebuvo statistiškai patikimi dėl galimo mažo imties skaičiaus, tačiau jie suteikia naudingų įžvalgų tolimesniems gliomų tyrimams. Tuomet atidžiau pažvelgėme į kamieniškumo balui skaičiuoti naudotus genus, todėl atlikome papildomą analizę. 17 iš 21 su kamieniškumu susijusių genų buvo įtraukti į skaičiavimus. Nustatėme, kad kamieniškumo genai atskiria pacientus į du skirtingus klasterius pagal patologiją, taip pat, kaip ir visų RRACH motyvų m^6A metilino lygis. C1 klasteryje dominavo LGG pacientai ir 2 GB, o C2 klasteryje – tik glioblastomos. Šis grupavimas parodo, kad kamieniškumo genai gali būti naudojami atskirti skirtingas gliomų grupes, ir pabrėžia, kaip jie svarbūs norint suprasti patogeninį gliomų kintamumą. Šis metodas leido mums nustatyti grupes, kurios atitiko gliomų patologijas, įrodydamas pacientų klasifikavimo tvirtumą. Be to, mes pavaizdavome nomogramą, į kurią įtraukėme ne tik pacientų klinikinės charakteristikas, bet ir kamieniškumo, bei m^6A metilino balus. Nomograma parodė, kad svarbiausi faktoriai buvo Ki-67 geno statusas, naviko vieta, patologija ir amžius. Nomogramos tikslumą gali riboti imties dydis ir tai gali turėti įtakos rizikos prognozėms, todėl

kad ji taptų pakankamai tiksli, reikia į analizę įtraukti daugiau pacientų mėginių.

Toliau buvo atliktas taikinių genų raiškos tyrimai gliomomis sergančiuose pacientuose.

Tikslinių genų raiškos analizė. Siekėme bendrai ištirti atrinktų genų raiškos skirtumus tarp klasterių ir įvertinti galimą poveikį pacientams. 7 taikinių genų raiška parodė tendenciją tarp klasterių, kad didesnė genų raiška fiksuojama C2 (glioblastomų) klasteryje ($p = 0,080$). Kadangi išgyvenamumo analizė neparodė reikšmingų skirtumų, įvertinome kiekvieno taikinio geno raišką atskirai minėtuose klasteriuose. Rezultatai parodė, kad geno *PIK3R2* raiška klasteriuose reikšmingai skyrėsi ($p = 0,019$) ir buvo didesnė klasteryje C1. Taip pat pastebima tendencija, klasteryje C2 geno *PAGRI* geno raiškos lygis buvo didesnis ($p = 0,051$). Papildomai atlikome koreliacijos analizę, siekdami ištirti ryšį tarp taikinių genų ir su gliomų kamieniškumu susijusių genų raiška klasteriuose. Tikėjomės atskleisti reikšmingas sąsajas su analizuojamais, taikiniaisiais genais ir su kamieniškumu susijusiais genais, kurie buvo panaudoti skaičiuojant kamieniškumo įvertį pacientams. Rezultatai parodė reikšmingas, teigiamas ir neigiamas koreliacijas. Klasteryje C1 (kuriame dominavo LGG pacientai), genai *PIK3R3*, *TOB1*, *GP1BB* ir *RETREG1* turėjo stiprią, statistiškai reikšmingą teigiamą ryšį ($p < 0,05$) su, atitinkamai, kamieniškumo genais *EZH2*, *HIF1A*, *LGR5* ir *PROM1*. Tai pat, *GP1BB* taikinytis genas turėjo stiprią, statistiškai reikšmingą neigiamą koreliaciją su *CD34* kamieniškumo genu, o *RETREG1* genas turėjo vidutinę, statistiškai reikšmingą neigiamą koreliaciją su *TWIST1* kamieniškumo genu ($p < 0,05$). Klasteryje C2 (tik glioblastomų pacientai) *PIK3R3* taikinytis genas turėjo stiprią teigiamą, statistiškai reikšmingą koreliaciją su kamieniškumu susijusiais genais *CD34* ir *KDM5B* ($p < 0,05$), o *GP1BB* genas, taip pat turėjo teigiamą statistiškai reikšmingą koreliaciją su *LGR5* ($p < 0,05$). Matomos tendencijos taikiniui genui *LUC7L3* turėti vidutinę teigiamą koreliaciją su *CD34* kamieniškumo genu ($p = 0,06$), taip pat kaip ir *PIK3R3* genui su *TWIST1* ($p = 0,05$) ir *GP1BB* turėti neigiamą koreliaciją su *CD44* kamieniškumo genu ($p = 0,06$). Šioje analizėje mes nustatėme reikšmingas koreliacijas tarp mūsų pasirinktų taikinių genų ir su kamieniškumu susijusiais genais. Kamieniškumas yra vėžio kamieninių ląstelių, kurios, kaip žinoma, skatina naviko atsiradimą, atsparumą gydymui, gliomų pasikartojimą ar progresavimą, požymis [196, 197]. Rastos asociacijos rodo, kad mūsų taikiniai genai gali atlikti svarbų vaidmenį išsaugant į kamieniškumą panašias savybes. Šios sąsajos taip pat rodo, kad mūsų tiksliniai genai gali būti naudojami kaip terapiniai žymenys, kurie galėtų sulėtinti navikų augimą ir padidinti gydymo veiksmingumą.

Taikinių genų raiškos ryšiai su m⁶A metiliniu. Visų pirma patikrinome bendrą taikinių genų metilinimo ryšį su jų genų raiška. Tirdami ryšį neradome jokių reikšmingų ar tiesioginių koreliacijų. Tai rodo, bendras metilinimo lygis RRACH motyvuose negali tiesiogiai numatyti genų raiškos pokyčių. Tačiau, svarbu sutelkti dėmesį į atskirų RRACH motyvų sąsajas su jų genų raiškos pokyčiais, kurie galėtų tiksliai nustatyti tam tikrus scenarijus reguliuojant genų raišką.

Individualių taikinių genų raiškos ryšiai su pacientų klinikinėmis charakteristikomis. Pirsono Chi kvadrato testas buvo naudojamas individualiai tikslinių genų raiškai įvertinti naudojant pacientų klinikinės duomenis, suskirstytus pagal metilinimo klasterius, siekiant iširti, kaip specifinė genų raiška yra susijusi su klinikiniais pacientų duomenimis. Remiantis mūsų rezultatais, C1 klasteryje nustatėme reikšmingą ryšį tarp *RETREG1* geno raiškos ir MGMT metilinimo statuso ($p = 0,034$) bei naviko vietos ($p = 0,027$). Gene *GP1BB* buvo reikšmingų sąsajų su kamieniškumo įverčiu C2 klasteryje, o tai parodė, kad aukšta genų raiška yra susijusi su aukštu kamieniškumo įverčiu ($p = 0,044$). Be to, *TOB1* genas parodė reikšmingą ryšį su pacientų amžiumi klasteryje C1 ($p = 0,031$) ir *PAGR1* genas su glioblastomų potipiais ($p = 0,004$). Galiausiai, pasitelkėme Cox proporcingą pavojaus analizę įvertinti skaitinius analizuojamų taikinių genų raiškos pokyčius susijusius su gliomomis sergančių pacientų išgyvenamumu. Didelę įtaką pacientų išgyvenamumui turėjo *LUC7L3*, *OS9* ir *TOB1* genų raiška. Didžiausi pacientų išgyvenamumo pavojaus pokyčiai buvo susiję su *OS9* genu, kas parodė padidėjusią mirties riziką net 8,9 karto, o tai reiškia, kad genas labiausiai siejamas su prastu išgyvenimu.

Baltymus koduojančių RNR signalinimo keliai, susiję su kamieniškumu m⁶A metilinimo klasteriuose. Signalinimo keliai atlieka lemiamą vaidmenį reguliuot kamieniškumą, kuris prisideda prie gliomos kamieninių ląstelių atsinaujinimo, diferenciacijos ir išgyvenimo. Keliai yra sudėtingi ir pažeidžia molekulinis signalus bei reguliavimo elementus susijusius su kamieniškumu [204]. Gliomų navikai yra kilę iš glijos ląstelių ir turi unikalių ląstelių ir molekulinį savybių, kurias dažnai sukelia sutrikęs signalinių kelių reguliavimas [205]. Gliomos ląstelės, sąveikaudamos su receptoriumi, gali kontroliuoti ryšius manipuluodamos informacija, kuri siunčiama į kitas ląsteles, tam kad sukurtų tam tikrą biologinį poveikį įskaitant citoskeleto pokyčius, ląstelių proliferaciją, o tai skatina angiogenezę ir gliomos navikų augimą [206]. Signalinimo kelių analizė yra labai svarbi ypatingai sprendžiant tokias problemas kaip heterogeniškumas, atsparumas terapijai ir naviko atsinaujinimas, o su kamieniškumu susijusių kelių stebėjimas gali padėti numatyti naviko vystymąsi ir progresavimą [207].

Mokslininkai jau nustatė signalinimo kelius susijusius su kamieniškumu, ir kiekvienas iš jų apima kamieniškumo žymenis. Taigi mes atlikome signalinių kelių praturtinimo analizę klasteriuose C1 ir C2. Abejuose klasteriuose buvo rasti 15 pagrindinių signalinių kelių. C2 klasteryje, kuriame buvo tik GB pacientai, buvo nustatyti kamieniškumu susiję keliai JAK-STAT ir PI3K-Akt. Šie keliai labai svarbūs palaikant ląstelių atsinaujinimą, naviko progresavimą ir atitinka agresyvių glioblastomų pobūdį. Su kamieniškumu susijusių kelių nustatymas rodo, kad GB ląstelės gali turėti didesnį navikų inicijavimo potencialą, atsparumo terapijai ir gebėjimą prisitaikyti prie naviko mikroaplinkos. Ši genų praturtinimo analizė rodo, kad GB pacientų prognozė gali būti prasta ir susijusi su agresyviu naviko elgesiu, lyginant su LGG pacientais. Šie keliai, galėtų būti potencialūs taikiniai, o nusitaikant į juos būtų galima sutrikdyti agresyvių GB elgesį. Rezultatai suteikia svarbių įžvalgų apie molekulinis mechanizmus, kuriais grindžiamas kamieniškumas ir gali būti naudingi nustatant galimus vėžio terapinės intervencijos tikslus ateities tyrimuose.

IŠVADOS

1. Įvertinus m⁶A modifikacijų profilį nustatėme aukštesnį metilinimo lygį gliomos kamieninėse ląstelėse lyginant su U87-MG ląstelėmis. Buvo atrinkti 8, su gliomos kamieninėmis ląstelėmis susiję m⁶A modifikuoti transkriptai genuose *OS9*, *PAGRI*, *TOB1*, *PIK3R2*, *GP1BB*, *RETREG1* ir *LUC7L3*.
2. Klasterinė analizė pagal 8 sumuotus gliomų kamieninėms ląstelėms specifinius m⁶A genų transkriptus, pacientus suskirstė žemo laipsnio gliomų ir glioblastomų klasterius. m⁶A modifikuotų transkriptų metilinimo lygis buvo 3,4 karto didesnis LGG lyginant su GB, kas parodė m⁶A modifikacijų sąsajas su gliomageneze.
- 2.1 Suminis, gliomos kamieninėms ląstelėms specifinių m⁶A modifikuotų transkriptų metilinimo lygis buvo reikšmingai susijęs su pacientų klinikinėmis charakteristikomis – amžiumi ir išgyvenamumu, o glioblastomų imtyje su naviko lokalizacija ir išgyvenamumu. Gliomos pacientų mėginiuose identifikuoti su kamieninėmis ląstelėmis ir m⁶A modifikacija susijęs RRACH motyvų rinkinys: AAACA|2129|*OS9*, AGACA|1210|*PAGRI*, GGACA|2173|*OS9*, GGACT|2187|*TOB1*, AAACC|3283|*PIK3R2*, GAACC|3068|*GP1BB*, GGACA|3110|*RETREG1* ir GGACT|3122|*LUC7L3*). Nustatyti reikšmingi m⁶A mRNR rinkinio ryšiai su pacientų

klinikinėmis charakteristikomis rodo taikinių tinkamumą gliomų klasifikavimui ir prognozei.

3. Atskirų gliomos kamieninėms ląstelėms specifiniai, m⁶A modifikuotų transkriptų analizė atskleidė ryšį su pacientų amžiumi, Ki-67 indeksu ir bendru išgyvenamumu GGACA|2173|OS9, AAACC|3283|PIK3R2 motyvuose; Ki-67 indeksu ir bendru išgyvenamumu GAACC|3068|GP1BB RRACH motyve; pacientų išgyvenamumu AAACA|2129|OS9 ir AGACA|1210|PAGRI ir, galiausiai, bendru išgyvenamumu, amžiumi, Ki-67 statusu ir naviko vieta GGACA|3110|RETREGI motyve, parodydama specifinės m⁶A metilinimo svarbą gliomos patogenezėje.

REFERENCES

1. Yang K, Wu Z, Zhang H, Zhang N, Wu W, Wang Z, et al. Glioma targeted therapy: insight into future of molecular approaches. *Mol Cancer*. 2022 Feb 8;21(1):39.
2. Wu W, Klockow JL, Zhang M, Lafortune F, Chang E, Jin L, et al. Glioblastoma multiforme (GBM): An overview of current therapies and mechanisms of resistance. *Pharmacol Res*. 2021 Sep;171:105780.
3. Guadagno E, Borrelli G, Califano M, Cali G, Solari D, Del Basso De Caro M. Immunohistochemical expression of stem cell markers CD44 and nestin in glioblastomas: Evaluation of their prognostic significance. *Pathol Res Pract*. 2016 Sep;212(9):825–32.
4. Li F, Lv B, Liu Y, Hua T, Han J, Sun C, et al. Blocking the CD47-SIRP α axis by delivery of anti-CD47 antibody induces antitumor effects in glioma and glioma stem cells. *Oncoimmunology*. 2018 Feb 1;7(2).
5. Jia G, Fu Y, Zhao X, Dai Q, Zheng G, Yang Y, et al. N6-Methyladenosine in nuclear RNA is a major substrate of the obesity-associated FTO. *Nat Chem Biol*. 2011 Dec 16;7(12):885–7.
6. Zheng G, Dahl JA, Niu Y, Fedorcsak P, Huang CM, Li CJ, et al. ALKBH5 Is a Mammalian RNA Demethylase that Impacts RNA Metabolism and Mouse Fertility. *Mol Cell*. 2013 Jan;49(1):18–29.
7. Wang T, Kong S, Tao M, Ju S. The potential role of RNA N6-methyladenosine in Cancer progression. *Mol Cancer*. 2020 Dec 12;19(1):88.
8. Cui Q, Shi H, Ye P, Li L, Qu Q, Sun G, et al. m⁶A RNA Methylation Regulates the Self-Renewal and Tumorigenesis of Glioblastoma Stem Cells. *Cell Rep*. 2017 Mar; 18(11):2622–34.
9. Sibbritt T, Patel HR, Preiss T. Mapping and significance of the mRNA methylome. *WIREs RNA*. 2013 Jul 16;4(4):397–422.
10. Dominissini D, Moshitch-Moshkovitz S, Schwartz S, Salmon-Divon M, Ungar L, Osenberg S, et al. Topology of the human and mouse m⁶A RNA methylomes revealed by m⁶A-seq. *Nature*. 2012 May 10;485(7397):201–6.
11. Liu H, Begik O, Lucas MC, Ramirez JM, Mason CE, Wiener D, et al. Accurate detection of m⁶A RNA modifications in native RNA sequences. *Nat Commun*. 2019 Sep 9;10(1):4079.
12. Schaff LR, Mellinghoff IK. Glioblastoma and Other Primary Brain Malignancies in Adults. *JAMA*. 2023 Feb 21;329(7):574.
13. Wrensch M, Lee M, Miike R, Newman B, Bargar G, Davis R, et al. Familial and Personal Medical History of Cancer and Nervous System Conditions among Adults with Glioma and Controls. *Am J Epidemiol*. 1997 Apr 1;145(7):581–93.
14. Ostrom QT, Fahmideh MA, Cote DJ, Muskens IS, Schraw JM, Scheurer ME, et al. Risk factors for childhood and adult primary brain tumors. *Neuro Oncol*. 2019 Nov 4; 21(11):1357–75.
15. Jonsson P, Lin AL, Young RJ, DiStefano NM, Hyman DM, Li BT, et al. Genomic Correlates of Disease Progression and Treatment Response in Prospectively Characterized Gliomas. *Clinical Cancer Research*. 2019 Sep 15;25(18):5537–47.
16. Kinnersley B, Mitchell JS, Gousias K, Schramm J, Idbaih A, Labussière M, et al. Quantifying the heritability of glioma using genome-wide complex trait analysis. *Sci Rep*. 2015 Dec 2;5(1):17267.

17. Ilic I, Ilic M. International patterns and trends in the brain cancer incidence and mortality: An observational study based on the global burden of disease. *Heliyon*. 2023 Jul;9(7):e18222.
18. Tan AC, Ashley DM, López GY, Malinzak M, Friedman HS, Khasraw M. Management of glioblastoma: State of the art and future directions. *CA Cancer J Clin*. 2020 Jul; 70(4):299–312.
19. Onishi S, Yamasaki F, Amatya VJ, Takayasu T, Yonezawa U, Taguchi A, et al. Characteristics and therapeutic strategies of radiation-induced glioma: case series and comprehensive literature review. *J Neurooncol*. 2022 Sep 3;159(3):531–8.
20. Stupp R, Hegi ME, Mason WP, van den Bent MJ, Taphoorn MJ, Janzer RC, et al. Effects of radiotherapy with concomitant and adjuvant temozolomide versus radiotherapy alone on survival in glioblastoma in a randomised phase III study: 5-year analysis of the EORTC-NCIC trial. *Lancet Oncol*. 2009 May;10(5):459–66.
21. Ostrom QT, Bauchet L, Davis FG, Deltour I, Fisher JL, Langer CE, et al. The epidemiology of glioma in adults: a “state of the science” review. *Neuro Oncol*. 2014 Jul 1;16(7):896–913.
22. Marenco-Hillebrand L, Wijesekera O, Suarez-Meade P, Mampre D, Jackson C, Peterson J, et al. Trends in glioblastoma: outcomes over time and type of intervention: a systematic evidence based analysis. *J Neurooncol*. 2020 Apr 9;147(2):297–307.
23. Louis DN, Perry A, Reifenberger G, von Deimling A, Figarella-Branger D, Cavenee WK, et al. The 2016 World Health Organization classification of tumors of the central nervous system: a summary. *Acta Neuropathol*. 2016 Jun 9;131(6):803–20.
24. Agnihotri S, Burrell KE, Wolf A, Jalali S, Hawkins C, Rutka JT, et al. Glioblastoma, a Brief Review of History, Molecular Genetics, Animal Models and Novel Therapeutic Strategies. *Arch Immunol Ther Exp (Warsz)*. 2013 Feb 7;61(1):25–41.
25. Couturier CP, Ayyadhury S, Le PU, Nadaf J, Monlong J, Riva G, et al. Single-cell RNA-seq reveals that glioblastoma recapitulates a normal neurodevelopmental hierarchy. *Nat Commun*. 2020 Jul 8;11(1):3406.
26. Parsons DW, Jones S, Zhang X, Lin JCH, Leary RJ, Angenendt P, et al. An Integrated Genomic Analysis of Human Glioblastoma Multiforme. *Science* (1979). 2008 Sep 26;321(5897):1807–12.
27. Ohgaki H, Kleihues P. The Definition of Primary and Secondary Glioblastoma. *Clinical Cancer Research*. 2013 Feb 15;19(4):764–72.
28. Nobusawa S, Watanabe T, Kleihues P, Ohgaki H. IDH1 Mutations as Molecular Signature and Predictive Factor of Secondary Glioblastomas. *Clinical Cancer Research*. 2009 Oct 1;15(19):6002–7.
29. Omuro A. Glioblastoma and Other Malignant Gliomas. *JAMA*. 2013 Nov 6;310(17):1842.
30. Campos B, Olsen LR, Urup T, Poulsen HS. A comprehensive profile of recurrent glioblastoma. *Oncogene*. 2016 Nov 10;35(45):5819–25.
31. Singh SK, Hawkins C, Clarke ID, Squire JA, Bayani J, Hide T, et al. Identification of human brain tumour initiating cells. *Nature*. 2004 Nov;432(7015):396–401
32. Thakur A, Faujdar C, Sharma R, Sharma S, Malik B, Nepali K, et al. Glioblastoma: Current Status, Emerging Targets, and Recent Advances. *J Med Chem*. 2022 Jul 14;65(13):8596–685.
33. Slepak TI, Guyot M, Walters W, Eichberg DG, Ivan ME. Dual role of the adhesion G-protein coupled receptor ADRGE5/CD97 in glioblastoma invasion and proliferation. *Journal of Biological Chemistry*. 2023 Sep;299(9):105105.

34. Lathia JD, Mack SC, Mulkearns-Hubert EE, Valentim CLL, Rich JN. Cancer stem cells in glioblastoma. *Genes Dev.* 2015 Jun 15;29(12):1203–17.
35. Rich JN. Cancer stem cells. *Medicine.* 2016 Sep;95(1S):S1.
36. Sarkar S, Greer J, Marlowe NJ, Medvid A, Ivan ME, Kolishetti N, et al. Stemness, invasion, and immunosuppression modulation in recurrent glioblastoma using nanotherapy. *WIREs Nanomedicine and Nanobiotechnology.* 2024 Jul 2;16(4).
37. Louis DN, Perry A, Wesseling P, Brat DJ, Cree IA, Figarella-Branger D, et al. The 2021 WHO classification of tumors of the central nervous system: a summary. *Neuro Oncol.* 2021 Aug 2;23(8):1231–51.
38. Gritsch S, Batchelor TT, Gonzalez Castro LN. Diagnostic, therapeutic, and prognostic implications of the 2021 World Health Organization classification of tumors of the central nervous system. *Cancer.* 2022 Jan 11;128(1):47–58.
39. Brat DJ, Aldape K, Colman H, Holland EC, Louis DN, Jenkins RB, et al. cIMPACT-NOW update 3: recommended diagnostic criteria for “Diffuse astrocytic glioma, IDH-wildtype, with molecular features of glioblastoma, WHO grade IV.” *Acta Neuropathol.* 2018 Nov 26;136(5):805–10.
40. Stichel D, Ebrahimi A, Reuss D, Schrimpf D, Ono T, Shirahata M, et al. Distribution of EGFR amplification, combined chromosome 7 gain and chromosome 10 loss, and TERT promoter mutation in brain tumors and their potential for the reclassification of IDHwt astrocytoma to glioblastoma. *Acta Neuropathol.* 2018 Nov 5;136(5):793–803.
41. Verhaak RGW, Hoadley KA, Purdom E, Wang V, Qi Y, Wilkerson MD, et al. Integrated Genomic Analysis Identifies Clinically Relevant Subtypes of Glioblastoma Characterized by Abnormalities in PDGFRA, IDH1, EGFR, and NF1. *Cancer Cell.* 2010 Jan;17(1):98–110.
42. Colman H, Zhang L, Sulman EP, McDonald JM, Shooshtari NL, Rivera A, et al. A multigene predictor of outcome in glioblastoma. *Neuro Oncol.* 2010 Jan 1;12(1):49–57.
43. Wang Q, Hu B, Hu X, Kim H, Squatrito M, Scarpace L, et al. Tumor Evolution of Glioma-Intrinsic Gene Expression Subtypes Associates with Immunological Changes in the Microenvironment. *Cancer Cell.* 2017 Jul;32(1):42-56.e6.
44. Chiu FY, Yen Y. Imaging biomarkers for clinical applications in neuro-oncology: current status and future perspectives. *Biomark Res.* 2023 Mar 29;11(1):35.
45. Biomarkers and surrogate endpoints: Preferred definitions and conceptual framework. *Clin Pharmacol Ther.* 2001 Mar;69(3):89–95.
46. Kim RK, Yoon CH, Hyun KH, Lee H, An S, Park MJ, et al. Role of lymphocyte-specific protein tyrosine kinase (LCK) in the expansion of glioma-initiating cells by fractionated radiation. *Biochem Biophys Res Commun.* 2010 Nov;402(4):631–6.
47. Binello E, Qadeer ZA, Kothari HP, Emdad L, Germano IM. Stemness of the CT-2A Immunocompetent Mouse Brain Tumor Model: Characterization In Vitro. *J Cancer.* 2012;3:166–74.
48. Wookey PJ, McLean CA, Hwang P, Furness SGB, Nguyen S, Kourakis A, et al. The expression of calcitonin receptor detected in malignant cells of the brain tumour glioblastoma multiforme and functional properties in the cell line A172. *Histopathology.* 2012 May 15;60(6):895–910.
49. Guo Y, Liu S, Wang P, Zhao S, Wang F, Bing L, et al. Expression profile of embryonic stem cell-associated genes Oct4, Sox2 and Nanog in human gliomas. *Histopathology.* 2011 Oct;59(4):763–75.

50. Zhang M, Song T, Yang L, Chen R, Wu L, Yang Z, et al. Nestin and CD133: valuable stem cell-specific markers for determining clinical outcome of glioma patients. *Journal of Experimental & Clinical Cancer Research*. 2008 Dec 24;27(1):85.
51. Mooney KL, Choy W, Sidhu S, Pelargos P, Bui TT, Voth B, et al. The role of CD44 in glioblastoma multiforme. *Journal of Clinical Neuroscience*. 2016 Dec;34:1–5.
52. Brown D V., Filiz G, Daniel PM, Hollande F, Dworkin S, Amiridis S, et al. Expression of CD133 and CD44 in glioblastoma stem cells correlates with cell proliferation, phenotype stability and intra-tumor heterogeneity. *PLoS One*. 2017 Feb 27;12(2):e0172791.
53. Zbinden M, Duquet A, Lorente-Trigos A, Ngwabyt SN, Borges I, Ruiz i Altaba A. NANOG regulates glioma stem cells and is essential in vivo acting in a cross-functional network with GLI1 and p53. *EMBO J*. 2010 Aug 4;29(15):2659–74.
54. Yu Q, Xue Y, Liu J, Xi Z, Li Z, Liu Y. Fibronectin Promotes the Malignancy of Glioma Stem-Like Cells Via Modulation of Cell Adhesion, Differentiation, Proliferation and Chemoresistance. *Front Mol Neurosci*. 2018 Apr 13;11.
55. Vieira de Castro J, Gonçalves CS, Hormigo A, Costa BM. Exploiting the Complexities of Glioblastoma Stem Cells: Insights for Cancer Initiation and Therapeutic Targeting. *Int J Mol Sci*. 2020 Jul 25;21(15):5278.
56. Kraboth Z, Kalman B. Longitudinal Characteristics of Glioblastoma in Genome-Wide Studies. *Pathology & Oncology Research*. 2020 Oct 3;26(4):2035–47.
57. Barthel FP, Johnson KC, Varn FS, Moskalik AD, Tanner G, Kocakavuk E, et al. Longitudinal molecular trajectories of diffuse glioma in adults. *Nature*. 2019 Dec 5;576(7785):112–20.
58. Körber V, Yang J, Barah P, Wu Y, Stichel D, Gu Z, et al. Evolutionary Trajectories of IDHWT Glioblastomas Reveal a Common Path of Early Tumorigenesis Instigated Years ahead of Initial Diagnosis. *Cancer Cell*. 2019 Apr;35(4):692-704.e12.
59. Wang J, Cazzato E, Ladewig E, Frattini V, Rosenbloom DIS, Zairis S, et al. Clonal evolution of glioblastoma under therapy. *Nat Genet*. 2016 Jul 6;48(7):768–76.
60. An Z, Aksoy O, Zheng T, Fan QW, Weiss WA. Epidermal growth factor receptor and EGFRvIII in glioblastoma: signaling pathways and targeted therapies. *Oncogene*. 2018 Mar 11;37(12):1561–75.
61. Touat M, Idbah A, Sanson M, Ligon KL. Glioblastoma targeted therapy: updated approaches from recent biological insights. *Annals of Oncology*. 2017 Jul;28(7):1457–72.
62. Platten M. EGFRvIII vaccine in glioblastoma – InACT-IVE or not ReACTive enough? *Neuro Oncol*. 2017 Oct 19;19(11):1425–6.
63. Neftel C, Laffy J, Filbin MG, Hara T, Shore ME, Rahme GJ, et al. An Integrative Model of Cellular States, Plasticity, and Genetics for Glioblastoma. *Cell*. 2019 Aug;178(4):835-849.e21.
64. Boulias K, Greer EL. Biological roles of adenine methylation in RNA. *Nat Rev Genet*. 2023 Mar 19;24(3):143–60.
65. Huang H, Weng H, Chen J. m⁶A Modification in Coding and Non-coding RNAs: Roles and Therapeutic Implications in Cancer. *Cancer Cell*. 2020 Mar;37(3):270–88.
66. Meyer KD, Jaffrey SR. The dynamic epitranscriptome: N⁶-methyladenosine and gene expression control. *Nat Rev Mol Cell Biol*. 2014 May 9;15(5):313–26.
67. Huang M, Xu S, Liu L, Zhang M, Guo J, Yuan Y, et al. m⁶A Methylation Regulates Osteoblastic Differentiation and Bone Remodeling. *Front Cell Dev Biol*. 2021 Dec 21;9.
68. Roundtree IA, Evans ME, Pan T, He C. Dynamic RNA Modifications in Gene Expression Regulation. *Cell*. 2017 Jun;169(7):1187–200.

69. Edupuganti RR, Geiger S, Lindeboom RGH, Shi H, Hsu PJ, Lu Z, et al. N6-methyladenosine (m⁶A) recruits and repels proteins to regulate mRNA homeostasis. *Nat Struct Mol Biol.* 2017 Oct 4;24(10):870–8.
70. Li S, Qi Y, Yu J, Hao Y, He B, Zhang M, et al. Nuclear Aurora kinase A switches m⁶A reader YTHDC1 to enhance an oncogenic RNA splicing of tumor suppressor RBM4. *Signal Transduct Target Ther.* 2022 Apr 1;7(1):97.
71. Alarcón CR, Lee H, Goodarzi H, Halberg N, Tavazoie SF. N6-methyladenosine marks primary microRNAs for processing. *Nature.* 2015 Mar 18;519(7544):482–5.
72. Heck AM, Russo J, Wilusz J, Nishimura EO, Wilusz CJ. YTHDF2 destabilizes m⁶A-modified neural-specific RNAs to restrain differentiation in induced pluripotent stem cells. *RNA.* 2020 Jun;26(6):739–55.
73. Edens BM, Vissers C, Su J, Arumugam S, Xu Z, Shi H, et al. FMRP Modulates Neural Differentiation through m⁶A-Dependent mRNA Nuclear Export. *Cell Rep.* 2019 Jul;28(4):845-854.e5.
74. Feng J, Zhang T, Sorel O, Meng W, Zhang X, Lai Z, et al. Global profiling reveals common and distinct N6-methyladenosine (m⁶A) regulation of innate immune responses during bacterial and viral infections. *Cell Death Dis.* 2022 Mar 14;13(3):234.
75. Ma Z, Ji J. N6-methyladenosine (m⁶A) RNA modification in cancer stem cells. *Stem Cells.* 2020 Dec 1;38(12):1511–9.
76. Yin H, Zhang X, Yang P, Zhang X, Peng Y, Li D, et al. RNA m⁶A methylation orchestrates cancer growth and metastasis via macrophage reprogramming. *Nat Commun.* 2021 Mar 2;12(1):1394.
77. Müller S, Glaß M, Singh AK, Haase J, Bley N, Fuchs T, et al. IGF2BP1 promotes SRF-dependent transcription in cancer in a m⁶A- and miRNA-dependent manner. *Nucleic Acids Res.* 2019 Jan 10;47(1):375–90.
78. Chai RC, Wu F, Wang QX, Zhang S, Zhang KN, Liu YQ, et al. m⁶A RNA methylation regulators contribute to malignant progression and have clinical prognostic impact in gliomas. *Aging.* 2019 Feb 27;11(4):1204–25.
79. Ceccarelli M, Barthel FP, Malta TM, Sabedot TS, Salama SR, Murray BA, et al. Molecular Profiling Reveals Biologically Discrete Subsets and Pathways of Progression in Diffuse Glioma. *Cell.* 2016 Jan;164(3):550–63.
80. Wang X, Lu Z, Gomez A, Hon GC, Yue Y, Han D, et al. N6-methyladenosine-dependent regulation of messenger RNA stability. *Nature.* 2014 Jan 27;505(7481):117–20.
81. Dixit D, Prager BC, Gimple RC, Poh HX, Wang Y, Wu Q, et al. The RNA m⁶A Reader YTHDF2 Maintains Oncogene Expression and Is a Targetable Dependency in Glioblastoma Stem Cells. *Cancer Discov.* 2021 Feb 1;11(2):480–99.
82. Liu J, Yue Y, Han D, Wang X, Fu Y, Zhang L, et al. A METTL3–METTL14 complex mediates mammalian nuclear RNA N6-adenosine methylation. *Nat Chem Biol.* 2014 Feb 6;10(2):93–5.
83. Zhao BS, Roundtree IA, He C. Post-transcriptional gene regulation by mRNA modifications. *Nat Rev Mol Cell Biol.* 2017 Jan 3;18(1):31–42.
84. Jia G, Fu Y, Zhao X, Dai Q, Zheng G, Yang Y, et al. N6-Methyladenosine in nuclear RNA is a major substrate of the obesity-associated FTO. *Nat Chem Biol.* 2011 Dec 16;7(12):885–7.
85. Zheng G, Dahl JA, Niu Y, Fedorcsak P, Huang CM, Li CJ, et al. ALKBH5 Is a Mammalian RNA Demethylase that Impacts RNA Metabolism and Mouse Fertility. *Mol Cell.* 2013 Jan;49(1):18–29.
86. Dong Z, Cui H. The Emerging Roles of RNA Modifications in Glioblastoma. *Cancers (Basel).* 2020 Mar 20;12(3):736.

87. Wang J, Sha Y, Sun T. m⁶A Modifications Play Crucial Roles in Glial Cell Development and Brain Tumorigenesis. *Front Oncol.* 2021 Feb 24;11.
88. Kane SE, Beemon K. Inhibition of methylation at two internal N⁶-methyladenosine sites caused by GAC to GAU mutations. *Journal of Biological Chemistry.* 1987 Mar; 262(7):3422–7.
89. Batista PJ, Molinie B, Wang J, Qu K, Zhang J, Li L, et al. m⁶A RNA Modification Controls Cell Fate Transition in Mammalian Embryonic Stem Cells. *Cell Stem Cell.* 2014 Dec;15(6):707–19.
90. Chen T, Hao YJ, Zhang Y, Li MM, Wang M, Han W, et al. m⁶A RNA Methylation Is Regulated by MicroRNAs and Promotes Reprogramming to Pluripotency. *Cell Stem Cell.* 2015 Mar;16(3):289–301.
91. Barbieri I, Tzelepis K, Pandolfini L, Shi J, Millán-Zambrano G, Robson SC, et al. Promoter-bound METTL3 maintains myeloid leukaemia by m⁶A-dependent translation control. *Nature.* 2017 Dec 27;552(7683):126–31.
92. Yankova E, Blackaby W, Albertella M, Rak J, De Brackeleer E, Tsagkogeorga G, et al. Small-molecule inhibition of METTL3 as a strategy against myeloid leukaemia. *Nature.* 2021 May 27;593(7860):597–601.
93. Murakami S, Jaffrey SR. Hidden codes in mRNA: Control of gene expression by m⁶A. *Mol Cell.* 2022 Jun;82(12):2236–51.
94. Yang Y, Lu Y, Wang Y, Wen X, Qi C, Piao W, et al. Current progress in strategies to profile transcriptomic m⁶A modifications. *Front Cell Dev Biol.* 2024 Jul 11;12.
95. Vu LP, Pickering BF, Cheng Y, Zaccara S, Nguyen D, Minuesa G, et al. The N⁶-methyladenosine (m⁶A)-forming enzyme METTL3 controls myeloid differentiation of normal hematopoietic and leukemia cells. *Nat Med.* 2017 Nov 18;23(11):1369–76.
96. Weng H, Huang H, Wu H, Qin X, Zhao BS, Dong L, et al. METTL14 Inhibits Hematopoietic Stem/Progenitor Differentiation and Promotes Leukemogenesis via mRNA m⁶A Modification. *Cell Stem Cell.* 2018 Feb;22(2):191-205.e9.
97. Li Z, Weng H, Su R, Weng X, Zuo Z, Li C, et al. FTO Plays an Oncogenic Role in Acute Myeloid Leukemia as a N⁶-Methyladenosine RNA Demethylase. *Cancer Cell.* 2017 Jan;31(1):127–41.
98. Tian J, Ying P, Ke J, Zhu Y, Yang Y, Gong Y, et al. ANKLE1 N⁶-Methyladenosine-related variant is associated with colorectal cancer risk by maintaining the genomic stability. *Int J Cancer.* 2020 Jun 15;146(12):3281–93.
99. Zhang J, Bai R, Li M, Ye H, Wu C, Wang C, et al. Excessive miR-25-3p maturation via N⁶-methyladenosine stimulated by cigarette smoke promotes pancreatic cancer progression. *Nat Commun.* 2019 Apr 23;10(1):1858.
100. Gu S, Sun D, Dai H, Zhang Z. N⁶-methyladenosine mediates the cellular proliferation and apoptosis via microRNAs in arsenite-transformed cells. *Toxicol Lett.* 2018 Aug; 292:1–11.
101. Yang F, Jin H, Que B, Chao Y, Zhang H, Ying X, et al. Dynamic m⁶A mRNA methylation reveals the role of METTL3-m⁶A-CDCP1 signaling axis in chemical carcinogenesis. *Oncogene.* 2019 Jun 22;38(24):4755–72.
102. Cui Q, Shi H, Ye P, Li L, Qu Q, Sun G, et al. m⁶A RNA Methylation Regulates the Self-Renewal and Tumorigenesis of Glioblastoma Stem Cells. *Cell Rep.* 2017 Mar;18(11):2622–34.
103. Suvà ML, Rheinbay E, Gillespie SM, Patel AP, Wakimoto H, Rabkin SD, et al. Reconstructing and Reprogramming the Tumor-Propagating Potential of Glioblastoma Stem-like Cells. *Cell.* 2014 Apr;157(3):580–94.

104. Galardi S, Michienzi A, Ciafrè SA. Insights into the Regulatory Role of m⁶A Epitranscriptome in Glioblastoma. *Int J Mol Sci.* 2020 Apr 17;21(8):2816.
105. Hyman G, Manglik V, Rousch JM, Verma M, Kinkebiel D, Banerjee HN. Epigenetic Approaches in Glioblastoma Multiforme and Their Implication in Screening and Diagnosis. In 2015. p. 511–21.
106. Zhang Y, Geng X, Li Q, Xu J, Tan Y, Xiao M, et al. m⁶A modification in RNA: biogenesis, functions and roles in gliomas. *Journal of Experimental & Clinical Cancer Research.* 2020 Dec 17;39(1):192.
107. Yuan F, Cai X, Cong Z, Wang Y, Geng Y, Aili Y, et al. Roles of the m⁶A Modification of RNA in the Glioblastoma Microenvironment as Revealed by Single-Cell Analyses. *Front Immunol.* 2022 Apr 26;13.
108. Meyer KD, Saletore Y, Zumbo P, Elemento O, Mason CE, Jaffrey SR. Comprehensive Analysis of mRNA Methylation Reveals Enrichment in 3' UTRs and near Stop Codons. *Cell.* 2012 Jun;149(7):1635–46.
109. Lavi U, Fernandez-Mufioz R, Darnell JE. Content of N-6 methyl adenylic acid in heterogeneous nuclear and messenger RNA of HeLa cells. *Nucleic Acids Res.* 1977;4(1):63–9.
110. Horowitz S, Horowitz A, Nilsen TW, Munns TW, Rottman FM. Mapping of N6-methyladenosine residues in bovine prolactin mRNA. *Proceedings of the National Academy of Sciences.* 1984 Sep;81(18):5667–71.
111. Ke S, Alemu EA, Mertens C, Gantman EC, Fak JJ, Mele A, et al. A majority of m⁶A residues are in the last exons, allowing the potential for 3' UTR regulation. *Genes Dev.* 2015 Oct 1;29(19):2037–53.
112. Zeng Y, Wang S, Gao S, Soares F, Ahmed M, Guo H, et al. Refined RIP-seq protocol for epitranscriptome analysis with low input materials. *PLoS Biol.* 2018 Sep 13; 16(9):e2006092.
113. Liu J, Li K, Cai J, Zhang M, Zhang X, Xiong X, et al. Landscape and Regulation of m⁶A and m⁶Am Methylome across Human and Mouse Tissues. *Mol Cell.* 2020 Jan;77(2):426-440.e6.
114. Liu H, Begik O, Lucas MC, Ramirez JM, Mason CE, Wiener D, et al. Accurate detection of m⁶A RNA modifications in native RNA sequences. *Nat Commun.* 2019 Sep 9;10(1):4079.
115. Chu X, Tian W, Ning J, Xiao G, Zhou Y, Wang Z, et al. Cancer stem cells: advances in knowledge and implications for cancer therapy. *Signal Transduct Target Ther.* 2024 Jul 5;9(1):170.
116. Sun L, Xu C, Chen G, Yu M, Yang S, Qiu Y, et al. A Novel Role of OS-9 in the Maintenance of Intestinal Barrier Function from Hypoxia-induced Injury via p38-dependent Pathway. *Int J Biol Sci.* 2015;11(6):664–71.
117. Su YA, Hutter CM, Trent JM, Meltzer PS. Complete sequence analysis of a gene (OS-9) ubiquitously expressed in human tissues and amplified in sarcomas. *Mol Carcinog.* 1996 Apr;15(4):270–5.
118. Satoh T, Chen Y, Hu D, Hanashima S, Yamamoto K, Yamaguchi Y. Structural Basis for Oligosaccharide Recognition of Misfolded Glycoproteins by OS-9 in ER-Associated Degradation. *Mol Cell.* 2010 Dec;40(6):905–16.
119. Gong Z, Cho YW, Kim JE, Ge K, Chen J. Accumulation of Pax2 Transactivation Domain Interaction Protein (PTIP) at Sites of DNA Breaks via RNF8-dependent Pathway Is Required for Cell Survival after DNA Damage. *Journal of Biological Chemistry.* 2009 Mar;284(11):7284–93.

120. Cho YW, Hong T, Hong S, Guo H, Yu H, Kim D, et al. PTIP Associates with MLL3- and MLL4-containing Histone H3 Lysine 4 Methyltransferase Complex. *Journal of Biological Chemistry*. 2007 Jul;282(28):20395–406.
121. Wang D, Li Y, Sui S, Cai M, Dong K, Wang P, et al. Involvement of TOB1 on autophagy in gastric cancer AGS cells via decreasing the activation of AKT/mTOR signaling pathway. *PeerJ*. 2022 Feb 4;10:e12904.
122. Minchenko OH, Sliusar MY, Viletska YM, Rudnytska OV, Kolybo DV. The impact of ERN1 endoribonuclease activity inhibition on TOB1, HBEGF, and TWIST1 genes expression in U87MG glioblastoma cells. *Endocr Regul*. 2025 Jan 1;59(1):24–32.
123. Wang D, Song H, Zhao T, Wang M, Wang Y, Yu L, et al. Human Genetic Resources and Disease Control in China [Internet]. Vol. 11, P. R. China. * Equal con-tributors. 2019. Available from: www.ajtr.org
124. Zhang J, Li Y, Chen J, Huang T, Lin J, Pi Y, et al. TOB1 modulates neutrophil phenotypes to influence gastric cancer progression and immunotherapy efficacy. *Front Immunol*. 2024 Mar 28;15.
125. Mengel B, Hunziker A, Pedersen L, Trusina A, Jensen MH, Krishna S. Modeling oscillatory control in NF- κ B, p53 and Wnt signaling. *Curr Opin Genet Dev*. 2010 Dec;20(6):656–64.
126. Uthamacumaran A. H3K4-H3K9 Histone Methylation Patterns and Oncofetal Developmental Networks as Drivers of Cell Fate Decisions in Pediatric High-Grade Gliomas. 2024.
127. Winkler GS. The mammalian anti-proliferative BTG/Tob protein family. *J Cell Physiol*. 2010 Jan 10;222(1):66–72.
128. Zhang S, Gu J, Shi L ling, Qian B, Diao X, Jiang X, et al. A pan-cancer analysis of anti-proliferative protein family genes for therapeutic targets in cancer. *Sci Rep*. 2023 Dec 7;13(1):21607.
129. Fruman DA. Regulatory Subunits of Class IA PI3K. In 2010. p. 225–44.
130. Ueki K, Algenstaedt P, Mauvais-Jarvis F, Kahn CR. Positive and Negative Regulation of Phosphoinositide 3-Kinase-Dependent Signaling Pathways by Three Different Gene Products of the p85 α Regulatory Subunit. *Mol Cell Biol*. 2000 Nov 1;20(21):8035–46.
131. Vanhaesebroeck B, Vogt PK, Rommel C. PI3K: From the Bench to the Clinic and Back. In 2010. p. 1–19.
132. Vallejo-Díaz J, Chagoyen M, Olazabal-Morán M, González-García A, Carrera AC. The Opposing Roles of PIK3R1/p85 α and PIK3R2/p85 β in Cancer. *Trends Cancer*. 2019 Apr;5(4):233–44.
133. Vallejo-Díaz J, Olazabal-Morán M, Cariaga-Martínez AE, Pajares MJ, Flores JM, Pio R, et al. Targeted depletion of PIK3R2 induces regression of lung squamous cell carcinoma. *Oncotarget*. 2016 Dec 20;7(51):85063–78.
134. Fruman DA, Chiu H, Hopkins BD, Bagrodia S, Cantley LC, Abraham RT. The PI3K Pathway in Human Disease. *Cell*. 2017 Aug;170(4):605–35.
135. Liu Y, Wang D, Li Z, Li X, Jin M, Jia N, et al. Pan-cancer analysis on the role of PIK3R1 and PIK3R2 in human tumors. *Sci Rep*. 2022 Apr 8;12(1):5924.
136. Chang M, He Y, Liu C, Lin R, Huang X, Liang D, et al. Downregulation of SEPTIN5 inhibits prostate cancer progression by increasing CD8 + T cell infiltration. *Int J Biol Sci*. 2022;18(16):6035–51.
137. Peter B, Scherer N, Liang WS, Pophal S, Nielsen C, Grebe TA. A phenotypically diverse family with an atypical 22q11.2 deletion due to an unbalanced 18q23;22q11.2 translocation. *Am J Med Genet A*. 2021 May 11;185(5):1532–7.

138. McDermid HE, Morrow BE. Genomic disorders on 22q11. *The American Journal of Human Genetics*. 2002 May;70(5):1077–88.
139. Bartsch I, Sandrock K, Lanza F, Nurden P, Hainmann I, Pavlova A, et al. Deletion of human GP1BB and SEPT5 is associated with Bernard-Soulier syndrome, platelet secretion defect, polymicrogyria, and developmental delay. *Thromb Haemost*. 2011 Nov 24;106(09):475–83.
140. Islam F, Gopalan V, Lam AK. RETREG1 (FAM134B): a new player in human diseases: 15 years after the discovery in cancer. *J Cell Physiol*. 2018 Jun 15;233(6):4479–89.
141. Zhou L, Tang C, Shuai R, Chen B, Yang X, He Y, et al. TIMP4 serves as a novel potential prognostic biomarker for oral squamous cell carcinoma. *Sci Rep*. 2025 Feb 21;15(1):6313.
142. Scheubert L, Schmidt R, Repsilber D, Lustrek M, Fuellen G. Learning Biomarkers of Pluripotent Stem Cells in Mouse. *DNA Research*. 2011 Aug 1;18(4):233–51.
143. Kurth I, Pamminer T, Hennings JC, Soehendra D, Huebner AK, Rothhler A, et al. Mutations in FAM134B, encoding a newly identified Golgi protein, cause severe sensory and autonomic neuropathy. *Nat Genet*. 2009 Nov 18;41(11):1179–81.
144. Murphy SM, Davidson GL, Brandner S, Houlden H, Reilly MM. Mutation in FAM134B causing severe hereditary sensory neuropathy: Figure 1. *J Neurol Neurosurg Psychiatry*. 2012 Jan;83(1):119–20.
145. Davidson GL, Murphy SM, Polke JM, Laura M, Salih MAM, Muntoni F, et al. Frequency of mutations in the genes associated with hereditary sensory and autonomic neuropathy in a UK cohort. *J Neurol*. 2012 Aug 1;259(8):1673–85.
146. Rivière JB, Ramalingam S, Lavastre V, Shekarabi M, Holbert S, Lafontaine J, et al. KIF1A, an Axonal Transporter of Synaptic Vesicles, Is Mutated in Hereditary Sensory and Autonomic Neuropathy Type 2. *The American Journal of Human Genetics*. 2011 Aug;89(2):219–30.
147. Kasem K, Gopalan V, Salajegheh A, Lu CT, Smith RA, Lam AKY. The roles of JK-1 (FAM134B) expressions in colorectal cancer. *Exp Cell Res*. 2014 Aug;326(1):166–73.
148. Haque MdH, Gopalan V, Chan K wah, Shiddiky MJA, Smith RA, Lam AK yin. Identification of Novel FAM134B (JK1) Mutations in Oesophageal Squamous Cell Carcinoma. *Sci Rep*. 2016 Jul 4;6(1):29173.
149. Kasem K, Gopalan V, Salajegheh A, Lu CT, Smith RA, Lam AKY. JK1 (FAM134B) gene and colorectal cancer: A pilot study on the gene copy number alterations and correlations with clinicopathological parameters. *Exp Mol Pathol*. 2014 Aug;97(1):31–6.
150. Zielke S, Kardo S, Zein L, Mari M, Covarrubias-Pinto A, Kinzler MN, et al. ATF4 links ER stress with reticulophagy in glioblastoma cells. *Autophagy*. 2021 Sep 2;17(9):2432–48.
151. Kung CP, Budina A, Balaburski G, Bergenstock MK, Murphy M. Autophagy in tumor suppression and cancer therapy. *Crit Rev Eukaryot Gene Expr*. 2011;21(1):71–100.
152. Batara DCR, Choi MC, Shin HU, Kim H, Kim SH. Friend or Foe: Paradoxical Roles of Autophagy in Gliomagenesis. *Cells*. 2021 Jun 6;10(6):1411.
153. Zhang X, Guo J, Shi X, Zhou X, Chen Q. LUC7L3 is a downstream factor of SRSF1 and prevents genomic instability. *Cell Insight*. 2024 Jun;3(3):100170.
154. Hou Y, Wang S, Zhang Y, Huang X, Zhang X, He F, et al. Proteomics Identifies LUC7L3 as a Prognostic Biomarker for Hepatocellular Carcinoma. *Curr Issues Mol Biol*. 2024 Apr 27;46(5):4004–20.

155. Hamperl S, Bocek MJ, Saldivar JC, Swigut T, Cimprich KA. Transcription-Replication Conflict Orientation Modulates R-Loop Levels and Activates Distinct DNA Damage Responses. *Cell*. 2017 Aug;170(4):774-786.e19.
156. Bao X, Zhu K, Liu X, Chen Z, Luo Z, Zhao Q, et al. MeRIPseqPipe: an integrated analysis pipeline for MeRIP-seq data based on Nextflow. *Bioinformatics*. 2022 Mar 28;38(7):2054-6.
157. Di Tommaso P, Chatzou M, Floden EW, Barja PP, Palumbo E, Notredame C. Nextflow enables reproducible computational workflows. *Nat Biotechnol*. 2017 Apr 11;35(4):316-9.
158. Danecek P, Bonfield JK, Liddle J, Marshall J, Ohan V, Pollard MO, et al. Twelve years of SAMtools and BCFtools. *Gigascience*. 2021 Jan 29;10(2).
159. Dobin A, Davis CA, Schlesinger F, Drenkow J, Zaleski C, Jha S, et al. STAR: ultrafast universal RNA-seq aligner. *Bioinformatics*. 2013 Jan 1;29(1):15-21.
160. <https://matk.renlab.org/#/home>.
161. Liu L, Zhang SW, Huang Y, Meng J. QNB: differential RNA methylation analysis for count-based small-sample sequencing data with a quad-negative binomial model. *BMC Bioinformatics*. 2017 Dec 31;18(1):387.
162. Love MI, Huber W, Anders S. Moderated estimation of fold change and dispersion for RNA-seq data with DESeq2. *Genome Biol*. 2014 Dec 5;15(12):550.
163. Liao Y, Smyth GK, Shi W. featureCounts: an efficient general purpose program for assigning sequence reads to genomic features. *Bioinformatics*. 2014 Apr 1;30(7):923-30.
164. Cappannini A, Ray A, Purta E, Mukherjee S, Boccaletto P, Moafinejad SN, et al. MODOMICS: a database of RNA modifications and related information. 2023 update. *Nucleic Acids Res*. 2024 Jan 5;52(D1):D239-44.
165. Smith MA, Ersavas T, Ferguson JM, Liu H, Lucas MC, Begik O, et al. Molecular barcoding of native RNAs using nanopore sequencing and deep learning. *Genome Res*. 2020 Sep;30(9):1345-53.
166. Cunningham F, Allen JE, Allen J, Alvarez-Jarreta J, Amode MR, Armean IM, et al. Ensembl 2022. *Nucleic Acids Res*. 2022 Jan 7;50(D1):D988-95.
167. Li H. Minimap2: pairwise alignment for nucleotide sequences. *Bioinformatics*. 2018 Sep 15;34(18):3094-100.
168. Danecek P, Bonfield JK, Liddle J, Marshall J, Ohan V, Pollard MO, et al. Twelve years of SAMtools and BCFtools. *Gigascience*. 2021 Jan 29;10(2).
169. Liu H, Begik O, Lucas MC, Ramirez JM, Mason CE, Wiener D, et al. Accurate detection of m⁶A RNA modifications in native RNA sequences. *Nat Commun*. 2019 Sep 9;10(1):4079.
170. Liao Y, Smyth GK, Shi W. featureCounts: an efficient general purpose program for assigning sequence reads to genomic features. *Bioinformatics*. 2014 Apr 1;30(7):923-30.
171. <https://www.R-project.org/>.
172. <https://www.graphpad.com/>.
173. Demšar J, Erjavec A, Hočvar T, Milutinović M, Možina M, Toplak M, et al. Orange: Data Mining Toolbox in Python Tomaž Curk Matija Polajnar Laň Zagar. *Journal of Machine Learning Research*. 2013;4(71):2349-53.
174. Wu T, Hu E, Xu S, Chen M, Guo P, Dai Z, et al. clusterProfiler 4.0: a universal enrichment tool for interpreting omics data. *The Innovation*. 2021 Aug;2(3):100141.
175. Vissers C, Sinha A, Ming G li, Song H. The epitranscriptome in stem cell biology and neural development. *Neurobiol Dis*. 2020 Dec;146:105139.

176. Hatakeyama J, Ono T, Takahashi M, Oda M, Shimizu H. Differentiating between Primary Central Nervous System Lymphoma and Glioblastoma: The Diagnostic Value of Combining F-fluorodeoxyglucose Positron Emission Tomography with Arterial Spin Labeling. *Neurol Med Chir (Tokyo)*. 2021;61(6):367–75.
177. Cho HR, Jeon H, Park CK, Park SH, Choi SH. Radiogenomics Profiling for Glioblastoma-related Immune Cells Reveals CD49d Expression Correlation with MRI parameters and Prognosis. *Sci Rep*. 2018 Oct 30;8(1):16022.
178. Mohan S, Wang S, Coban G, Kural F, Chawla S, O'Rourke DM, et al. Detection of occult neoplastic infiltration in the corpus callosum and prediction of overall survival in patients with glioblastoma using diffusion tensor imaging. *Eur J Radiol*. 2019 Mar; 112:106–11.
179. Fyllingen EH, Bø LE, Reinertsen I, Jakola AS, Sagberg LM, Berntsen EM, et al. Survival of glioblastoma in relation to tumor location: a statistical tumor atlas of a population-based cohort. *Acta Neurochir (Wien)*. 2021 Jul 20;163(7):1895–905.
180. Li HY, Sun CR, He M, Yin LC, Du HG, Zhang JM. Correlation Between Tumor Location and Clinical Properties of Glioblastomas in Frontal and Temporal Lobes. *World Neurosurg*. 2018 Apr;112:e407–14.
181. Liu TT, Achrol AS, Mitchell LA, Du WA, Loya JJ, Rodriguez SA, et al. Computational Identification of Tumor Anatomic Location Associated with Survival in 2 Large Cohorts of Human Primary Glioblastomas. *American Journal of Neuroradiology*. 2016 Apr;37(4):621–8.
182. Lee JE, Cho YW, Deng CX, Ge K. MLL3/MLL4-associated PAGR1 Regulates Adipogenesis by Controlling Induction of C/EBP β and C/EBP δ . *Mol Cell Biol*. 2020 Aug 14;40(17).
183. Liu B, Li Z. PTIP-associated Protein 1: More Than a Component of the MLL3/4 Complex. *Front Genet*. 2022 Jun 9;13.
184. Bai Y, Qiao L, Xie N, Li Y, Nie Y, Pan Y, et al. TOB1 suppresses proliferation in K-Ras wild-type pancreatic cancer. *Cancer Med*. 2020 Feb 31;9(4):1503–14.
185. Zhang YW, Nasto RE, Varghese R, Jablonski SA, Serebriiskii IG, Surana R, et al. Acquisition of estrogen independence induces TOB1-related mechanisms supporting breast cancer cell proliferation. *Oncogene*. 2016 Mar 31;35(13):1643–56.
186. Cortés I, Sánchez-Ruíz J, Zuluaga S, Calvanese V, Marqués M, Hernández C, et al. p85 β phosphoinositide 3-kinase subunit regulates tumor progression. *Proceedings of the National Academy of Sciences*. 2012 Jul 10;109(28):11318–23.
187. Hübner CA, Dikic I. ER-phagy and human diseases. *Cell Death Differ*. 2020 Mar 28;27(3):833–42.
188. Phi LTH, Sari IN, Yang YG, Lee SH, Jun N, Kim KS, et al. Cancer Stem Cells (CSCs) in Drug Resistance and their Therapeutic Implications in Cancer Treatment. *Stem Cells Int*. 2018;2018:1–16.
189. Lai J, Lin X, Zheng H, Xie B, Fu D. Characterization of stemness features and construction of a stemness subtype classifier to predict survival and treatment responses in lung squamous cell carcinoma. *BMC Cancer*. 2023 Jun 8;23(1):525.
190. Barbie DA, Tamayo P, Boehm JS, Kim SY, Moody SE, Dunn IF, et al. Systematic RNA interference reveals that oncogenic KRAS-driven cancers require TBK1. *Nature*. 2009 Nov 21;462(7269):108–12.
191. Malta TM, Sokolov A, Gentles AJ, Burzykowski T, Poisson L, Weinstein JN, et al. Machine Learning Identifies Stemness Features Associated with Oncogenic Dedifferentiation. *Cell*. 2018 Apr;173(2):338-354.e15.

192. Miranda A, Hamilton PT, Zhang AW, Pattnaik S, Becht E, Mezheyeuski A, et al. Cancer stemness, intratumoral heterogeneity, and immune response across cancers. *Proceedings of the National Academy of Sciences*. 2019 Apr 30;116(18):9020–9.
193. Qu S, Huang J, Liu J, Wang H. Prognostic significance of cancer stemness-associated genes in patients with gliomas. *Clin Transl Med*. 2020 Sep 27;10(5).
194. Ye S, Yang B, Yang L, Wei W, Fu M, Yan Y, et al. Stemness subtypes in lower-grade glioma with prognostic biomarkers, tumor microenvironment, and treatment response. *Sci Rep*. 2024 Jun 26;14(1):14758.
195. Xue J, Liu H, Jiang L, Yin Q, Chen L, Wang M. Limitations of nomogram models in predicting survival outcomes for glioma patients. *Front Immunol*. 2025 Mar 18;16.
196. Battle E, Clevers H. Cancer stem cells revisited. *Nat Med*. 2017 Oct 1;23(10):1124–34.
197. Huang T, Song X, Xu D, Tiek D, Goenka A, Wu B, et al. Stem cell programs in cancer initiation, progression, and therapy resistance. *Theranostics*. 2020;10(19):8721–43.
198. McCown PJ, Ruszkowska A, Kunkler CN, Breger K, Hulewicz JP, Wang MC, et al. Naturally occurring modified ribonucleosides. *WIREs RNA*. 2020 Sep 16;11(5).
199. Eisenberg E, Levanon EY. A-to-I RNA editing – immune protector and transcriptome diversifier. *Nat Rev Genet*. 2018 Aug 24;19(8):473–90.
200. Sun H, Li K, Liu C, Yi C. Regulation and functions of non-m6A mRNA modifications. *Nat Rev Mol Cell Biol*. 2023 Oct 27;24(10):714–31.
201. Lv D, Gimple RC, Zhong C, Wu Q, Yang K, Prager BC, et al. PDGF signaling inhibits mitophagy in glioblastoma stem cells through N-methyladenosine. *Dev Cell*. 2022 Jun;57(12):1466-1481.e6.
202. Zhang S, Zhao BS, Zhou A, Lin K, Zheng S, Lu Z, et al. m6A Demethylase ALKBH5 Maintains Tumorigenicity of Glioblastoma Stem-like Cells by Sustaining FOXM1 Expression and Cell Proliferation Program. *Cancer Cell*. 2017 Apr;31(4):591-606.e6.
203. Price M, Ballard C, Benedetti J, Neff C, Cioffi G, Waite KA, et al. CBTRUS Statistical Report: Primary Brain and Other Central Nervous System Tumors Diagnosed in the United States in 2017–2021. *Neuro Oncol*. 2024 Oct 6;26(Supplement_6):vi1–85.
204. Talukdar J, Srivastava TP, Sahoo OS, Karmakar A, Rai AK, Sarma A, et al. Cancer stem cells: Signaling pathways and therapeutic targeting. *MedComm – Oncology*. 2023 Dec 28;2(4).
205. Mehta S, Lo Cascio C. Developmentally regulated signaling pathways in glioma invasion. *Cellular and Molecular Life Sciences*. 2018 Feb 18;75(3):385–402.
206. Liu M, Xu Z, Du Z, Wu B, Jin T, Xu K, et al. The Identification of Key Genes and Pathways in Glioma by Bioinformatics Analysis. *J Immunol Res*. 2017;2017:1–9.
207. Sevastre AS, Buzatu IM, Baloi C, Oprita A, Dragoi A, Tataranu LG, et al. ELTD1 – An Emerging Silent Actor in Cancer Drama Play. *Int J Mol Sci*. 2021 May 13;22(10):5151.
208. De Sousa e Melo F, Vermeulen L. Wnt Signaling in Cancer Stem Cell Biology. *Cancers (Basel)*. 2016 Jun 27;8(7):60.
209. Abel E V., Kim EJ, Wu J, Hynes M, Bednar F, Proctor E, et al. The Notch Pathway Is Important in Maintaining the Cancer Stem Cell Population in Pancreatic Cancer. *PLoS One*. 2014 Mar 19;9(3):e91983.
210. Koury J, Zhong L, Hao J. Targeting Signaling Pathways in Cancer Stem Cells for Cancer Treatment. *Stem Cells Int*. 2017;2017:1–10.
211. Zeng F, Chen H, Zhang Z, Yao T, Wang G, Zeng Q, et al. Regulating glioma stem cells by hypoxia through the Notch1 and Oct3/4 signaling pathway. *Oncol Lett*. 2018 Sep 17;

212. Rane SG, Reddy EP. Janus kinases: components of multiple signaling pathways. *Oncogene*. 2000 Nov 20;19(49):5662–79.
213. Stine RR, Matunis EL. JAK-STAT Signaling in Stem Cells. In 2013. p. 247–67.
214. de Freitas RM, da Costa Maranduba CM. Myeloproliferative neoplasms and the JAK/STAT signaling pathway: an overview. *Rev Bras Hematol Hemoter*. 2015 Sep; 37(5):348–53.
215. Peñuelas S, Anido J, Prieto-Sánchez RM, Folch G, Barba I, Cuartas I, et al. TGF- β Increases Glioma-Initiating Cell Self-Renewal through the Induction of LIF in Human Glioblastoma. *Cancer Cell*. 2009 Apr;15(4):315–27.
216. Sherry MM, Reeves A, Wu JK, Cochran BH. STAT3 Is Required for Proliferation and Maintenance of Multipotency in Glioblastoma Stem Cells. *Stem Cells*. 2009 Oct 1;27(10):2383–92.
217. Clement V, Sanchez P, de Tribolet N, Radovanovic I, Ruiz i Altaba A. HEDGEHOG-GLI1 Signaling Regulates Human Glioma Growth, Cancer Stem Cell Self-Renewal, and Tumorigenicity. *Current Biology*. 2007 Jan;17(2):165–72.
218. Takezaki T, Hide T, Takanaga H, Nakamura H, Kuratsu J, Kondo T. Essential role of the Hedgehog signaling pathway in human glioma-initiating cells. *Cancer Sci*. 2011 Jul 3;102(7):1306–12.
219. Skoda AM, Simovic D, Karin V, Kardum V, Vranic S, Serman L. The role of the Hedgehog signaling pathway in cancer: a comprehensive review. *Bosn J Basic Med Sci*. 2018 Feb 20;18(1):8–20.
220. Xu J, Zhang Z, Qian M, Wang S, Qiu W, Chen Z, et al. Cullin-7 (CUL7) is over-expressed in glioma cells and promotes tumorigenesis via NF- κ B activation. *Journal of Experimental & Clinical Cancer Research*. 2020 Dec 6;39(1):59.
221. Li X, Wu C, Chen N, Gu H, Yen A, Cao L, et al. PI3K/Akt/mTOR signaling pathway and targeted therapy for glioblastoma. *Oncotarget*. 2016 May 31;7(22):33440–50.
222. Chakravarti A, Zhai G, Suzuki Y, Sarkesh S, Black PM, Muzikansky A, et al. The Prognostic Significance of Phosphatidylinositol 3-Kinase Pathway Activation in Human Gliomas. *Journal of Clinical Oncology*. 2004 May 15;22(10):1926–33.
223. Zahonero C, Sánchez-Gómez P. EGFR-dependent mechanisms in glioblastoma: towards a better therapeutic strategy. *Cellular and Molecular Life Sciences*. 2014 Sep 27;71(18):3465–88.
224. Chehelgerdi M, Behdarvand Dehkordi F, Chehelgerdi M, Kabiri H, Salehian-Dehkordi H, Abdolvand M, et al. Exploring the promising potential of induced pluripotent stem cells in cancer research and therapy. *Mol Cancer*. 2023 Nov 28;22(1):189.
225. Ediriweera MK, Tennekoon KH, Samarakoon SR. Role of the PI3K/AKT/mTOR signaling pathway in ovarian cancer: biological and therapeutic significance. *Semin Cancer Biol*. 2019 Dec;59:147–60.
226. Zhang C, Wang Y, Shao W, Zhou D, Yu D, Hou S, et al. A novel NFAT1-IL6/JAK/STAT3 signaling pathway related nomogram predicts overall survival in gliomas. *Sci Rep*. 2023 Jul 14;13(1):11401.
227. Goenka A, Tiek D, Song X, Huang T, Hu B, Cheng SY. The Many Facets of Therapy Resistance and Tumor Recurrence in Glioblastoma. *Cells*. 2021 Feb 24;10(3):484.
228. Esmatabadi MJD, Bakhshinejad B, Motlagh FM, Babashah S, Sadeghizadeh M. Therapeutic resistance and cancer recurrence mechanisms: unfolding the story of tumour coming back. *J Biosci*. 2016 Sep 13;41(3):497–506.
229. Yalamarty SSK, Filipczak N, Li X, Subhan MA, Parveen F, Ataide JA, et al. Mechanisms of Resistance and Current Treatment Options for Glioblastoma Multiforme (GBM). *Cancers (Basel)*. 2023 Apr 1;15(7):2116.

230. Chaulagain D, Smolanka V, Smolanka A, Havryliv T. Гліобластома: огляд літератури. *International Neurological Journal*. 2023 Jan 27;18(8):32–7.
231. Yalamarty SSK, Filipczak N, Li X, Subhan MA, Parveen F, Ataide JA, et al. Mechanisms of Resistance and Current Treatment Options for Glioblastoma Multiforme (GBM). *Cancers (Basel)*. 2023 Apr 1;15(7):2116.
232. Liu Y, Zhou F, Ali H, Lathia JD, Chen P. Immunotherapy for glioblastoma: current state, challenges, and future perspectives. *Cell Mol Immunol*. 2024 Oct 15;21(12):1354–75.
233. Kotecha R, Odia Y, Khosla AA, Ahluwalia MS. Key Clinical Principles in the Management of Glioblastoma. *JCO Oncol Pract*. 2023 Apr;19(4):180–9.
234. Sharma P, Aaroe A, Liang J, Puduvali VK. Tumor microenvironment in glioblastoma: current and emerging concepts. *Neurooncol Adv*. 2023 Jan 1;5(1).
235. Eramo A, Ricci-Vitiani L, Zeuner A, Pallini R, Lotti F, Sette G, et al. Chemotherapy resistance of glioblastoma stem cells. *Cell Death Differ*. 2006 Jul 3;13(7):1238–41.
236. Muftuoglu Y, Pajonk F. Targeting Glioma Stem Cells. *Neurosurg Clin N Am*. 2021 Apr;32(2):283–9.
237. Lathia JD, Gallagher J, Myers JT, Li M, Vasanji A, McLendon RE, et al. Direct In Vivo Evidence for Tumor Propagation by Glioblastoma Cancer Stem Cells. *PLoS One*. 2011 Sep 22;6(9):e24807.
238. Tchoghandjian A, Baeza N, Colin C, Cayre M, Metellus P, Beclin C, et al. A2B5 Cells from Human Glioblastoma have Cancer Stem Cell Properties. *Brain Pathology*. 2010 Jan 7;20(1):211–21.
239. Sun T, Chen G, Li Y, Xie X, Zhou Y, Du Z. Aggressive invasion is observed in CD133–/A2B5+ glioma-initiating cells. *Oncol Lett*. 2015 Dec;10(6):3399–406.
240. Wu B, Sun C, Feng F, Ge M, Xia L. Do relevant markers of cancer stem cells CD133 and Nestin indicate a poor prognosis in glioma patients? A systematic review and meta-analysis. *Journal of Experimental & Clinical Cancer Research*. 2015 Dec 14;34(1):44.
241. Lopes Abath Neto O, Aldape K. Morphologic and Molecular Aspects of Glioblastomas. *Neurosurg Clin N Am*. 2021 Apr;32(2):149–58.
242. Bhat K, Saki M, Vlashi E, Cheng F, Duhachek-Muggy S, Alli C, et al. The dopamine receptor antagonist trifluoperazine prevents phenotype conversion and improves survival in mouse models of glioblastoma. *Proceedings of the National Academy of Sciences*. 2020 May 19;117(20):11085–96.
243. Xie GS, Richard HT. m⁶A mRNA Modifications in Glioblastoma: Emerging Prognostic Biomarkers and Therapeutic Targets. *Cancers (Basel)*. 2024 Feb 9;16(4):727.
244. Fang R, Chen X, Zhang S, Shi H, Ye Y, Shi H, et al. EGFR/SRC/ERK-stabilized YTHDF2 promotes cholesterol dysregulation and invasive growth of glioblastoma. *Nat Commun*. 2021 Jan 8;12(1):177.
245. Visvanathan A, Patil V, Arora A, Hegde AS, Arivazhagan A, Santosh V, et al. Essential role of METTL3-mediated m⁶A modification in glioma stem-like cells maintenance and radioresistance. *Oncogene*. 2018 Jan 9;37(4):522–33.
246. Deng X, Sun X, Hu Z, Wu Y, Zhou C, Sun J, et al. Exploring the role of m⁶A methylation regulators in glioblastoma multiforme and their impact on the tumor immune microenvironment. *The FASEB Journal*. 2023 Sep 22;37(9).
247. Li F, Zhang C, Zhang G. m⁶A RNA Methylation Controls Proliferation of Human Glioma Cells by Influencing Cell Apoptosis. *Cytogenet Genome Res*. 2019;159(3):119–25.
248. Batool SM, Khan SM, Muralidharan K, Escobedo AK, Lee H, Ekanyake E, et al. Epitranscriptome Mapping of m⁶A RNA Modifications in Glioma Tumor Tissue. 2024.

249. Jiang X, Liu B, Nie Z, Duan L, Xiong Q, Jin Z, et al. The role of m⁶A modification in the biological functions and diseases. *Signal Transduct Target Ther.* 2021 Feb 21;6(1):74.
250. Zheng X, Li S, Yu J, Dai C, Yan S, Chen G, et al. N6-methyladenosine reader IGF2BP3 as a prognostic Biomarker contribute to malignant progression of glioma. *Transl Cancer Res.* 2023 Apr;12(4):992–1005.
251. Yu M, Ji W, Yang X, Tian K, Ma X, Yu S, et al. The role of m6A demethylases in lung cancer: diagnostic and therapeutic implications. *Front Immunol.* 2023 Nov 29;14.
252. Huang W, Chen TQ, Fang K, Zeng ZC, Ye H, Chen YQ. N6-methyladenosine methyltransferases: functions, regulation, and clinical potential. *J Hematol Oncol.* 2021 Jul 27;14(1):117.
253. Zhang G, Zheng P, Lv Y, Shi Z, Shi F. m⁶A Regulatory Gene-Mediated Methylation Modification in Glioma Survival Prediction. *Front Genet.* 2022 Apr 26;13.
254. Wei B, Wang L, Zhao J. Identification of an autophagy-related 10-lncRNA-mRNA signature for distinguishing glioblastoma multiforme from lower-grade glioma and prognosis prediction. *Gen Physiol Biophys.* 2021 Jul;40(4):257–74.
255. Valenzuela-Fuenzalida JJ, Moyano-Valarezo L, Silva-Bravo V, Milos-Brandenberg D, Orellana-Donoso M, Nova-Baeza P, et al. Association between the Anatomical Location of Glioblastoma and Its Evaluation with Clinical Considerations: A Systematic Review and Meta-Analysis. *J Clin Med.* 2024 Jun 13;13(12):3460.
256. Corr F, Grimm D, Saß B, Pojskić M, Bartsch JW, Carl B, et al. Radiogenomic Predictors of Recurrence in Glioblastoma – A Systematic Review. *J Pers Med.* 2022 Mar 4;12(3):402.
257. Lynes J, Khan I, Aguilera C, Rubino S, Thompson Z, Etame AB, et al. Development of a “Geo-Tagged” tumor sample registry: intra-operative linkage of sample location to imaging. *J Neurooncol.* 2023 Dec 28;165(3):449–58.
258. Jallo GI, Biser-Rohrbaugh A, Freed D. Brainstem gliomas. *Child’s Nervous System.* 2004 Mar 1;20(3):143–53.
259. Guidara S, Seyve A, Poncet D, Leonce C, Bringuier PP, McLeer A, et al. Characteristics of H3K27M-mutant diffuse gliomas with a non-midline location. *J Neurooncol.* 2024 Sep 27;169(2):391–8.
260. Raysi Dehcordi S, Galzio R, Marrone F, Di Vitantonio H, Marzi S, Fasano T, et al. Brain location and tumor biological markers in high- and low-grade gliomas. *J Neurosurg Sci.* 2023 Apr;67(2).
261. Wen PY, Weller M, Lee EQ, Alexander BM, Barnholtz-Sloan JS, Barthel FP, et al. Glioblastoma in adults: a Society for Neuro-Oncology (SNO) and European Society of Neuro-Oncology (EANO) consensus review on current management and future directions. *Neuro Oncol.* 2020 Aug 17;22(8):1073–113.
262. Galon J, Bruni D. Approaches to treat immune hot, altered and cold tumours with combination immunotherapies. *Nat Rev Drug Discov.* 2019 Mar 4;18(3):197–218.
263. Nduom EK, Wei J, Yaghi NK, Huang N, Kong LY, Gabrusiewicz K, et al. PD-L1 expression and prognostic impact in glioblastoma. *Neuro Oncol.* 2016 Feb;18(2):195–205.
264. Hambardzumyan D, Gutmann DH, Kettenmann H. The role of microglia and macrophages in glioma maintenance and progression. *Nat Neurosci.* 2016 Jan 29;19(1):20–7.
265. Quail DF, Joyce JA. The Microenvironmental Landscape of Brain Tumors. *Cancer Cell.* 2017 Mar;31(3):326–41.
266. He J, Zhu S, Liang X, Zhang Q, Luo X, Liu C, et al. LncRNA as a multifunctional regulator in cancer multi-drug resistance. *Mol Biol Rep.* 2021 Aug 31;48(8):1–15.

267. Vembar SS, Brodsky JL. One step at a time: endoplasmic reticulum-associated degradation. *Nat Rev Mol Cell Biol.* 2008 Dec 12;9(12):944–57.
268. Bernasconi R, Pertel T, Luban J, Molinari M. A Dual Task for the Xbp1-responsive OS-9 Variants in the Mammalian Endoplasmic Reticulum. *Journal of Biological Chemistry.* 2008 Jun;283(24):16446–54.
269. Hüttner S, Veit C, Schoberer J, Grass J, Strasser R. Unraveling the function of Arabidopsis thaliana OS9 in the endoplasmic reticulum-associated degradation of glycoproteins. *Plant Mol Biol.* 2012 May 11;79(1–2):21–33.
270. Seayfan E, Defontaine N, Demaretz S, Zaarour N, Laghmani K. OS9 Protein Interacts with Na-K-2Cl Co-transporter (NKCC2) and Targets Its Immature Form for the Endoplasmic Reticulum-associated Degradation Pathway. *Journal of Biological Chemistry.* 2016 Feb;291(9):4487–502.
271. Sun YW, Chen YF, Li J, Huo YM, Liu DJ, Hua R, et al. A novel long non-coding RNA ENST00000480739 suppresses tumour cell invasion by regulating OS-9 and HIF-1 α in pancreatic ductal adenocarcinoma. *Br J Cancer.* 2014 Nov 14;111(11):2131–41.
272. Arrillaga-Romany I, Chi AS, Allen JE, Oster W, Wen PY, Batchelor TT. A phase 2 study of the first imipridone ONC201, a selective DRD2 antagonist for oncology, administered every three weeks in recurrent glioblastoma. *Oncotarget.* 2017 Oct 3;8(45):79298–304.
273. Morson S, Yang Y, Price DJ, Pratt T. Expression of Genes in the 16p11.2 Locus during Development of the Human Fetal Cerebral Cortex. *Cerebral Cortex.* 2021 Jul 29;31(9):4038–52.
274. van Schie JJM, de Lint K, Molenaar TM, Moronta Gines M, Balk JA, Rooimans MA, et al. CRISPR screens in sister chromatid cohesion defective cells reveal PAXIP1-PAGR1 as regulator of chromatin association of cohesin. *Nucleic Acids Res.* 2023 Oct 13;51(18):9594–609.
275. Ashkin EL, Tang YJ, Xu H, Hung KL, Belk JA, Cai H, et al. A STAG2-PAXIP1/PAGR1 axis suppresses lung tumorigenesis. *Journal of Experimental Medicine.* 2025 Jan 6;222(1).
276. Mayayo-Peralta I, Gregoricchio S, Schuurman K, Yavuz S, Zaalberg A, Kojic A, et al. PAXIP1 and STAG2 converge to maintain 3D genome architecture and facilitate promoter/enhancer contacts to enable stress hormone-dependent transcription. *Nucleic Acids Res.* 2023 Oct 13;51(18):9576–93.
277. Takeshita T, Yamamoto-Ibusuki M, Yamamoto Y, Omoto Y, Honda Y, Iyama K ichi, et al. PTIP Associated protein 1, PA1, Is an Independent Prognostic Factor for Lymphnode Negative Breast Cancer. *PLoS One.* 2013 Nov 18;8(11):e80552.
278. Zeng W, Cheng Q, Wen Z, Wang J, Chen Y, Zhao J, et al. Aberrant ASPM expression mediated by transcriptional regulation of FoxM1 promotes the progression of gliomas. *J Cell Mol Med.* 2020 Sep 15;24(17):9613–26.
279. Zhao T, Meng W, Chin Y, Gao L, Yang X, Sun S, et al. Identification of miR-25-3p as a tumor biomarker: Regulation of cellular functions via TOB1 in breast cancer. *Mol Med Rep.* 2021 Mar 26;23(6):406.
280. Wang D, Song H, Zhao T, Wang M, Wang Y, Yu L, et al. Phosphorylation of TOB1 at T172 and S320 is critical for gastric cancer proliferation and progression. *Am J Transl Res.* 2019;11(8):5227–39.
281. Sliusar MY, Minchenko DO, Khita OO, Tsymbal DO, Viletska YM, Luzina OY, et al. Hypoxia controls the expression of genes responsible for serine synthesis in U87MG cells on ERN1-dependent manner. *Endocr Regul.* 2023 Jan 1;57(1):252–61.

282. Peng X, Ma L, Chen X, Tang F, Zong X. Inhibition of FBP1 expression by KMT5A through TWIST1 methylation is one of the mechanisms leading to chemoresistance in breast cancer. *Oncol Rep.* 2024 Jul 3;52(2):110.
283. Xu T, Yin F, Shi K. TMEM158 functions as an oncogene and promotes lung adenocarcinoma progression through the PI3K/AKT pathway via interaction with TWIST1. *Exp Cell Res.* 2024 Apr;437(1):114010.
284. Bi Y, Mao Y, Su Z, Du J, Ye L, Xu F. Long noncoding RNA HNF1A-AS1 regulates proliferation and apoptosis of glioma through activation of the JNK signaling pathway via miR-363-3p/MAP2K4. *J Cell Physiol.* 2021 Feb 10;236(2):1068–82.
285. Glaviano A, Foo ASC, Lam HY, Yap KCH, Jacot W, Jones RH, et al. PI3K/AKT/mTOR signaling transduction pathway and targeted therapies in cancer. *Mol Cancer.* 2023 Aug 18;22(1):138.
286. Lyu P, Zhang SD, Yuen HF, McCrudden CM, Wen Q, Chan KW, et al. Identification of TWIST-interacting genes in prostate cancer. *Sci China Life Sci.* 2017 Apr 22;60(4):386–96.
287. Mao X, Zhang X, Zheng X, Chen Y, Xuan Z, Huang P. Curcumin suppresses LGR5(+) colorectal cancer stem cells by inducing autophagy and via repressing TFAP2A-mediated ECM pathway. *J Nat Med.* 2021 Jun 13;75(3):590–601.
288. Blanco-Luquin I, Acha B, Urdániz-Casado A, Gómez-Orte E, Roldan M, Pérez-Rodríguez DR, et al. NXN Gene Epigenetic Changes in an Adult Neurogenesis Model of Alzheimer's Disease. *Cells.* 2022 Mar 22;11(7):1069.
289. Zhang Z, Chen J, Huang W, Ning D, Liu Q, Wang C, et al. FAM134B induces tumorigenesis and epithelial-to-mesenchymal transition via Akt signaling in hepatocellular carcinoma. *Mol Oncol.* 2019 Apr 24;13(4):792–810.
290. Tang W, Chui C, Fatima S, Kok S, Pak K, Ou T, et al. Oncogenic properties of a novel gene JK-1 located in chromosome 5p and its overexpression in human esophageal squamous cell carcinoma. *Int J Mol Med.* 2007 Jun 1;
291. Lee KTW, Islam F, Vider J, Martin J, Chruścik A, Lu CT, et al. Overexpression of family with sequence similarity 134, member B (FAM134B) in colon cancers and its tumor suppressive properties in vitro. *Cancer Biol Ther.* 2020 Oct 2;21(10):954–62.
292. Islam F, Gopalan V, Pillai S, Lu C, Kasem K, Lam AK. Promoter hypermethylation inactivate tumor suppressor FAM134B and is associated with poor prognosis in colorectal cancer. *Genes Chromosomes Cancer.* 2018 May 30;57(5):240–51.
293. Parker NR, Hudson AL, Khong P, Parkinson JF, Dwight T, Ikin RJ, et al. Intratumoral heterogeneity identified at the epigenetic, genetic and transcriptional level in glioblastoma. *Sci Rep.* 2016 Mar 4;6(1):22477.
294. Delahaye C, Nicolas J. Sequencing DNA with nanopores: troubles and biases. *PLoS One.* 2021 Oct 1;16(10):e0257521.

LIST OF PUBLICATIONS

Thesis publications:

1. Steponaitis, G., Stakaitis, R., Valiulytė, I., Krušnauskas, R., **Dragūnaitė, R.**, Urbanavičiūtė, R., Tamašauskas, A., and Skiriutė, D. (2022). Transcriptome-wide analysis of glioma stem cell specific m⁶A modifications in long-non-coding RNAs. *Scientific Reports*. London : Nature Publishing Group, 2022, Vol. 12, No. 1., 1-11. <https://doi.org/10.1038/s41598-022-08616-z> [Impact factor: 4.6, quartile: Q2].
2. Steponaitis, G., **Dragūnaitė, R.**, Stakaitis, R., Sharma, A., Tamasauskas, A., Skiriute, D. m⁶A-LncRNA landscape highlights reduced levels of m⁶A modification in glioblastoma as compared to low-grade glioma. 2025, <https://doi.org/10.1186/s10020-025-01254-x> [Impact factor: 6.0, quartile: Q1].

Thesis scientific conferences:

1. **Dragūnaitė, R.**, Stakaitis, R., Skiriutė, D. (2024). Revealing the relationship between glioblastoma stem cells and patient outcome through the expression patterns of lncRNAs. *International Health Sciences Conference for All (IHSC for All) “Precision Medicine”*: Abstract Book 2024: [March 25–26, 2024, Kaunas] Edited by Ignas Lapeikis, Livija Petrokaitė, 466-467. <https://smd.lt/uploads/publications/IHSCforAll2024.pdf>.
2. **Dragūnaitė, R.**, Steponaitis, G., Stakaitis, R., Skiriutė, D. (2024). Uncovering transcriptome-wide lncRNA methylation and expression patterns in human glioma. *FENS Forum 2024*: 25–29 June 2024, Vienna, Austria, 1-1. <https://fens2024.abstractserver.com/program/#!/details/presentations/>.
3. Skiriutė, D., **Dragūnaitė, R.**, Stakaitis, R., Steponaitis, G., Vaitkienė, P. (2024). m⁶A modified lncRNA profile of glioblastoma and healthy brain. 1st Net4Brain Annual Meeting “Closing the Translational Gap in Brain Cancer Treatment”: September 4th–6th, 2024 : *Book of Abstracts Editors: Barbara Breznik, Metka Novak*, 49–49. <https://hdl.handle.net/20.500.12512/249952>.
4. Žvinakytė, G., Balion, Z., Skiriutė, D., Vaitkienė, P., **Dragūnaitė, R.**, Urbanavičiūtė-Orentė, R., Steponaitis, G. (2024). Therapeutic Potential of Non-Coding RNAs in NSC-Generated EVs. *Join Baltic and Polish Societies of Extracellular Vesicles Meeting “The Good, the Bad and the Unknown – Roles of EVs in Health and Disease”*: 6–7 September 2024, Riga, Latvia, 30-30. <https://hdl.handle.net/20.500.12512/246877>.

5. **Dragūnaitė, R.**, Stakaitis, R., Skiriutė, D. (2023). Gliomagenesis associated lncRNAs *LINC00461*, *GAS5* and *NEAT1* are post-transcriptionally m⁶A modified in gliomas. *Medicina : Abstracts of the International Scientific Conference on Medicine Organized Within the Frame of the 81st International Scientific Conference of the University of Latvia : 10 February 2023, Riga University of Latvia ; Editor-in-Chief Edgaras Stankevičius. Kaunas ; Basel : LSMU ; MDPI, 2023, Vol. 59, Suppl. 1., 116–116. <https://hdl.handle.net/20.500.12512/117127>.*
6. **Dragūnaitė, R.**, Steponaitis, G., Stakaitis, R., Skiriutė, D. (2023). Epi-transcriptomic m⁶A modifications in glioma associated long-noncoding RNAs. *Health for All: 2023 – International Conference Health for All “Rare diseases” : Abstract Book : Kaunas, Lithuania, 19-20th April, 2023 [organised: Council of LSMU Doctoral Students]. Kaunas : Lithuanian University of Health Sciences, 2023, 31–32. <https://hdl.handle.net/20.500.12512/117846>.*
7. **Dragūnaitė, R.**, Steponaitis, G., Stakaitis, R., Skiriutė, D. (2023). Identifying modified long non-coding RNA targets in gliomas by direct RNA-SEQ. *International Conference of Life Sciences The COINS 2023 : Book of Abstracts : [April 24–27, 2023, Vilnius, Lithuania] Vilnius University. Vilnius : Vilnius University, 2023, 143–143. <https://hdl.handle.net/20.500.12512/2862>.*
8. Kriščiukaitis, A., Petrolis, R., **Dragūnaitė, R.**, Stakaitis, R., Skiriutė, D. (2023). Challenges in the Next Generation (Oxford Nanopore) Direct RNA Sequencing (dRNA-seq) Data Processing: Coping With Normalisation of Gene Expression Levels by Principal Component Analysis. *DAMSS 2023 : 14th [International] Conference on Data Analysis Methods for Software Systems : November 30 – December 2, 2023, Druskininkai, Lithuania, 41–42. <https://doi.org/10.15388/DAMSS.14.2023>.*
9. Skiriutė, D., **Dragūnaitė, R.**, Stakaitis, R., Steponaitis, G. (2023). Does posttranscriptional m⁶A lncRNAs landscape in glioblastoma matter? *XVIth International Conference of the Lithuanian Biochemical Society “Biochemistry Targeting Diseases” : Taujėnai, Lithuania, June 28–30, 2023 : programme and abstract book / Lietuvos Biochemikų Draugija. (p. 32-32). Lietuvos Biochemikų Draugija, 2023. <https://hdl.handle.net/20.500.12512/237914>.*
10. Steponaitis, G., **Dragūnaitė, R.**, Stakaitis, R., Vaitkienė, P., Tamašauskas, A., Skiriutė, D. (2023). RNA Modifications in Tumors – the New Black in Gene Regulation. *15th International Conference of the Lithuanian Neuroscience Association „Neurodiversity: From Theory through Artificial Intelligence to Clinical Practice“ : 24th November 2023, Kaunas, Lithuania Lithuanian Neuroscience Association. Neuroscience*

- Institute. Lithuanian University of Health Sciences, 12–12. https://www.neuromokslai.lt/wp-content/uploads/2023/10/15th_international_conference_of_the-Lithuanian-Neuroscience-2.pdf.
11. Širvinskas, D., **Dragūnaitė, R.**, Stakaitis, R., Steponaitis, G., Skiriutė, D., Vaitkienė, P. (2023). Glioma classification and prognosis through lncRNA. 15th International Conference of the Lithuanian Neuroscience Association „Neurodiversity: From Theory through Artificial Intelligence to Clinical Practice“ : 24th November 2023, Kaunas, Lithuania Lithuanian Neuroscience Association. Neuroscience Institute. Lithuanian University of Health Sciences., 28–28. https://www.neuromokslai.lt/wp-content/uploads/2023/10/15th_international_conference_of_the-Lithuanian-neuroscience-2.pdf.
 12. **Dragūnaitė, R.** (2022). Advances on the detection of N6-methyladenosine (m⁶A) modifications in glioma stem cells. Health for All: 2022 – International Conference Health for All “Our Planet, Our health” : Abstract Book : Kaunas, Lithuania, 6–7 April, 2022 [organized: Doctoral Student’s Committee of Lithuanian University of Health Sciences]. Kaunas: Lithuanian University of Health Sciences, 2022, 32–33. <https://hdl.handle.net/20.500.12512/113451>.
 13. **Dragūnaitė, R.**, Skiriutė, D. (2022). Analysis of M6A Modification Level at RRACH Motifs in *LINC00461*, *GAS5*, and *NEAT1* Genes in Gliomas. 14th International Conference of the Lithuanian Neuroscience Association: 25 November 2022, Vilnius, Lithuania: Abstract Book Lithuanian Neuroscience Association. Vilnius University. Vilnius: Vilnius University Press, 2022. ISBN 9786090707968, 26–26. <https://hdl.handle.net/20.500.12512/116189>.
 14. **Dragūnaitė, R.**, Steponaitis, G., Stakaitis, R., Skiriutė, D. (2022). Investigation of m6A modified lncRNAs in different grade gliomas. Brain Tumors 2022: From Biology to Therapy : Abstract Book : June 22-24, 2022, Warsaw, Poland Scientific Committee: Ety (Tika) Benveniste, Dolores Hambarzumyan, Christel Herold-Mende, Dinorah Friedmann-Morvinski, Bozena Kaminska. Warsaw: Nencki Institute of Experimental Biology, 2022, 35–35. <https://hdl.handle.net/20.500.12512/115191>.
 15. Kaur, G., Carbonell-Sala, S., Arnan, C., Palumbo, E., Uszczynska-Ratajczak, B., Lagarde, J., **Dragūnaitė, R.**, Guigo, R. (2022). Digging into the hidden layer of the human and mouse transcriptomes. X Bioinformatics and Genomics Symposium (BGS-X): Burjassot, Spain, December 15th–16th, 2022 Cavanilles Institute of Biodiversity and Evolutionary Biology (ICBiBE). Institute for Integrative Systems Biology (I2SysBio), 35-35. <https://hdl.handle.net/20.500.12512/240982>.

16. Stakaitis, R., Valiulytė, I., Steponaitis, G., **Dragūnaitė, R.**, Urbanavičiūtė, R., Krušnauskas, R., Skiriutė, D. (2021). Investigation of m6A modified lncRNAs for glioma prognosis. Symposium for the Next Generation of Stem Cell Researchers (SY-Stem): 3–5 March 2021, Vienna, Austria Organized Research Institute of Molecular Pathology (IMP). Institute of Molecular Biotechnology (IMBA). Vienna, 2021., 49–49. <https://hdl.handle.net/20.500.12512/110353>.

PHD CANDIDATE'S CONTRIBUTION

The contribution of author Rugilė Dragūnaitė is presented below concerning each of the publications related to the dissertation (A1–A2 listed in the list of scientific papers).

A1: Steponaitis, G., **Dragūnaitė, R.**, Stakaitis, R., Sharma, A., Tamašauskas, A., Skiriutė, D. m⁶A-lncRNA landscape highlights reduced levels of m⁶A modification in glioblastoma as compared to low-grade glioma. *Molecular Medicine*, 2025, 31(1), 1–16.

- Prepared 26 snap-frozen glioma tissues for the direct RNA Nanopore sequencing:
 1. Isolated total RNA from tumor tissues, enriched polyA RNA.
 2. Prepared polyA RNA libraries quantified the purity of the libraries and conducted direct RNA Nanopore sequencing.
- Assisted in formal analysis, writing original draft preparation and writing/reviewing.

A2: Steponaitis, G., Stakaitis, R., Valiulytė, I., Krušnauskas, R., **Dragūnaitė, R.**, Urbanavičiūtė, R., Tamašauskas, A., Skiriutė, D. (2022). Transcriptome-wide analysis of glioma stem cell specific m⁶A modifications in long-non-coding RNAs. *Scientific Reports*. London: Nature Publishing Group, 2022, Vol. 12, No. 1., 1–11.

- Assisted in preparing cell lines (NCH421k and U87-MG) for the MeRIP sequencing.
- Performed polyA enrichment, m⁶A immunoprecipitation.
- Assisted in writing original draft preparation.

Co-authors' contribution:

- **Daina Skiriutė** contributed to supervision and conceptualization of the studies, approved the final versions of the manuscripts, performed writing and editing of the article A1, A2; organized funding acquisition and resources; contributed to formal data analysis and investigation for the article A1.
- **Giedrius Steponaitis** contributed to conceptualization of the article A1, A2, laboratory work of the article A2; study conception and design, formal data analysis, investigation, writing-review and editing of the article A1, A2.
- **Arimantas Tamašauskas** contributed to conceptualization of the article A2; organized biological material from the participants for article A1.

- **Rūta Urbanavičiūtė, Indrė Valiulytė** performed part of investigations and experiments related to article A2.
- **Rytis Stakaitis** contributed to study conception and design, formal data analysis and investigation, writing-review and editing of the article A1; performed bioinformatic analysis and analyzed data of the article A2.
- **Raulas Krušnauskas** performed part of investigations and experiments, contributed to preparation of original A2 draft.
- **Amit Sharma** contributed to writing-review and editing of the article A1.

CURRICULUM VITAE

Name, Surname: Rugilė Dragūnaitė
Address: Lithuanian university of Health Sciences,
Mickevičiaus Str. 9, LT-44307 Kaunas
E-mail: rugile.dragunaite@lsmu.lt
Phone: +370 636 01283

Education:

2020–2024 LSMU, PhD in Biology
2017–2019 KTU, LSMU, master's degree in medicinal chemistry
2013–2017 VDU, bachelor's degree in environmental science

Work experience:

2020–present Junior researcher, LSMU, Neuroscience Institute,
Laboratory of Molecular Neurooncology

Scientific project:

2023–2026 Junior researcher at LRC project – *Molecular response of neural stem cells to the extracellular vesicles secreted by cells of different brain pathologies (ERONSC)*

01/2024–08/2024 Project leader at LSMU Science Fund funded project – *SELECT-based detection of specific m⁶A modification marks in gliomas*

01/2023–12/2023 Project leader at LSMU Science Fund funded project – *Culturing and growing adult human neural stem cells*

01/2022–12/2022 Project leader at LSMU Science Fund funded project – *Long non-coding RNA epitranscriptome profiling in tumors for identification of novel biomarkers*

Professional memberships:

2020–2024 LSMU PhD Students Council
2021–2024 LSMU Science Fund
2021–2024 LSMU Neuroscience Institute Council

Traineeships:

- 06/06/2022–
13/06/2022 Department of Life Sciences, Ben-Gurion University of
Negev (Beer Sheva, Israel)
- 12/09/2022–
12/12/2022 Centre for Genomic Regulation, the Laboratory of
Bioinformatics and Genomics (Barcelona, Spain)
- 02/02/2023–
02/03/2023 Centre for Genomic Regulation, the Laboratory of
Bioinformatics and Genomics (Barcelona, Spain)

Honors and Awards:

- 2023 The Lithuanian Research Council Scholarship for the
academic achievements
- 2023 The Lithuanian Research Council Foundation for
Professional Internship in Barcelona, Spain

ACKNOWLEDGMENTS

I would like to take this opportunity to express my heartfelt gratitude to all those who have supported me throughout my PhD ride.

I would like to begin with Lithuanian university of Health Sciences for providing me with the opportunity to pursue my PhD studies. I am also thankful to the Research Council of Lithuania for funding the project (No S-SEN-20-7) and LSMU Neuroscience Institute, for resources and support I received, which have been instrumental in my journey. I really appreciate for all the effort, organizational guidance, and scientific insights.

I am sincerely grateful to the entire team of the Laboratory of Molecular Neurobiology. Their collaboration played a crucial role in my academic development. Their expertise, technical assistance and involvement were truthfully valuable. Thanks for the professional and productive partnership.

I want to acknowledge my supervisor Dr. Daina Skiriutė for their feedback, invaluable insights, and critical thinking during my research process. Her ambitious standards and thorough feedback influence both the quality of this dissertation and my growth as a researcher.

Thanks to my lab colleagues of the Laboratory of Molecular Neurooncology. I am grateful for the knowledge I gained, all of you have created an environment that fostered both my academic and personal development. Especially thanks to Dr. Giedrius Steponaitis, Dr. Rytis Stakaitis, Dr. Rūta Urbanavičiūtė-Orentė and Dr. Indrė Valiulytė-Simaitė they made significant contributions to the experiment's execution and outcomes interpretation.

I am so grateful to all my friends. All your belief in me has been a constant source of strength, and for that, I am profoundly grateful. A special shoutout to my best friend Kotryna. I always feel uplifted and better equipped to face the world after our conversations. Thank you for being a shining light in my life.

I want to take a moment to express my deepest gratitude to my beloved family. To my mother Aldona. Your unwavering support and love have been the foundation of my journey. Thank you for giving me the freedom to choose. Your sacrifices and encouragement have inspired me to reach for my dreams. To my sister Goda, thank you for always being there for me, sharing in my joys and challenges. Together, you both have been my greatest support, and I deeply appreciate everything you have done for me. Part of this dissertation belongs to you – your love and guidance have shaped my path. Thank you for being my pillars of strength.